MASSEY UNIVERSITY

DOCTORAL THESIS

Non-destructive and Cost-effective 3D Plant Growth Monitoring System in Outdoor Conditions

Student:
Abhipray PATURKAR

Supervisors:
Prof. Gourab SEN GUPTA and
Prof. Donald BAILEY

A thesis presented in partial fulfilment of the requirements for the degree of
Doctor of Philosophy

in

School of Food and Advanced Technology
at Massey University,
Palmerston North, New Zealand.

June 21, 2022

Declaration of Authorship

I, Abhipray PATURKAR, declare that this thesis titled, "Non-destructive and Cost-effective 3D Plant Growth Monitoring System in Outdoor Conditions" and the work presented in it are my own. I confirm that:

- This work was done wholly or mainly while in candidature for a research degree at this University.
- Where any part of this thesis has previously been submitted for a degree or any other qualification at this University or any other institution, this has been clearly stated.
- Where I have consulted the published work of others, this is always clearly attributed.
- Where I have quoted from the work of others, the source is always given. With the exception of such quotations, this thesis is entirely my own work.
- I have acknowledged all main sources of help.
- Where the thesis is based on work done by myself jointly with others, I have made clear exactly what was done by others and what I have contributed myself.

Signed:

Date:

Abstract

Plant growth monitoring is one of the crucial steps within plant phenotyping. Traditional manual measurement techniques are error-prone and destructive. In recent times there has been substantial progress in computer vision-based methods. Due to their non-destructive nature and increased accuracy, imaging techniques are becoming state-of-the-art in plant phenotyping. However, most of the associated cameras, sensors, and processors are expensive, resulting in their reduced applicability in this area.

This thesis proposes a framework for low-cost plant growth monitoring. A novel, cost-effective and non-destructive 3D method is proposed. It uses a smartphone's camera and is based on the structure-from-motion algorithm to construct 3D plant models. This algorithm uses several overlapped images to build the model. The modelling speed and quality largely depend on the number of input images used. It is challenging to select the right number of images to generate an accurate plant model - too few images might generate false points in the 3D point cloud, whereas too many images will result in redundant processing, which will inevitably increase computation time. An analytical method is proposed to determine the appropriate number of images for modelling to solve this problem. Once the 3D model is generated, it is essential to segment the various plant components such as leaves and stem to measure traits. The segmentation method needs to be able to work regardless of particular plant architecture. This thesis proposes a segmentation method using Euclidean distance to segment the point cloud. Finally, plant traits for growth monitoring are measured: leaf length, leaf width, number of leaves, stem height, and leaf area. Methods to accurately measure leaf length, width and stem height when curled are proposed. To conclude, this thesis demonstrated that the proposed framework could monitor plant growth and calculate structure and growth parameters in different outdoor conditions. The framework was tested using five different plants with different architectures: cauliflower, lettuce, tomato, chilli, and maize. Hence, this framework is a potential alternative to costly state-of-the-art systems.

Acknowledgements

It's a marathon, not a sprint. I recall my father's valuable advice when I started this beautiful journey. The last five years have felt like a bit of both. For whatever it was that I thought I would be doing during this PhD, it was nothing like it. This has been a complex and challenging but eventually most rewarding journey. From rushing to submit the journals and conference papers seconds before a deadline to planning my experiments years in advance, my way through this PhD experience has been anything but monotonous. From not having a clue about "research" or what I wanted to work on to letting myself wander aimlessly through life, five years on, I am proud of the ideas I have explored and am closer to being the person I have always aspired to be.

It is inconceivable that I would have persisted through the duration of the program had it not been for the constant and dedicated support of an army of people, far too many to name. I am grateful to my primary supervisor, Prof Gourab Sen Gupta, for his continuous support and valuable guidance. Dr Sen's critical analysis of my work helped me improve how I now conduct research. I must admit that I have learned ways of thinking clearly and thoroughly under the guidance of Dr Sen. I am also very thankful to my co-supervisor, Prof Donald Bailey. His critiques on my research was a significant factor in improving the quality of this thesis. Thank you for being patient with me for innumerable knocks on your office door for my questions. I want to thank both of my supervisors; their patience and constant encouragement are the chief sources of my academic and research successes at Massey University. They have also demonstrated that success in one's career can gracefully coexist with the kindness of personality. Their words of wisdom and advising style have left a deep impression on me–lessons I hope to emulate in my own career. Also, thank you for the many hours you spent reading and correcting my articles for various conferences and journals.

Many thanks to the Centre for Research in Image and Signal Processing (CRISP) for their input to my research. I am very grateful to Prof Donald Bailey and Murray Milner for their counselling and support through the IEEE NZ Central Section platform. Thank you, Massey University, for MU doctoral scholarship and MU presentation grants; these uplifted me financially.

When I was about to start writing this thesis, COVID-19 struck the world. Like most of the world, my life was also affected: my lovely grandparents and dear uncle passed away due to COVID-19 in a year. It was a difficult time in life, knowing that we could not travel home to see them for the last time during this unprecedented time. Like much else, I owe a lot of things to them, and I would like to thank them for all the things they did for me.

I want to thank my friends for keeping me sane during this journey: Abhijit, Ajinkya, Anup, Chitra, Chanjief, Gunjan, Kanwal, Karan, Makrand, Monika, Nikhil, Pawan, Pournima, Pratik, Raunak, Rayson, Sai, Sashi, Sayali, Shan, and Yugant (the list goes on). I am blessed to have close and devoted friends. Their friendship has sustained me at every step along my way and I cannot imagine my life without each and every one of them. I am indebted to all my friends and extended family for their kindness and faith in me.

The love of my life, Ankita, whom I met during this PhD journey, is, without doubt, my most enthusiastic advocate. Without her presence, love, and levelheadedness, this body of work may not have seen the light of day for another year, at least. And it is not just a matter of emotional support. Ankita has also paid keen attention to the finer details of my research and developed an acute understanding of this area. For any researcher, having a captive audience is priceless, and Ankita's attention and feedback have given me tremendous confidence in my work's merits. It has been a remarkable journey so far, and I have Ankita to thank for it all. Knowing the journey we shared, all the ups and downs, we know each other in and out. This begs the most important question of my life, Dr. Ankita Jena, daughter of Commodore Surgeon Pramod Kumar Jena and Dr. Sudhansu Bala Pattnaik, **will you marry me?**

I am a firm believer in divine interventions. It can only be due to fortune that I was blessed with parents and a brother who have sacrificed everything for me. They have all selflessly vested themselves in my career and have experienced all the joys and disappointments as their own. Without their sacrifices, this PhD would have been inconceivable. Academics themselves, understand firsthand what this journey entails, and this journey would have been impossible without their unwavering support and encouragement. I wouldn't be anywhere near where I am today without their sacrifices and devotion. It is also worth mentioning how they fought COVID-19 by themselves; knowing I was coming home to support them, they did not allow me to come home; instead, they asked me to focus on my studies. It has been my elder brother's (Dada) dream for me to get my PhD, whom I lost just before starting this PhD in an accident. I dedicate this thesis to him and know that he will celebrate it as his own accomplishment from wherever he is.

Contents

Declaration of Authorship iii

Abstract v

Acknowledgements vii

1 Introduction 1
1.1 Introduction . . . 1
1.1.1 Plant Growth Monitoring . . . 1
1.1.2 Problem Statement and Research Contribution . . . 1
1.2.1 Cost-effective Image Capture Technique: . . . 2
1.2.2 Reduction in Computation time: . . . 3
1.2.3 Efficient 3D model Segmentation: . . . 3
1.2.4 Accurate Plant Trait Measurement: . . . 4
1.1.3 Thesis Outline . . . 4

2 Imaging for Monitoring Plant Growth 5
2.1 Introduction . . . 5
2.1.1 Research Contribution . . . 6
2.2 3D Imaging Techniques . . . 7
2.2.1 Active Techniques . . . 7
Laser Triangulation . . . 7
Structured Light . . . 7
Time-of-flight . . . 8
LiDAR . . . 9
2.2.2 Passive Techniques . . . 9
Stereo Vision . . . 9
Structure-from-motion . . . 10
Light Field Cameras . . . 11
2.2.3 A Constructive Comparison of 3D Imaging Techniques . . . 11
2.3 Plant Separation in Clusters and Row Structure . . . 11
2.3.1 Raster-Based Algorithms . . . 13
Plant-top Detection . . . 13
Segmentation and Post-processing of the Result . . . 13
2.3.2 Point Cloud Based Methods . . . 14
K-means Clustering . . . 14
Voxel Based Single Tree Segmentation . . . 14
Other Point Cloud Based Methods . . . 14
2.3.3 Fused Method Combining Raster, Point, and *a Priori* Data . . . 14
Adaptive Plant Detection . . . 14
Combined Image and Point Cloud Analyses . . . 15
2.3.4 Plant Shape Reconstruction Algorithms . . . 15
Convex Hull . . . 15

Alpha Shapes . . . 15
2.3.5 Key Takeaways: . . . 15
2.4 Initial Scene Rendering . . . 16
2.4.1 Point Cloud . . . 16
2.4.2 Voxel Grids . . . 16
2.4.3 Depth Map . . . 17
2.5 3D Model Processing . . . 18
2.5.1 Preprocessing . . . 18
Background Removal . . . 18
Outlier Removal . . . 18
Denoising . . . 19
Down-sampling . . . 19
2.5.2 Lower-level 3D Model Representation . . . 19
Octree . . . 19
Polygon Mesh . . . 20
Undirected Graph . . . 20
2.6 3D Model Analysis . . . 20
2.6.1 Segmentation . . . 20
Point Cloud Surface Feature-based Segmentation: . . . 21
Graph-based Segmentation: . . . 22
Voxel-based Segmentation: . . . 22
Mesh-based Segmentation: . . . 22
Deep Learning-based Segmentation: . . . 23
2.6.2 Skeletonization . . . 23
2.6.3 Surface Fitting . . . 24
Non-uniform Rational Basis Splines: . . . 24
Cylinder Fitting: . . . 25
2.6.4 Key Takeaways . . . 25
2.7 Plant Traits to Consider for Growth Monitoring and Extraction of the Traits . . . 25
2.7.1 Individual Plant Trait Measurements: . . . 25
2.7.2 Whole Plant Measurements: . . . 26
2.7.3 Canopy-based Measurements: . . . 27
2.8 Plant Growth . . . 27
2.8.1 Key Takeaways . . . 29
2.9 Current Challenges and Research Directions . . . 29
2.10 Summary . . . 30

3 3D Reconstruction of Plants using Smartphone's Camera in Outdoor Conditions 31
3.1 Introduction . . . 31
3.1.1 Overview of 3D Reconstruction Techniques . . . 31
3.1.2 Research Contribution . . . 32
3.2 Methods and Materials . . . 32
3.2.1 Testing Site . . . 32
3.2.2 Types of Plant . . . 33
3.2.3 Plant Settings . . . 33
3.2.4 Imaging Sensor . . . 33
3.2.5 Image Acquisition Scheme . . . 33
3.2.6 Number of Samples Generated . . . 33
3.2.7 Structure-from-Motion Work-flow . . . 35

3D Reconstruction . . . 35
Post-Processing . . . 35
3.3 Results . . . 36
3.3.1 3D Reconstruction of Chilli Plant . . . 36
3.3.2 3D Reconstruction of all the Plants . . . 36
3.3.3 Quality Assessment of the 3D Models . . . 41
3.3.4 Discussion . . . 41

4 Reducing Computation Cost for Accurate 3D Modelling **49**
4.1 Introduction . . . 49
4.1.1 Overview of Structure-from-motion . . . 50
4.1.2 Research Contribution . . . 50
4.1.3 Materials and Methods . . . 50
Computer Platform and Software . . . 50
Dataset . . . 51
Investigating Parameters . . . 51
4.1.4 Measurement of plant features from the reconstructed 3D model . . . 51
4.1.5 Results and Discussion . . . 52
3D Modeling . . . 52
4.1.6 Investigation Parameters . . . 53
Change in number of input images for 3D modeling . . . 53
Change in Image Resolution . . . 55
4.1.7 Conclusion . . . 57

5 Plant Trait Segmentation for Plant Growth Monitoring **59**
5.1 Introduction . . . 59
5.1.1 Research Contribution . . . 62
5.1.2 Materials and Methods . . . 62
Computer Platform and Software . . . 62
Dataset . . . 62
Point cloud down-sampling: . . . 62
5.1.3 Plant Point Cloud Segmentation . . . 62
5.1.4 Results . . . 63
5.1.5 Performance Evaluation . . . 68
5.1.6 Determination of Best (r_{th}) Value . . . 69
5.1.7 Conclusion . . . 69

6 Plant Traits Measurement in 3D **71**
6.1 Introduction . . . 71
2D Systems For Plant Measurement . . . 71
3D Systems For Plant Measurement . . . 72
6.1.1 Research Contribution . . . 74
6.1.2 Materials and Methods . . . 74
Plant Trait Measurements . . . 74
Leaf Length . . . 74
Leaf Width . . . 76
Stem Height . . . 76
Number of Leaves . . . 77
Leaf Area . . . 77
6.1.3 Ground Truth Measurements . . . 78

6.1.4 Results . . . 78
Leaf Length . . . 79
Leaf Width . . . 79
Stem Height . . . 79
Number of Leaves . . . 80
Leaf Area . . . 80
6.1.5 Comparison with the State-of-the-art . . . 80
6.1.6 Discussion and Conclusion . . . 82

7 Conclusion and Future Scope **85**
7.1 Conclusion . . . 85
7.1.1 Performance of various stages in the framework on the considered plants . . . 86
3D Reconstruction of Plants . . . 86
Reducing Computation Cost . . . 86
7.1.2 Plant Trait Segmentation . . . 86
Plant Trait Measurement . . . 86
7.2 Future Scope . . . 87

A Supplementary Material **89**
A.1 Chapter 4: Reducing Computation Cost for Accurate 3D Modeling . . . 89

B Supplementary Material **101**
B.1 Chapter 6: Plant Traits Measurement in 3D . . . 101
B.2 Videos . . . 101

References **109**

List of Figures

1.1 A team of experts assessing the plant growth [175] 2

2.1 Classification of 3D acquisition methods 6
2.2 Outline of processing and analysis stages for 3D plant growth monitoring 7
2.3 General configuration of laser triangulation 8
2.4 Structured-light for 3D measurement 8
2.5 ToF measurement principle 9
2.6 Stereo vision technique 10
2.7 Illustration of structure-from-motion technique 10

3.1 Testing site 32
3.2 Illustration of image acquisition scheme 34
3.3 A sample of the captured images with different view angles and distances of a chilli plant 34
3.4 Leaf mesh consisting different sizes of triangular polygons 36
3.5 Sparse 3D point cloud of the plant. The triangles in the image represent the viewpoint of the plant 37
3.6 3D Models of chilli plant 37
3.7 3D models of tomato plant at different growth stages 39
3.8 3D models of cauliflower plant at different growth stages 39
3.9 3D models of lettuce plant at different growth stages 39
3.10 3D models of chilli plant at different growth stages 40
3.11 3D models of maize plant at different growth stages 40
3.12 The approximate calculation of stem height from the reconstructed 3D model 42
3.13 Comparison of manual and measured measurements of the plants . . . 43
3.13 Comparison of manual and measured steam height measurements of the plants 44
3.14 Comparison of manual and measured measurements of the plants . . . 45
3.14 Comparison of manual and measured measurements of the plants(cont.) 46

4.1 Example 3D reconstructions of a chilli plant with different numbers of input images 52
4.2 Extracted stem height from reconstructed 3D model with change in number of input images for chilli plant 53
4.3 Extracted number of leaves from reconstructed 3D model with change in number of input images for chilli plant 55
4.4 Number of 3D data points detected for different image resolutions for chilli plant 56

5.1 Results of the proposed algorithm of different plants at various growth stages 64

5.2 Comparison of overall performance of the proposed and standard algorithms . . . 66

6.1 Flowchart of 3D plant reconstruction and plant trait measurements . . 75
6.2 Leaf length measurement. . . . 75
6.3 Leaf width measurement . . . 76
6.4 Stem height measurement . . . 77
6.5 Leaf triangular polygonal mesh . . . 78
6.6 Leaf area calculation using ImageJ . . . 79
6.7 Correlation between Ground Truth and Measured Leaf Length . . . 80
6.8 Correlation between ground truth and measured leaf width . . . 81
6.9 Correlation between ground truth and measured values for (A) stem height and (B) number of leaves . . . 81
6.10 Correlation between ground truth and measured values for leaf area (cm^2) . . . 82

A.1 Example 3D reconstructions of a cauliflower plant with different numbers of input images . . . 90
A.2 Example 3D reconstructions of a lettuce plant with different numbers of input images . . . 91
A.3 Example 3D reconstructions of a maize plant with different numbers of input images . . . 92
A.4 Example 3D reconstructions of a tomato plant with different numbers of input images . . . 93
A.5 Extracted stem height from reconstructed 3D model with change in number of input images for cauliflower plant . . . 93
A.6 Extracted stem height from reconstructed 3D model with change in number of input images for tomato plant . . . 94
A.7 Extracted stem height from reconstructed 3D model with change in number of input images for maize plant . . . 94
A.8 Extracted number of leaves from reconstructed 3D model with change in number of input images for cauliflower plant . . . 95
A.9 Extracted number of leaves from reconstructed 3D model with change in number of input images for tomato plant . . . 95
A.10 Extracted number of leaves from reconstructed 3D model with change in number of input images for maize plant . . . 96
A.11 Extracted number of leaves from reconstructed 3D model with change in number of input images for lettuce plant . . . 96
A.12 Number of 3D data points detected for different image resolutions for cauliflower plant . . . 97
A.13 Number of 3D data points detected for different image resolutions for lettuce plant . . . 98
A.14 Number of 3D data points detected for different image resolutions for maize plant . . . 99
A.15 Number of 3D data points detected for different image resolutions for tomato plant . . . 100

B.1 Leaf length measurement for cauliflower . . . 102
B.2 Leaf width measurement for cauliflower . . . 102
B.3 Stem measurement for cauliflower . . . 103
B.4 Leaf length measurement for cauliflower . . . 103

B.5 Leaf length measurement for cauliflower . . . 104
B.6 Correlation between ground truth and measured leaf length for Cauliflower plant . . . 104
B.7 Correlation between ground truth and measured leaf length for Tomato plant . . . 104
B.8 Correlation between ground truth and measured leaf length for Maize plant . . . 105
B.9 Correlation between ground truth and measured leaf length for Lettuce plant . . . 105
B.10 Correlation between ground truth and measured leaf width for Cauliflower plant . . . 105
B.11 Correlation between ground truth and measured leaf width for Tomato plant . . . 106
B.12 Correlation between ground truth and measured leaf width for Lettuce plant . . . 106
B.13 Correlation between ground truth and measured values for leaf area (cm^2) for Cauliflower plant . . . 106
B.14 Correlation between ground truth and measured values for leaf area (cm^2) for Tomato plant . . . 107
B.15 Correlation between ground truth and measured values for leaf area (cm^2) for Maize plant . . . 107
B.16 Correlation between ground truth and measured values for leaf area (cm^2) for Lettuce plant . . . 107

List of Tables

2.1 Comparative analysis of state-of-the-art 3D acquisition systems. The values of XYZ represents coordinates, I stands for intensity or reflectance, and RGB is image combination 6
2.2 Comparative analysis of 3D imaging techniques 12

3.1 Mean squared error for stem height and number of leaves 41

4.1 Total number of captured images for each plant in the advanced vegetative growth stage 51
4.2 Execution time taken based on number of images used for 3D reconstruction 54

5.1 Comparative analysis of clustering algorithms 61
5.2 Plant and algorithm wise performance assessment 67
5.3 Comparative analysis of standard algorithms 68
5.4 Algorithm performance based on ARI 68

6.1 Comparative analysis of state-of-the-art systems 82
6.2 Comparative analysis of of all the remaining plant 83

List of Abbreviations

ARI	Adjusted rand index
CHM	Canopy height model
CT	Computerised tomography
DSM	Digital surface model
FCN	Fully convolutional network
FPFH	Fast point feature histograms
LME	Linear mixed-effects
MAPE	Mean absolute percentage error
MRI	Magnetic resonance imaging
NDVI	Normalised difference vegetation index
NURBS	Non-uniform rational Bsplines
PFH	Point feature histograms
RANSAC	Random sample consensus
R-CNN	Region-based convolutional neural network
RF	Random forest
RGB	Red, Green, Blue
RMSE	Root mean square error
SFH	Surface feature histograms
SfM	Structure-from-motion
SMLR	Stepwise multiple linear regression
SVM	Support vector machine
TLS	Terrestrial laser scanning
ToF	Time of flight
UAV	Unmanned aerial vehicle

This thesis is dedicated to the memory of my brother

Akshay Prakash Paturkar
24/07/1988 - 13/04/2015

Chapter 1

Introduction

1.1 Introduction

In New Zealand, horticulture is an important industry. The horticulture industry represents the interest of nearly 6000 growers and employs around 60,000 people [1]. In 2019, horticulture contributed approximately $6.3 billion to the New Zealand economy [1], making it significant for the New Zealand economy. However, with the rapidly increasing world population, the production of plants for food is very important. The United Nations have included a goal in their 17 sustainable goals to promote sustainable agriculture to provide sufficient food for everyone to end hunger [189]. Enhancing crop production and plant breeding efficiency is critical to the success of achieving the growing food demands of more than nine billion population by 2050 [56]. In addition, environmental issues and labour constraints are also important factors for the growth of the horticulture industry.

1.1.1 Plant Growth Monitoring

Growth monitoring provides vital information about plants for plant phenotyping which is helpful to farmers in their decision making process [28]. Plant-phenotyping is a set of protocols and techniques used to calculate plant architecture, composition, and growth with precision at different plant growth stages. Popular plant traits for growth monitoring include stem height, stem diameter, leaf area, leaf length, leaf width, number of leaves or fruits on the plant, and biomass. However, the measurement of growth parameters is difficult, tedious and mostly depends on destructive approaches.

Plant growth monitoring is an important task, and plants are monitored throughout the growth stages for the plant's health. Nowadays, commercial lands or glasshouses are automated, but growth monitoring is still done manually. Currently, plants are monitored based on experience and frequent visual inspection. The assessment approach used by the experts in this field includes plucking a leaf from the plant for inspection, which can influence the growth patterns of the plants and their neighbours, thus interfering with the plant growth [129]. Also, this manual approach is prone to errors and is tedious. Finally, subjective factors and uncertainty are associated with manual measurements. There is a great demand for non-destructive, cost-effective, and accurate plant growth monitoring [129].

1.1.2 Problem Statement and Research Contribution

In recent years, the computer vision community has developed dramatically. Computer vision algorithms have been developed that can perform complex tasks on an

FIGURE 1.1: A team of experts assessing the plant growth [175]

almost routine basis. Developments in 3D imaging techniques are being broadly applied in precision agriculture and plant science. Computer vision techniques have proven their potential in non-destructive growth monitoring. For many years, 2D imaging techniques have been used for this application. Such methods have limitations such as the inability to handle occlusion, not providing sufficient information about plant traits, and plant measurements depending on the camera and leaf orientation. These limitations lead to inaccurate plant trait measurements. For instance, consider calculating leaf area; if the leaf is curled, the 3D area will be different from the leaf area calculated from its 2D image. To overcome these issues, 3D imaging techniques have been used. These produce geometrically precise 3D plant models which help to extract plant features accurately.

This thesis contributes to the recent advancements of computer vision-based plant growth monitoring technologies. This thesis addresses four problems in the literature, these are discussed in the following subsections.

1.2.1 Cost-effective Image Capture Technique:

In recent years, 3D laser scanners, structured light, time-of-flight cameras etc. are frequently used in this area to get the plant data. However, the cost of these sensors is significantly greater than that of commodity 2D cameras. For instance, the camera used in [155] costs around $9000 and laser scanning system costs around $111k. Also, the cost of commercial software for processing the data captured from the sensors/camera is around $7200 [155]. This makes the overall system expensive, stretching the budget to buy the sensors and associated software. To tackle this problem, we propose use of the smartphone's rear camera to capture the images and use computer vision methods to stitch the images together to form a 3D model.

The idea behind using a smartphone's rear camera is that commodity smartphones with good camera specifications are readily available for a reasonable cost and most people have smartphones.

Using a smartphone's camera has several advantages over expensive laser scanning sensors: it does not need bulky set-up to capture the plant data, it is easy to use, no need for prior training to the user, it is highly flexible and can be moved anywhere around the plant, and most importantly it is cost-effective. This allows us to capture plant images from multiple viewpoints. Other image capture sensors such as RGB-D cameras are not considered in this study due to they produce low-resolution point clouds. The results exhibit that the proposed image capture technique performs well when compared to costly state-of-the-art systems.

1.2.2 Reduction in Computation time:

There are a plethora of computer vision methods to build 3D models suitable for plant trait measurement. The computation time required to process the data differs from method to method. For instance, stereo vision uses a stereo camera set-up to capture the scene; however, the user has to determine the camera's intrinsic and extrinsic parameters. If the scene changes, then user has to again recalibrate these parameters which are time-consuming. Structure-from-motion (SfM) uses a single camera to capture the images. SfM calculates the intrinsic and extrinsic camera parameters as part of the 3D modelling process, which saves time. However, since the computation time depends on the number of images used to generate the 3D model, it is important to know the appropriate number of input images required to generate an accurate 3D model.

We conducted an analytical study to address this trade-off between the number of input images and computation time. The process of generating a 3D model using structure-from-motion is applied on different subsets of randomly selected images for a particular set of input images. The size of the subset is varied from 25 images through to 80 images. The experiment is repeated five times for each subset size, selecting a different random subset. The quality of the reconstructed 3D model was determined by comparing features extracted from the model with ground truth data (manually measured values of the actual plant). By exploring the correlation of extracted features with ground truth values, the number of images required to accurately reconstruct the plant was determined.

1.2.3 Efficient 3D model Segmentation:

Once the 3D model is generated, it is important to segment the plant traits accurately. There are several segmentation algorithms presented in the literature [132]. The segmentation should be able to separate the various plant components such as leaves and stem robustly to measure traits. Also, the segmentation method needs to work on a range of plant architectures with good accuracy and computation time. This study proposes a segmentation method using Euclidean distance to segment the point cloud generated. The proposed algorithm requires no prior information about the plant point cloud. The results illustrate that our proposed method can effectively segment the plant point cloud irrespective of its architecture and growth stage.

1.2.4 Accurate Plant Trait Measurement:

After segmentation, important plant traits for growth monitoring are measured: leaf length, leaf width, number of leaves, stem height, and leaf area. These traits are important as leaf size plays a vital role in plant growth. This study proposes techniques to measure leaf length, width, and stem height accurately even if it is curled at any growth stage of the plant.

1.1.3 Thesis Outline

The rest of the thesis can be summarized as follows:

1. **Chapter 2** reviews the background of various methods that are used in the rest of the chapters. The following areas are surveyed: imaging techniques for plant growth monitoring, 3D scene representation, 3D model analysis, plant traits to consider, plant trait measurement.
   This work was published in *Image and Vision Computing New Zealand* (IVCNZ) conference in 2017 [130] and expanded and published in special issue, 3D Point Clouds for Agriculture Applications, Remote Sensing in 2021 [132].

2. **Chapter 3** explains the use of a smartphone's camera for the image acquisition process. It investigates the effects of different adverse outdoor scenarios which affect the quality of the 3D model. Also, it compares the results with state-of-the-art image acquisition sensors.

   This work resulted as a book chapter published in [127] and subsequently expanded and published in *Multimedia Tools and Application* journal in 2020 [129].

3. **Chapter 4** analyses the appropriate number of input images required to generate an accurate 3D model. We briefly discuss the trade-off between the number of input images used and computation time.

   This work was published as a book chapter in *Advances in Signal and Data Processing* [128].

4. **Chapter 5** describes the proposed plant point cloud segmentation algorithm. We show that it is possible to accurately segment the plant point cloud at various growth stages and architectures.

   This work was published in *Image and Vision Computing New Zealand* (IVCNZ) conference in 2020 [131].

5. **Chapter 6** applies the methods developed in the previous chapters to 5 different plant species at various growth stages. The results demonstrate the applicability of the proposed framework. This work is currently under review for the *Plant Methods* journal.

6. **Chapter 7** summarises the whole thesis and possible future research directions are identified.

MASSEY UNIVERSITY
TE KUNENGA KI PŪREHUROA
UNIVERSITY OF NEW ZEALAND

GRADUATE RESEARCH SCHOOL

STATEMENT OF CONTRIBUTION
DOCTORATE WITH PUBLICATIONS/MANUSCRIPTS

We, the candidate and the candidate's Primary Supervisor, certify that all co-authors have consented to their work being included in the thesis and they have accepted the candidate's contribution as indicated below in the *Statement of Originality*.

Name of candidate:	Abhipray Paturkar
Name/title of Primary Supervisor:	Professor Gourab Sen Gupta
In which chapter is the manuscript /published work:	Chapter 2

Please select one of the following three options:

(●) The manuscript/published work is published or in press

- Please provide the full reference of the Research Output:

A. Paturkar, G. Sen Gupta, and D. Bailey, "Making Use of 3D Models for Plant Physiognomic Analysis: A Review," in special issue, 3D Point Clouds for Agriculture Applications, Remote Sensing, vol. 13, no. 11, p. 2232, 2021

( ) The manuscript is currently under review for publication – please indicate:

- The name of the journal:

- The percentage of the manuscript/published work that was contributed by the candidate: 90.00

- Describe the contribution that the candidate has made to the manuscript/published work:

The candidate performed the literature search, read, analysed the relevant literature, determined the research gaps, generated figures, and drafted the manuscript.

( ) It is intended that the manuscript will be published, but it has not yet been submitted to a journal

Candidate's Signature:	Abhipray Paturkar Digitally signed by Abhipray Paturkar Date: 2022.03.09 13:18:56 +13'00'
Date:	09-Mar-2022
Primary Supervisor's Signature:	Gourab Sen Gupta Digitally signed by Gourab Sen Gupta DN: cn=Gourab Sen Gupta, c=NZ, o=Massey University, ou=School of Food and Advanced Technology, email=g.sengupta@massey.ac.nz Date: 2022.03.10 10:34:18 +13'00'
Date:	10-Mar-2022

This form should appear at the end of each thesis chapter/section/appendix submitted as a manuscript/ publication or collected as an appendix at the end of the thesis.

MASSEY UNIVERSITY
TE KUNENGA KI PŪREHUROA
UNIVERSITY OF NEW ZEALAND

GRADUATE RESEARCH SCHOOL

STATEMENT OF CONTRIBUTION
DOCTORATE WITH PUBLICATIONS/MANUSCRIPTS

We, the candidate and the candidate's Primary Supervisor, certify that all co-authors have consented to their work being included in the thesis and they have accepted the candidate's contribution as indicated below in the *Statement of Originality*.

Name of candidate:	Abhipray Paturkar
Name/title of Primary Supervisor:	Professor Gourab Sen Gupta
In which chapter is the manuscript /published work:	Chapter 2

Please select one of the following three options:

(●) The manuscript/published work is published or in press

- Please provide the full reference of the Research Output:

A. Paturkar, G. Sen Gupta and D. Bailey, "Overview of image-based 3D vision systems for agricultural applications," International Conference on Image and Vision Computing New Zealand (IVCNZ), pp. 1-6,2017

( ) The manuscript is currently under review for publication – please indicate:

- The name of the journal:

- The percentage of the manuscript/published work that was contributed by the candidate: 90.00

- Describe the contribution that the candidate has made to the manuscript/published work:

The candidate performed the literature search, read, analysed the relevant literature, determined the research gaps, and drafted the manuscript.

( ) It is intended that the manuscript will be published, but it has not yet been submitted to a journal

Candidate's Signature:	Abhipray Paturkar Digitally signed by Abhipray Paturkar Date: 2022.03.09 13:15:07 +13'00'
Date:	09-Mar-2022
Primary Supervisor's Signature:	Gourab Sen Gupta Digitally signed by Gourab Sen Gupta DN: cn=Gourab Sen Gupta, c=NZ, o=Massey University, ou=School of Food and Advanced Technology, email=g.sengupta@massey.ac.nz Date: 2022.03.10 10:36:22 +13'00'
Date:	10-Mar-2022

This form should appear at the end of each thesis chapter/section/appendix submitted as a manuscript/ publication or collected as an appendix at the end of the thesis.

Chapter 2

Imaging for Monitoring Plant Growth

This thesis is composed of different types of problems and techniques related to plant growth monitoring. We discuss the related literature in various sections below. This work resulted in the following conference and journal publication:

1. A. Paturkar, G. Sen Gupta and D. Bailey, "Overview of image-based 3D vision systems for agricultural applications," *International Conference on Image and Vision Computing New Zealand* (IVCNZ), pp. 1-6,2017.

   DOI: 10.1109/IVCNZ.2017.8402483

2. A. Paturkar, G. Sen Gupta, and D. Bailey, "Making Use of 3D Models for Plant Physiognomic Analysis: A Review," in special issue, 3D Point Clouds for Agriculture Applications *Remote Sensing*, vol. 13, no. 11, article 2232, 2021. DOI: 10.3390/rs13112232

2.1 Introduction

In recent years, a plethora of studies has been conducted on plant trait measurement in 3D [198, 123, 135]. Plant phenotyping is an important area of research for plant growth monitoring. It is implemented by a fusion of techniques, such as spectroscopy, non-destructive imaging, and high performance computing. Plant phenotyping provides vital information about plants for monitoring growth which is helpful to farmers for their decision making process. Plant phenotyping is a set of protocols and techniques used to precisely calculate plant architecture, composition, and growth at different growth stages. Popular plant traits for growth monitoring include stem height, stem diameter, leaf area, leaf length, leaf width, number of leaves or fruits on the plant, and biomass. However, the measurement of plant structure and growth parameters is difficult, tedious and mostly depends on destructive approaches. 3D modelling helps to access the complex plant architecture [51] which allows plant related information to be extracted, such as characterization of plants and their growth development. Conventionally all these elements have been evaluated by experts in this field using a subjective visual score, which can result in dissimilarity between expert judgements. Primarily, plant phenotyping aims to calculate plant features precisely without subjective biases [130]. Therefore 3D measurement techniques are potentially suitable as these allow measurement of plant traits and can accurately model plant geometry.

The range of 3D measurement methods includes LiDAR, laser scanning, structured light, structure-from-motion, and time-of-flight sensors. Each of these methods has its own merits and demerits. All these methods produce a point cloud, in

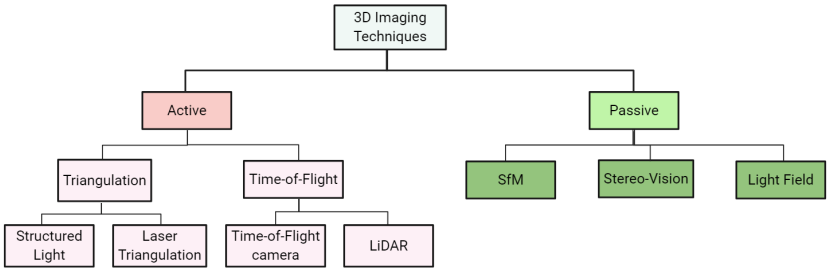

FIGURE 2.1: Classification of 3D acquisition methods

TABLE 2.1: Comparative analysis of state-of-the-art 3D acquisition systems. The values of XYZ represents coordinates, I stands for intensity or reflectance, and RGB is image combination

Method	**Price**	**Type**	**Output**	**Resolution**
Structured light	$$	Active	XYZIRBG	$<mm$
Laser triangulation	$$$	Active	XYZI	$< mm$
Structure-from-motion	$	Passive	XYZRGB	mm
LiDAR	$$$	Active	XYZ(I/RGB)	cm
Field cameras	$$$	Passive	XYZRGB	mm
Time-of-flight	$$	Active	XYZI	mm

which every 3D point represents a point detected on the plant's surface. Based on the measuring technique, the coordinates can be augmented by colour information or the intensity of the reflected light. Current 2.5D techniques such as range imaging calculate distances from a single point of view (range images). In contrast, 3D models describe point clouds captured from different angles and views displaying various spatial levels of points and therefore demonstrate less occlusion, higher accuracy, spatial resolution, and sample density.

A detailed technical classification of 3D acquisition methods is shown in fig 2.1. Active techniques use their own source of illumination for measurement and passive techniques use ambient light in the scene. Active sensing techniques are classified into two types: triangulation based methods and time-of-flight based methods. Structured light (early Kinect sensor) and laser triangulation approaches are triangulation based methods. LiDAR and time-of-flight cameras are time-of-flight based methods. Field cameras and structure-from-motion (SfM) methods are types of passive techniques. A comparison between these techniques is given in Table 2.1. Fig. 2.1 and Table 2.1 are adapted from [133].

2.1.1 Research Contribution

Several papers have reviewed 3D image acquisition for plant phenotyping [193, 108, 54, 123, 133, 190]. However, a review of approaches used for 3D model processing and analysis in the context of plant physiognomic analysis is lacking, which will be the focus of this review. For 3D plant model analysis, a wide set of tools is needed, because of the variety of plant architectures across species. This chapter aims to identify standard processing and analysis stages and review techniques used in each of these stages. An overview of the stages covered in this chapter is shown in fig.

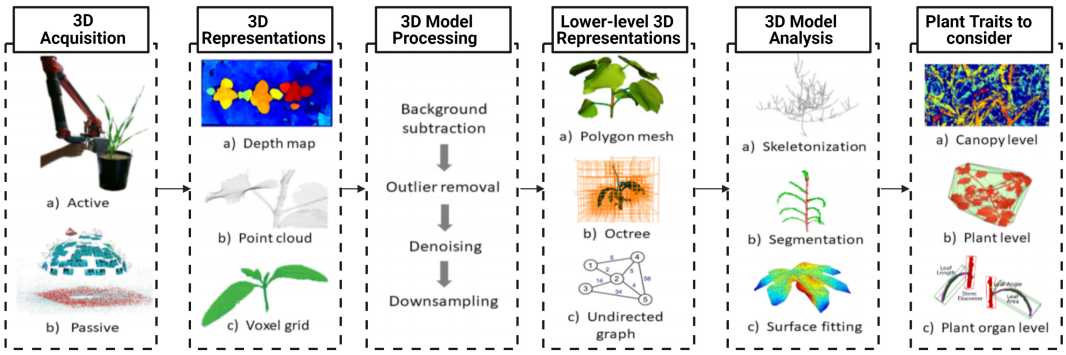

FIGURE 2.2: Outline of processing and analysis stages for 3D plant growth monitoring

2.2 which is adapted from [190]. Also, this is the first work to have done extensive review of all the stages involved in 3D plant growth monitoring.

This review addresses the questions related to 3D plant physiognomic analysis. What sensing methods can be used for such analysis? Are there any potential cost-effective and non-destructive methods? What are the various scene representations? What type of plant traits should be extracted? What are the current challenges and research directions?

2.2 3D Imaging Techniques

In this section we detail 3D imaging techniques, reviewing active and passive techniques. We also provide a constructive comparison of these techniques.

2.2.1 Active Techniques

Active techniques use their own light source to illuminate a target and collect the reflection from an object.

Laser Triangulation

Laser triangulation describes distance calculation techniques based on differing laser and sensor positions. A laser ray is transmitted to illuminate the target surface, and the position of the laser spot is detected using an image sensor (see fig. 2.3). Since the laser and sensor are in different positions, the 3D location of the laser spot can be found through triangulation. A 3D point cloud can be generated by scanning the laser spot.

Laser triangulation has a trade-off between the target volume and point resolution. It can either measure a small target with the highest possible resolution or a large target with low resolution. This approach needs a prior estimation of the required resolution and the target volume. Laser triangulation is mainly used in laboratory settings because of its high accuracy, high resolution readings and easy set-up [137, 37].

Structured Light

Structured light projects patterns, a grid, in temporal order on the target. For every pattern, an image is captured by the camera. The 2D points on the grid pattern are

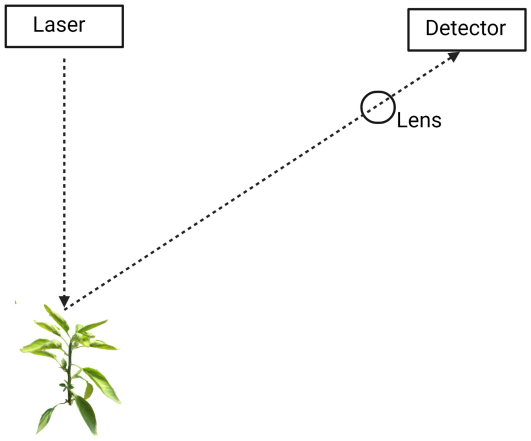

FIGURE 2.3: General configuration of laser triangulation

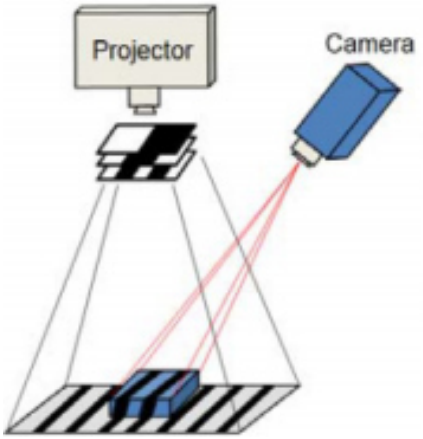

FIGURE 2.4: Structured-light for 3D measurement

linked to their 3D data by calculating the distortion of the pattern (see fig. 2.4) [50, 207]. Structured light has a bulky set-up and requires more time than other sensing techniques.

To achieve a 3D model, either the set-up or the target object has to be moved. Structured light is mostly used for industrial applications to check the quality of an object, providing high accuracy and resolution [91]. The early Kinect sensor is an example of a structured light sensor.

Time-of-flight

Time-of-flight (ToF) uses high frequency modulated illumination, and calculates the range from the phase shift (see fig. 2.5) [143]. This process can be repeated for thousands of points at the same time [130]. The set-up for ToF cameras is smaller than other methods and captures images with lower resolution. These cameras are suitable for indoor applications [153] or in the gaming industry [27]. ToF cameras are required to move in order to build a complete 3D point cloud. The cameras are slow and have low resolution, compared to laser triangulation and structure-from-motion (SfM).

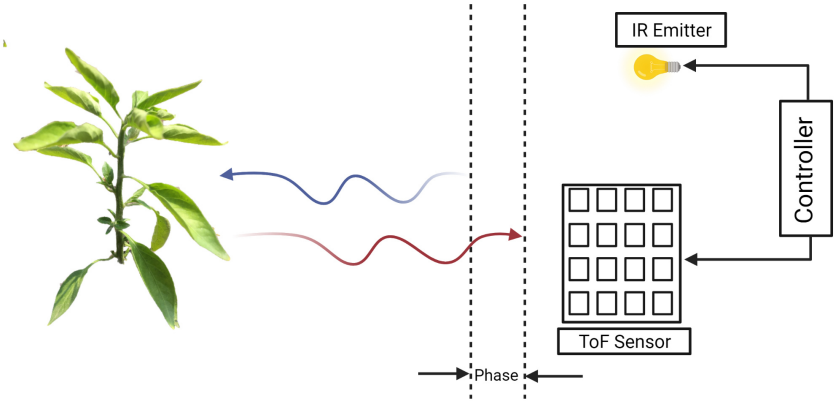

FIGURE 2.5: ToF measurement principle

LiDAR

Lidar is basically an extension of the principles employed in radar technology. It calculates the distance between the scanner and the target object by illuminating the object using a laser and measuring the time taken for the reflected light to return [130]. A terrestrial LiDAR has a bulky set-up and to deal with occlusion issues, the plant has to be scanned from multiple positions. This approach has already proved its worth in surveying applications, such as landslide detection and measurement [154]. For plant growth monitoring, LiDAR has the advantage that it can measure any target volume with high accuracy. However, this approach is costly, time consuming, and bulky, making it less suitable for plant growth monitoring.

Airborne LiDAR has also been used in some studies [145, 102] to determine plant height and crown diameter measurement. Airborne LiDAR offers accurate and detailed measurements; data can be collected quickly and from a variety of locations. However, there are some limitations such as underestimating vegetation height compared to field measurements [176, 42]. It struggles with dense vegetation canopy where the dense undergrowth may be confused with bare ground. The underestimation of vegetation height is also dependent on plant species and growth stage [205].

2.2.2 Passive Techniques

In these techniques, natural light is used to illuminate the object and to collect the object information through image sequence.

Stereo Vision

Stereo vision has three main processing stages: camera calibration, feature extraction, and correspondence matching. A stereo camera captures a pair of images (right and left). By using this stereo pair, the disparity can be calculated between the camera coordinates of matching points in the scene, thus the depth can then be calculated through triangulation (see fig. 2.6).

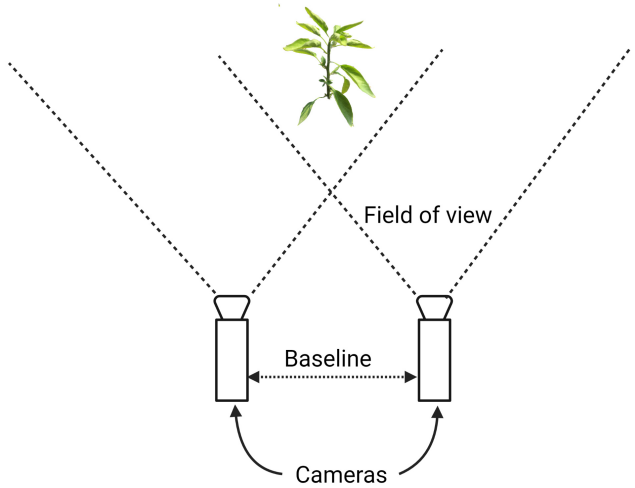

FIGURE 2.6: Stereo vision technique

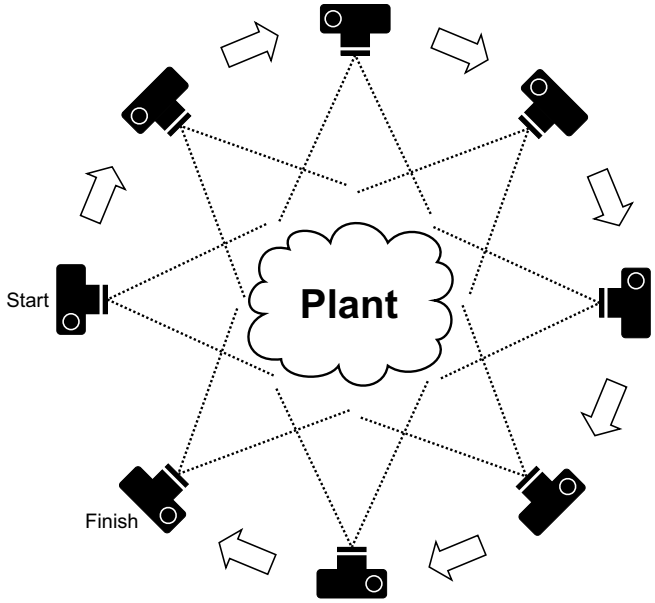

FIGURE 2.7: Illustration of structure-from-motion technique

Structure-from-motion

Structure-from-motion (SfM) uses a set of 2D images acquired by an RGB camera at different positions to generate a 3D model of the target [60] (see fig. 2.7). Corresponding points in the images are extracted [186] and matched to stitch the images together and generate the 3D model. The 3D point cloud includes colour and intensity information depending on the type of camera used [155].

The point resolution achieved from SfM is comparable to laser triangulation. However, it depends on the camera resolution and number of images used for 3D modelling [155].

Structure-from-motion can be used by mounting a camera on an unmanned aerial vehicle (UAV). This set-up is cheaper than airborne LiDAR. It is easy to gather data on a small study area, and overcast or partly cloudy conditions have less effect on the acquisition process. However, it is computationally demanding and it cannot penetrate the plant's canopy.

In contrast with laser triangulation, which requires more time for acquisition and the direct result is the point cloud, SfM requires less time for acquiring the images, but needs more time for reconstruction. SfM can be used in outdoor environments as it does not require special illumination or a complex set-up. This method requires only an off-the-shelf camera to capture the images, the set-up is cost-effective and easy.

Light Field Cameras

Field cameras [181] give depth information with colour images by calculating the direction of the light coming in using camera arrays. This allows the reconstruction of the target. However, similar to time-of-flight sensors, field cameras also need to move with a bulky set-up, making them difficult in outdoor applications.

2.2.3 A Constructive Comparison of 3D Imaging Techniques

Active techniques provide a high-resolution point cloud for further plant analysis such as plant trait segmentation and measurement. However, the influence of the laser on plant tissue has to be considered when active illumination techniques are used, especially laser triangulation. Even though laser-based techniques are described as non-penetrating, recent studies have found that plant tissue below cuticle (protecting covering) has significant impact on the trait measurement and accuracy due to laser intensity [133]. In addition, because of the edge effect [136, 38], plant trait measurements of partial leaves can generate outliers or errors in the measurement. Other active techniques such as structured light, time-of-flight, and LiDAR have proven their worth for plant phenotyping demands. However, the resolution and accuracy have to be improved for high throughput plant physiognomic analysis. Table 2.2 summarises the advantages and disadvantages of the various 3D imaging techniques.

In contrast, structure-from-motion gives an easy and cost-effective solution, and this makes them best suited for outdoor applications. However, the point cloud resolution depends on the number of images captured. Also, SfM requires more computation time than the other methods. Summing up, SfM is a reliable technique for 3D modelling of plants while resolving occlusion, self occlusion, correspondence problems, and providing high resolution information.

Researchers have used different sensors and techniques to derive a 3D model in all these studies. In conclusion, every sensor and technique has its merits and demerits [130] and their accuracy may vary. Depending on the budget and requirements, one should choose the sensors and techniques [127]. However, suppose budget is a limiting factor, based on the comparison provided in table 1. In that case, one can choose structure-from-motion as it is not only a cost-effective and non-destructive solution, but also it provides better point cloud resolution at the lowest price.

2.3 Plant Separation in Clusters and Row Structure

In some scenarios, plants are planted in a row or a cluster. Various active and passive methods have been developed in the literature [77, 192] to detect individual plants. In particular, LiDAR has been widely used over the past decade. Due to the airborne laser scanner (ALS), its data provides important information for individual tree detection [80, 174]. In the last 20 years, many fully- and semi-automatic algorithms have been developed to detect individual plants. However, even if one algorithm

TABLE 2.2: Comparative analysis of 3D imaging techniques

Technique	Type	Advantages	Disadvantages
Laser Triangulation	Active	-High precision -High speed data acquisition & 3D model generation -Does not rely on external light source	-High cost -Sensitive to sunlight
Structured Light	Active	-Low cost -High speed -High spatial resolution	-Small field-of-view -Poor with shiny surfaces -Limited sensing range -Sensitive to sunlight
Time-of-Flight	Active	-Performs well in dim/dark light conditions -High pixel resolution -Accurate depth sensors	-High cost -sensitive to sunlight
LiDAR	Active	-Robust against sunlight -Performs well in dim/dark light conditions -Robust against interference	-High cost -Bulky set-up -Poor in edge detection
Stereo Vision	Passive	-off-the-shelf cameras used -Cost-effective -Easy implementation -Provides efficient RGB stream	-Correspondence problem -Depth range depends on baseline -Sensitive to sunlight -Computationally costly
Structure-from-Motion	Passive	-Low cost -Excellent portability -Easy to use -Works with economical cameras	-High computation time -Poor in dim light

is best for a specific application, it may not be ideal for other situations. For instance, some algorithms may work well on canopies with large variations in plant growth stage, plant spacing, or plant crowns with a high degree of occlusion [88, 211]. It is challenging to decide on an ideal algorithm to detect individual plants as there is no standard method to assess the algorithm's accuracy [78]. This section will cover the work related to LiDAR information using a canopy height model (CHM), digital surface model (DSM), and passive methods to generate a point cloud to detect individual plants. Individual plant detection algorithms are grouped into four categories by Koch et al. [105]: (1) raster-based algorithms; (2) point cloud based algorithms; (3) fused method combining raster, point, and a priori data; and (4) plant shape reconstruction algorithms.

The individual plant detection algorithms are outlined below, but the reader must refer to the primary publications for detailed description.

2.3.1 Raster-Based Algorithms

Plant-top Detection

To use local maxima detection on CHM, the canopy height has to be derived from the laser point cloud data, interpolated and smoothed. The smoothing process results in the loss of detail about the plants. However, the smoothing process is needed to achieve an accurate number of local maxima as a starting point for plant segmentation. CHM underestimates the actual canopy height. To overcome this limitation, Solberg et al. [174] demonstrated a residual height adjustment method, in which the initial echoes from ALS were interpolated into a DSM with 25 cm spatial resolution by a minimum curvature algorithm. A 3×3 Gaussian filter was used to smooth the DSM. The local maxima in 3×3 neighbourhoods were considered as plant candidates. The height deviation of the initial echoes from the DSM was estimated providing a residual height distribution, and the local maxima and DSM were adjusted by adding specified residual height percentile. The filter window size and residual height percentile adjustment can be set according to the row structure or cluster.

However, all the algorithms based on CHM smoothing need a specific smoothing factor. A large smoothing factor may lead to an under-estimation of the number of local height maxima corresponding to plant-tops. In contrast, a low smoothing factor may lead to an over-estimation of the number of local maxima. In addition, all the algorithms based on analysing local maxima struggle to detect plants that are not shown in the CHM. For instance, plants in the undergrowth are covered by a neighbouring plant's crown.

A study conducted by Popescu et al. [145] used LiDAR to extract individual plants from a cluster used the local maxima on the assumption that the maximum heights in a given spatial neighbourhood represent the tips of the plant. The heights help to locate the individual plants in the cluster.

Segmentation and Post-processing of the Result

Two widely used raster-based algorithms for segmentation are the pouring and watershed algorithms [105]. The pouring algorithm starts "flowing water" from a given maximum height towards the lower heights and the region is divided into areas according to the water flow. The watershed algorithm uses an identical but inverse concept: the areas are extended as long as the neighbouring pixels with the same or lower height exist. The segmentation of plant crowns with the pouring algorithm works well for uniform heights. However, the result may have segmented areas

not resembling plant crowns, e.g.areas too small to be planted, non-plant like structures and so on. Solberg et al. [174] restricted region growing by applying polygon convexity rules when considering the regions' growth directions.

Geometrical models can be used to identify geometrical shapes combined with specific dimensions. Holmgren et al. [66] used geometric models for tree crown segmentation. A correlation surface was formed as the maximum pixel-wise correlation between the geometric plant crown model and CHM, defined as generalised ellipsoids of revolutions [144]. The correlation surface and CHM was used for segmentation, and merging and splitting criteria were used according to the geometric models.

2.3.2 Point Cloud Based Methods

K-means Clustering

K-means is one of the most popular clustering algorithms, with many attempts to partition ALS information into various clusters [74] and in single plant crowns [116]. The k-means algorithm needs seed points, derived as smoothed CHM based local maxima [116]. The unnecessary local maxima were removed by 3D Euclidean distance criteria, which were specified according to training data tests. A k-means algorithm is used to cluster the point cloud according to the seed points. However, it is important to note that the k-means algorithm works well when the point cloud has isolated or compact clusters [106]. Therefore, adaptive alternatives have been developed for different cluster structures [58].

Voxel Based Single Tree Segmentation

Point data was projected on a voxel space, which estimated density images from sequential height layers [202]. The images are scanned from top to bottom by a hierarchical morphological algorithm, assuming that the plant crown has a higher number of points. The method was then further developed with an algorithm for splitting and merging the plant crowns based on the horizontal projection.

Other Point Cloud Based Methods

In another study based on structure-from-motion, Jay et al. [79] analysed the plants planted in a row structure using overall excess green distribution in the image. Generally, the excess green value changes for the plant and the background, which helps to extract the individual plants when planted continuously.

To extract individual potato plants, planted in a row structure, Zhang et al. [207] defined regions of interest and then the regions were classified as different colours for plants and the background. Supervised maximum likelihood classification clusters pixels into pre-defined classes. Maximum likelihood classification presumes that the statistics for each class in every band is normally distributed and estimates the probability that a specific pixel belongs to a particular class. In this way, individual plants were extracted from a row structure.

2.3.3 Fused Method Combining Raster, Point, and *a Priori* Data

Adaptive Plant Detection

Ene et al. [41] introduced an adaptive method for single tree delineation and CHM generation. They adjusted the CHM resolution and filter size based on the prior

information achieved in the form of area-based stem number estimates. Considering that plants are distributed according to the Poisson process, one can estimate a rough plant-to-plant distance for optimizing the filter size and CHM resolution. A set of CHMs in varying resolution is formed for each training data. Two runs of the pit-filling algorithm by Ben-Arie et al. [7] were applied to every CHM, followed by low-pass filtering using a binomial kernel with a size relative to the expected nearest-neighbour distance between plants.

Combined Image and Point Cloud Analyses

Some methods combine point cloud and raster data to enhance the segmentation of single plants [151, 65]. Reitberger et al. [151] applied a normalized cut graph by Malik et al. [161] for segmentation using full waveform LiDAR point data. The method is based on graph partitioning and a measure to calculate within or between group dissimilarity. Reitberger et al. [151] used a watershed algorithm for crude segmentation. This segmentation was run to a smoothed CHM to generate an under-segmented result. The reflections extracted from full-waveform data were arranged in voxels; this was cut to areas based on graph partitioning to within-segment similarity. This similarity between voxels was calculated by echo, point distribution, and intensity. This algorithm generated a higher detection rate compared to using the watershed algorithm alone, yet still had some false detections.

2.3.4 Plant Shape Reconstruction Algorithms

Plant shape can be reconstructed using the following algorithms.

Convex Hull

Point cloud clusters shaped like plant crowns can be geometrically reconstructed using the convex hull [116, 81], representing the outer boundary of the point cloud. Gupta et al. [58] compared k-means clustering, modified k-means, and hierarchical clustering using a weighted average distance algorithm to detect plants, followed by an adapted convex hull algorithm, called Quick hull (QHull), for 3D plant shape reconstruction. Outdoor conditions, point density, plant crown, terrain type, and plant density are the important factors that affect the shape and the number of extracted plants.

Alpha Shapes

As an alternative to the convex hull, the number of facets corresponding to the minimum convex polygon may be controlled to achieve a detailed shape. A specifically useful method to perform this restriction is the idea of 3D alpha shapes [40], in which a pre-specified factor alpha is used as a size-criterion to estimate the level of detail in the achieved triangulation. Vauhkonen et al. [191] used the alpha shape method to select plant objects for predicting a range of factors, including species, plant crown volume, and crown base height, and noticed that this method is sensitive to the applied point density.

2.3.5 Key Takeaways:

Individual plant detection algorithms are widely based on raster-image analysis methods such as watershed segmentation and local maxima detection. However,

extracting the local maxima from raster-based CHMs misses plants below the dominant canopy, and methods developed to adjust the level of CHM smoothing cannot resolve this limitation. The detection of small plants or plants in early growth stages may be improved by a local refinement approach [151] or by performing detailed analysis of 3D point clouds [86, 179]. These techniques are computationally expensive and time consuming. Despite these limitations, the segmented plants possess useful information for applications such as plant growth monitoring, plant phenotyping, and plant physiognomic analysis.

2.4 Initial Scene Rendering

3D objects or scenes can be described as a point cloud, voxel grid, or depth map.

2.4.1 Point Cloud

Generally, active techniques directly provide point cloud information following the data acquisition. The point clouds are uniformly sampled points on the described object's surface. In contrast, the point cloud density obtained using passive techniques will mainly depend on the object's surface features. The reason is that passive techniques often depend on searching corresponding points on numerous overlapped images. Feature-less areas of the object or plant are poorly represented in the point cloud. Also, these feature-less areas can provide false points because of feature mismatching if the scene has similar structures. In outdoor conditions, it is often noticed that if there is excess sunlight present in the scene during image acquisition, the plant's leaves saturate, with a resulting loss of information which can lead to an inaccurate or incomplete 3D model. In addition [127], any movement during the image acquisition process, for example from wind, results in poor scene representation.

Point clouds usually provide accurate surface topology information [190]. This makes it easier to precisely estimate the curvature or underlying surface information and calculate surface traits. For passive techniques, the quality of the point cloud largely depends on the number of images used as well as the plant architecture. Paturkar et al. [128] provided a detailed analytical study on selecting an appropriate number of images for 3D modeling. This can help to generate a precise point cloud using fewer images. Point clouds are appropriate for segmentation and further analysis of segmented point clouds is possible.

2.4.2 Voxel Grids

A 3D plant can also be described by a 3D array of cells, in which each cell (voxel) has one of two values, showing if the plant occupies a voxel or not. The most common techniques which result in a voxel grid representation are voxel colouring [168], space carving [85], generalised voxel colouring [31, 39], and shape-from-silhouette [6].

If the plant architecture is simple, these techniques are fast, easy to implement and generate accurate estimations. For instance, Kumar et al. [84] used shape-from-silhouette to reconstruct young corn and barley plants. Similarly, Golbach et al. [52] used the same technique to reconstruct tomato seedlings. In another study, Phattaralerphong et al. [142] also used shape-from-silhouette to achieve voxel grid representations of tree canopies. The goal of this study was to calculate features like

canopy volume, tree crown diameter, and tree height which usually do not need precise 3D representation. Kumar et al. [84] examined maize root volume using shape-from-silhouette. These studies were conducted on the plants in the early growth stages.

However, if the plant architecture is complex, e.g. heavy overlapping between plant organs, or very complex, one must use principle volumetric techniques. For instance, Klodt et al. [79] proposed a fast approach which searches a segmentation of the volume surrounded by the visual hull, by reducing the surface area of an object, based on the factor that the volume of the segmented object should be 90% of the volume surrounded by its visual hull. The authors applied their approach for 3D reconstruction of fully grown barley plants and obtained precise fine-scale features of the plant.

X-ray computed tomography (CT) and magnetic resonance imaging (MRI), generally used in medical imaging, can also be applied to the plant phenotyping domain. Studies show that these techniques have been used to visualise plant root systems [104, 112, 167, 45]. These techniques generate voxels that have intensity data, either describing the density for CT, or the ability of the material to absorb and emit radio frequency energy in the presence of a magnetic field for MRI (detecting hydrogen atoms associated with water molecules).

2.4.3 Depth Map

A depth map is nothing but a 2D image in which the value of every pixel shows the distance from the camera. It is also referred to as 2.5D imaging. In such descriptions, parts of a plant occluded by a projected surface are not calculated. 3D imaging techniques which provide a depth map as output are mainly stereo vision or other active techniques. Stereo vision calculates depth of the scene from a single viewing location by analysing the disparity between two images captured from slightly different positions.

Depth maps can be obtained of single plants, of which the leaves are flattened, have orientation perpendicular to the camera. Xia et al. [203] proposed implementing depth maps only to give a robust segmentation of individual leaves of bell pepper plants. In this scenario, 2D imaging has struggled to separate overlapping of leaves. Dornbusch et al. [35] utilised depth maps to inspect and analyse the daytime patterns of leaf hyponasty (which is an upward bending of leaves) in *Arabidopsis*. Chéné et al. [23] examined the implementation of depth maps for the calculation of plant traits such as leaf angle, leaf curvature, and leaf segmentation.

In a few studies, depth maps are used on canopies, where deriving complete 3D structure is unimportant. Muller-Linow et al. [117] and Ivanov et al. [72] used depth maps to estimate structural features of canopies from top-view stereo vision set-ups, in sugar beat and maize, respectively. Using a side-view stereo set-up, Baharav et al. [4] estimated plant height and stem width.

Depth maps can also be used for segmentation but keep in mind that segmentation of depth maps may struggle with occlusions. Depth maps can be augmented to a real 3D point cloud by capturing the 3D scene from various angles and directions with overlapping images. An iterative closest point algorithm [10] can be used to match point clouds from overlapping depth maps.

2.5 3D Model Processing

Preprocessing of 3D model involves several steps, namely background removal, outlier removal, denoising, and down-sampling.

2.5.1 Preprocessing

When working on a point cloud, background removal, outlier removal, denoising, and down-sampling are important steps in the processing. The generated point cloud often has parts of the surrounding scene and some erroneous points, which need to be carefully removed. Also, the primary size of the point cloud is often too large for processing in a feasible time and hence down-sampling may be required.

Background Removal

If the point cloud is generated using an active imaging technique, it usually does not include colour information. Additional efforts need to be taken to acquire as little of the surrounding area as possible. If the point cloud still holds some surrounding information, then the background can be removed via the detection of geometric structures like cylinders, planes, and cones which might correlate with the plant surface, the plant's stem or pot. Points can then be removed by considering their relative position to these features. The detection of these geometric structures is generally done using the RANSAC algorithm [44]. For instance, Garrido et al. [73] modelled maize plants using LiDARs firmly fixed on an autonomous vehicle and later used RANSAC to segment point clouds into plants and ground.

If the point cloud is generated using passive techniques, it often includes colour information as an RGB camera is used for image acquisition. This colour information can then be used for background removal. Efforts to control the lighting conditions during image acquisition will determine the reliability of simple colour-based thresholding, classification or clustering approaches to differentiate between background and plant. Jay et al. [79] proposed a clustering method based on both colour and height above the ground to differentiate between background points in the point cloud generated from structure-from-motion and a plant.

3D model processing is an important step when working on point clouds. Background removal from a point cloud generated using active imaging techniques is tedious and prone to error because of the lack of information about the background.

Outlier Removal

Two approaches are mainly used for outlier removal for point clouds: statistical and radius outlier removal. Statistical outlier removal uses the mean distance to the k-nearest neighbors. Points are discarded if the mean distance exceeds a particular threshold, depending on the global mean distance to the k-nearest neighbours and the standard deviation of mean distances.

Radius outlier removal calculates the number of neighboring points within a given radius and discards points that have fewer than a specified minimum number of neighbors. Both outlier removal approaches perform well on the point clouds, and the only limitation is that the user has to give input value of the radius and k-nearest neighbors.

Denoising

Before advancing to further analysis, it might be important to correct some irregularities such as noise and misaligned points in the data. Moving least squares repetitively project points on their neighborhoods' weighted least squares surface, requiring the newly sampled points to lie near an underlying surface [87].

Denoising using moving least squares is effectively eliminates the noise present in the point cloud. Even after applying outlier removal, there can still be some irregularity present in the point cloud, which can be removed using this approach.

Down-sampling

Primary point clouds may need to be down-sampled to process them in a shorter time. The most reliable down-sampling approach is the voxel-grid filter [69]. In this approach, the point cloud is arranged into a 3D voxel grid and points within every voxel are replaced by the centroid of all the points within that voxel.

Another approach that uses random sampling designed to retain important structures in the point cloud is the dart-throwing filter [26]. In this, points from the primary point cloud are successively added to the down-sampled point cloud if they do not possess neighbours within a fixed radius in the resultant point cloud.

However, down-sampling the point cloud may lose important information about the plant, particularly fine structures such as parts of the leaf or stem. Therefore, depending on the plant species, architecture, and quality of a 3D model, one should select the down-sampling rate. If it is not essential to down-sample the point cloud, one can simply skip this step.

2.5.2 Lower-level 3D Model Representation

For further analysis, it may be beneficial to convert the 3D depictions into the following lower-level representations:

Octree

An octree [110] is a tree-like representation of the data which repeatedly sub-divides a 3D space into eight octants, only if the parent octant has at most one point. This way, the expanding tree depths show the point cloud in increasing resolution. This representation can help overcome memory limitations when points must be scanned within a large point cloud. A key advantage is that little memory is used for empty areas. Also, the octree representation does not struggle with complex plant architecture. One disadvantage of an octree representation is that an object or scene can only be approximated and not fully represented. This is because the octree breaks everything down into smaller and smaller blocks.

There are multiple algorithms for skeletonization and clustering in the literature that use the octree data format that is also appropriate for plant phenotyping. SkelTre [17] and Campino [16] are examples of the skeletonization and clustering algorithms. Scharr et al. [164] proposed a method for voxel carving of maize and banana seedlings which provides an octree depiction as an output. Duan et al. [36] exploited octrees to separate wheat seedling's point clouds into initial groups of points; later, these initial groups were combined manually to correlate them with distinctive plant organs.

Polygon Mesh

This is a 3D depiction comprised of faces, edges, and vertices that describes an object's shape. Polygon meshes are formed from a point cloud using α-shape triangulation [40] or from voxels utilising the marching cubes algorithm [99]. Nonetheless, a precise voxel depiction or point cloud is essential to produce an accurate polygon mesh. The complex plant architecture makes the generation of polygon mesh of the whole plant difficult. However, the polygon mesh is conceptually simple. Generally, surface fitting is applied to various plant organs.

McCormick et al. [109] generated polygonal meshes acquired through laser scanning to measure leaf widths, lengths, angles, area, and shoot height in sorghum. Paproki et al. [126] also generated polygon meshes of cotton plants from multi-view stereo and applied phenotypic analysis based on this depiction. In this study, they measured individual leaves. Chaudhary et al. [22] constructed a polygon mesh of *Arabidopsis* plant using α-shape triangulation to find the volume and surface area of the plant.

Undirected Graph

This representation is a structure comprised of vertices linked by the edges. These edges are allocated weights corresponding with the distance between the connected points. The shortest path can be calculated using Dijkstra's algorithm [34], graph-based clustering, e.g. spectral clustering [76], and minimum spanning tree [146] which use undirected graphs as an input.

This undirected graph can be generated from a point cloud by linking neighboring points to the query point. These neighbors can be chosen using a particular radius r around the query point, or the k-nearest neighbors are selected. If r or k are selected very high, many redundant edges will be created, whereas important edges will be missed if r or k are very low. However, undirected graphs struggle with redundant edges. Therefore, it is important to select the correct values of r and k. Hetroy-Wheeler et al. [64] generated an undirected graph of various seedlings acquired using laser scanning. These undirected graphs are then used as a base for spectral clustering into plant organs. To prevent redundant edges and speed up the computation process while simultaneously not missing any important edges, they reduced the edges that contain neighbors within a particular radius r, depending on the angles between the edges.

2.6 3D Model Analysis

The following processing stages convert the original 3D model as preparation for further analysis. During these stages, supplementary information is obtained from the 3D model.

2.6.1 Segmentation

A critical and complex stage in extracting the plant trait measurements is the segmentation of the 3D model into distinctive plant traits. There is no standard method that can be applied because segmentation depends strongly on the quality of the 3D model and the particular plant architecture.

Point Cloud Surface Feature-based Segmentation:

Surface feature-based approaches exploit surface normals and extracted features as measures for classification or clustering. This can allow for classification between traits with various geometrical shapes, like straight stems, flat leaves or other geometries.

The point cloud consists of a set of points on a surface. The surface normals can be derived by executing an eigendecomposition or principal component analysis on the co-variance matrix of nearest-neighbours around the query point. The nearest-neighbours can be selected either by defining a particular radius r or the number of neighbours k. These two parameters must be selected carefully because if r or k are selected very small, the normal calculation will be noisy; in contrast, if these parameters are selected very large, too many points are included and edges between planar surfaces will be blurred.

1. **Saliency Features:** In a study conducted by Dey et al. [33] on yield estimation, saliency features, along with colour information, were used to segment the point clouds of grapevines generated using structure-from-motion (SfM) [171], into fruits, leaves, and branches. They estimated saliency features at three spatial scales and integrated colour in RGB to achieve a 12-dimensional feature vector for segmentation.

   In another study, Moriondo et al. [115] also used structure-from-motion to obtain point clouds of the canopy of olive trees. Using a random forest classifier, they exploited saliency at one spatial scale and colour information as features to segment the point cloud into leaves and stems. Li et al. [94] used surface curvatures to classify linear stems and flat leaves. They used Markov random fields to achieve a spatially understandable unsupervised binary classification.

2. **Point Feature Histograms:** Point feature histograms [160] and its more efficient version, fast point feature histograms [159], provide distinctive features of a point's neighborhood that can be used for matching. This approach relies on the angular relationships between pairs of points and their respective normals within a given radius r around each query point. This information, generally four angular features, are binned into a histogram, and then these histogram bins can be utilised as features in a classification or clustering method. The study by Paulus et al. [138] illustrates the difference in the PFHs between point clouds with various surface properties.

   PFHs rely on the approximate representation of the plant trait shapes and surfaces, mostly achieved using active 3D imaging techniques like LiDAR or laser scanning. PFHs have been exploited as features of point clouds of wheat, barley, and grapevine generated by laser scanning [138, 134, 197]. In a study on sorghum plants, Sodhi et al. [172] used less accurate point clouds derived from multi-view stereo and robustly segmented stems and leaves because the sorghum plant's traits are easily classified.

3. **Segmentation Post-processing:** Point cloud segmentation methods that depend on local features, e.g. surface feature-based techniques, generally result in inaccurate classifications. A standard post-processing stage to enhance the accuracy is implementing a fully connected pairwise conditional random field [83], which considers the spatial context to greatly enhance the results. Sodhi

et al. [172] and Dey et al. [33] used a conditional random field as a post-processing stage of segmentation using saliency features and PFHs, respectively. The outcome of this post-processing is shown in [173].

Graph-based Segmentation:

Spectral clustering is a group of clustering methods that considers connectivity between points in an undirected graph [103]. The points are projected onto a lower dimensional graph which maintains the distances between the connected points. After that, a common clustering method is applied on this graph.

While implementing the spectral dimension reduction on a graph of a plant, this plant should be identifiable in the lower dimensional graph, whereas other morphological traits of the plant will be suppressed. Bolrcheva et al. [13] and Hetroy-Wheeler et al. [64] used a similar approach to segment poplar plants' point cloud into stems and leaves. They were able to identify the branching structure of the lower dimensional graph, which corresponds to the plant traits in the original point cloud.

Voxel-based Segmentation:

Golbach et al. [52] used a shape-from-silhouette to generate a 3D voxel structure of tomato seedlings. A breath-first-flood-fill algorithm with a 26 connected neighborhood is used, which repeatedly fills the structure. The algorithm starts with a lowest point in the voxel structure, which is the bottom of the stem. As the algorithm passes through the stem, all neighboring points are close together. However, when the first leaves and branches appear, the distance of the newly added point increases. If the distance threshold exceeds a specified threshold, the iteration is terminated, and a new iteration is started. The threshold depends on the voxel resolution and plant architecture. Once the flood-fill is carried out, a leaf tip is detected as the last added point and consequently backtracks the flood-fill until the last point of the stem is reached.

In another study, Klodt and Cremers et al. [79] segmented the 3D voxel structures of barley into parts using the eigenvalues of the second-moment tensor of the surfaces. These give information of the gradient directions of the structure, and permits classification between flat, long, or structures without any direction. This method resulted in classification between the plant traits.

The following examples of voxel-based segmentation methods can be modified depending on the plant architectures [52, 79]. The first method which uses shape-from-silhouette to generate the voxel model and relies on the plants with rosette-like structure of narrow leaves. The second method exploits the opposite arrangement of the cotyledons of dicot seedlings. The main advantage of these highly modified methods is that they can be easily customized according to plant architecture.

Mesh-based Segmentation:

Based on polygonal meshes, there are two standard methods for segmentation. The first method is a region growing from seed points on the mesh surface, constrained by curvature changes that correspond with edges [169, 195]. The second method is fitting shape primitives e.g. spheres, cylinders, and planes [3].

Paproki et al. [126] used a hybrid segmentation approach that uses both methods on cotton plants- at first achieved a coarse mesh segmentation into individual leaves

and stem by using region growing. Then, detailed segmentation of the stem into petioles and internodes was achieved using cylinder fitting.

Nguyen et al. [118] looked at segmentation and measurements of dicotyl plant traits. For this, they used region growing constrained by curvature. Using this method, they measured leaf width, length, surface area, and perimeter.

Deep Learning-based Segmentation:

3D point cloud segmentation using deep-learning is a new field. Some general techniques exist, which can be divided into two classes. One class of techniques is point-based which directly works with unordered 3D point clouds. Networks such as SGPN [200], PointNet [147], PointNet++ [149], and 3DmFV [8] take the 3D point cloud as input and provide class labels for each point as output. However, these architectures are limited in the number of points in each model. If the size of the point cloud is large, there is no reliable solution for the network training and interface.

The other class of techniques is based on multiple views, which generates many 2D projections from the 3D point cloud. It then uses deep-learning based segmentation techniques on the produced 2D images, later connecting the various projections into a 3D point cloud segmentation. For example, SnapNet [14] was applied for semantic segmentation of a 3D model by producing a number of virtual geometry-encoded 2D RGB images of the 3D object. The predicted labels from the 2D images were then back-propagated to the 3D model to provide each point a label.

Shi et al. [170] proposed a plant trait segmentation approach using a multi-view camera system combined with deep-learning. This approach segments the 2D images and integrates the data from multiple viewpoints into a 3D point cloud of the plant. They used a Mask R-CNN architecture [62] for instance-segmentation and an FCN architecture [98] for semantic-segmentation. A new 3D voting system was then proposed for segmenting the plant's 3D point cloud. However, the performance of this approach was unsatisfactory. The reason is that deep-learning methods require a lot of ground-truth training data, which is time-consuming and cumbersome. This field needs further exploration in the context of plant phenotyping.

2.6.2 Skeletonization

Skeletonization thins a shape to simplify and highlight its topological and geometrical properties, such as branching of the stem or leaf, which are important for calculating phenotypic features. Plenty of methods has been introduced to produce curve skeletons. Methods exploit various theoretical frameworks, e.g. medial axes or topological thinning. The outcome of skeletonization is generally a set of points or voxels which are connected to form an undirected graph, on which further analysis can be conducted.

A plethora of studies has proposed methods to structure the 3D model of plants by skeletonization for phenotyping or computer graphics. In Mei et al. [111] and Livny et al. [97], LiDAR was used to generate point clouds of trees and skeletonization was performed on these point clouds, not to generate a precise 3D representation of the trees, but to produce models of trees with convincing visual appearance for computer graphics.

Cote et al. [29] generated 3D models of pine trees using skeletonization to achieve realistic models to study transmitted and reflected light signatures of trees, incorporating the results into a 3D radiative transfer model. In this study, the aim was not to

achieve the phenotypic measurements of the trees but to study the radiative properties related to the tree canopy structure. They produced credible tree canopy structures from a skeleton frame describing the branches and trunk. The skeletonization approach applied to build this structural frame is comparatively easy and it uses the Dijkstra's algorithm employed on an undirected graph [194]. Delagrange et al. [32] proposed a software tool (PypeTree) to extract the skeleton of trees using the same skeletonization approach but with more editing functionality.

In another study, Bucksch et al. [17] proposed a skeletonization method using the direction the point cloud traverses through octree cell sides. They assessed their method by comparing the dispersions of skeleton branch lengths and manually calculating branch lengths with good results [15]. This method is fast but does not work well on varying point densities and is less applicable to plants different from the leafless trees which they examined.

The 3D analysis of the branching architecture of root systems is an additional application that has been addressed by skeletonization. Clark et al. [25] proposed a software tool for the 3D modeling and analysis of the roots. In this study, the thinning method is executed on the voxel representation generated using shape-from-silhouette.

Regardless of its efficiency for the calculation of certain plant features, skeletonization has barely been used for phenotyping of leafy vegetables. The reason is that skeletonization struggles with diverse topographies, complex plant architectures, and with heavy occlusions. Chaivivatrakul et al. [20] developed an axis-based skeletonization method for simple plant architectures, such as young corn plants, to extract leaf angle measurements. However, they assessed that their skeletonization algorithm did not perform well when compared to plane fitting.

2.6.3 Surface Fitting

When working with point clouds, surface fitting can be helpful for segmentation and also can serve as a prior stage before plant trait measurement. The fit can be based on geometric structures such as planes, cylinders, and flexible structures like non-uniform rational B-splines (NURBS) [182].

Non-uniform Rational Basis Splines:

NURBS are mathematical models commonly used for producing and representing smooth surfaces and curves in computer graphics. A NURBS surface is defined by a list of 3D coordinates of surface points and related weights. Wang et al. [201] explains various fitting methods of NURBS. NURBS surfaces and curves can be triangulated and the surface area is estimated by adding up the areas of each triangle.

NURBS have been used for the calculation of leaf surface area in several works: Gerald et al. [48, 49] used structure-from-motion to generate point clouds of sunflowers and fitted NURBS to segmented leaves after the stem was extracted and discarded using cylinder fitting. Santos et al. [162, 163] also used structure-from-motion to produce point clouds of soya beans and then segmented the 3D point cloud using spectral clustering. After that, they fitted NURBS surfaces to the segments related to leaves. In another study, Chaivivatrakul et al. [20] fitted NURBS surfaces to a set of points corresponding to corn leaves.

Cylinder Fitting:

Usually, plant stems can be locally described as a cylinder. A cylinder fitting method using least-squares fitting is explained in Pfeifer et al. [141]. Paulus et al. [134] used laser scanning to generate point clouds of barley. Point feature histograms were used to segment the 3D point clouds, and then cylinders were fitted to the stems to measure stem height.

However, the stem doesn't need to always be straight; it can also be curved. Gerald et al. [49] addressed this issue by developing an alternative method in which they propagated a radius along the stem of the plant with normal constraints to structure the stem as a curled tube. Nonetheless, the results were not accurate.

2.6.4 Key Takeaways

The 3D model analysis is a complex stage because it mainly depends on the plant architecture. Different analysis methods can be used for different architectures, and not all methods are applicable for a given plant architecture. Skeletonization is good for the overall structure but is not appliable for 2D structures such as leaves. Skeletonization and surface fitting work well on less complex architectures but struggle with heavy occlusion. Segmentation methods performed well on the complex and less complex plant architectures and have been widely used. Deep learning-based segmentation methods have shown potential but require huge ground-truth data to train the model.

2.7 Plant Traits to Consider for Growth Monitoring and Extraction of the Traits

After the complex stages of segmentation, surface fitting, and skeletonization, plant trait measurement of either single plant organs or the whole plant is comparatively easy, and various approaches may provide accurate estimates.

2.7.1 Individual Plant Trait Measurements:

1. **Leaf Measurements:** A mesh is the most natural description for estimating leaf dimensions. Leaf area can be easily calculated as the sum of triangular polygon mesh faces [83, 48, 49]. Leaf length can be estimated by calculating the shortest path on the mesh represented as a graph. Sodhi et al. [83, 173] calculated leaf width by determining a minimum area enclosing rectangle around a leaf point cloud and then measuring the shortest dimension of the enclosing rectangle.

   Golbach et al. [52] extracted the leaf measurements of tomato seedlings from a voxel description to reduce computing time. For leaf length, they considered the distance between the two points on the leaf surface which are farthest away from each other. For leaf width, they scanned for the highest leaf width perpendicular to the leaf midrib. For leaf area, they considered an approximation based on the number of surface voxels. The authors used simple calculations and traded precision for fast computation. When leaves are curled, it can be difficult to measure the leaf precisely.

2. **Fruit or Ear Volumes:** Plant yield is calculated by the estimated plant fruits or ears volume. For instance, Paulus et al. [138] determined that kernel weight, number of kernels, and ear weight in wheat plants was correlated with ear

volume, which they measured by calculating α-shape volumes on the point clouds representing the ears.

3. **Stem Measurements:** Cylinder fitting or curve skeletons can estimate the inter-node length and stem height. Paulus et al. [138] extracted stem height by fitting a cylinder to the stems. Golbach et al. [52] exploited the voxel skeleton corresponding to the stem of tomato plant seedlings.

   The inter-node length can be calculated by estimating the shortest distance between the branch points by considering the skeleton graph. This was developed by Balfer et al. [5] on grape clusters which was first skeletonized by using a technique introduced by Livny et al. [97]. Stem width can be calculated by cylinder fitting. Sodhi et al. [83, 173] fitted a cylinder shape to a segmented point cloud of corn plants to derive the stem diameters.

   However, similar to leaf measurements, stem measurements are difficult when the stem is not straight. Cylinder fitting is not applicable in this case. Therefore, a robust stem measurement method is required, which can work on curved stems as well.

2.7.2 Whole Plant Measurements:

1. **Height:** Point cloud height can be defined as the maximum distance between points corresponding to a plant projected on the vertical axis. This method was used by Nguyen et al. [120] for cucumber seedlings and cabbage and Paulus et al. [85] for sugar beet. Height can also be estimated from a top-view depth map which is the difference between the closest pixel in the image and the ground plane [23].

2. **Volume and Area:** 3D meshes are mostly used to estimate plant volume and area in the case of point cloud representations. By using Heron's formula, the surface area of a mesh can be calculated by summing up the area of its triangular mesh faces. The mesh volume can also be estimated by using the technique proposed in [206], which first calculates the features for each elementary shape and then adds up all the mesh values.

   If the plant model is represented as an octree or voxel grid, the plant volume can be calculated by summing up the volumes of all voxels covering the plant, as proposed by Scharr et al. [164]. However, this method has shown some inaccuracies in the measurements because of the discrete nature of voxels. If the representation is derived from space carving, then occlusion and concavities will also cause inaccuracies.

3. **Convex Hull:** This is defined as the shape of a plant that is formed by connecting its outermost points. The volume of the convex hull is an excellent indicator of plant size. In the root systems, it is very helpful for indication of the soil exploration [185]. Estimation of the convex hull of plant's point clouds needs minimum pre-processing to remove outliers but gives very crude estimation. Rose et al. [155] estimated the convex hull of a tomato plant's point cloud, and the convex hull was calculated on root systems by Topp et al. [185], Mairhover et al. [104], and Clark et al. [25].

4. **Number of Leaves:** Once the voxel representations or point clouds are segmented to classify between stem and leaves, the number of connected components can be used to derive the number of leaves, only after the conversion of leaf points into a graph if point cloud is used.

   In some cases, such as in monocot plants, leaves are elongated and not always different from the stem. However, a precise segmentation of stems and leaves is not required if leaf counting is the only goal. For instance, Klodt and Cremers [79] classified between only the outer part of leaves and the stem by analysing the gradient direction of a 3D model. This was enough to count the number of leaves.

   Another way to count the number of leaves for elongated leaves is to count the number of leaf tips, which are usually described by the endpoints of the plant's skeleton. However, care must be taken for plants with jagged leaves to avoid many false tips.

2.7.3 Canopy-based Measurements:

3D imaging techniques may not give sufficient information to calculate individual plant traits when used on a larger field. The important information can still be estimated on the level of a tree or plant canopies. These traits consist of leaf area index, leaf angle distribution, or canopy height.

1. **Leaf Angle Distribution:** 3D imaging techniques allow examining patterns of leaf orientation, which is a very dynamic feature that varies with change in the environment. Biskup et al. [11] proposed a top-view stereo imaging set-up method. The depth maps were segmented using graph-based segmentation [43] to achieve a crude segmentation of leaves. After that, planes were fitted to each and every segment based on RANSAC to get leaf inclination angles. Muller-Linow et al. [117] proposed a software tool to study leaf angles in plant canopies based on similar methods.

2. **Canopy Profiling:** LiDAR can penetrate tree or plant canopies; therefore, in LiDAR, the laser interception frequency by a canopy can be considered an index of foliage area. In ecological research on forest stands [123, 90], this canopy profiling by airborne LiDAR has been mostly employed. In a study by Hosoi and Omasa et al. [68], they used a set-up of LiDAR and mirror to estimate vertical plant area density of a rice canopy at various growth stages. Their approach used a voxel representation of canopy to calculate leaf area density [123]. The leaf area index also can be extracted from the vertical integration of leaf area density.

   Cabrera et al. [18] used a voxel model of corn plants to examine the light interception of corn plant species by building virtual canopies of corn. In these virtual canopies, the average leaf angles and cumulative leaf area were estimated using the 3D models of the individual plants.

2.8 Plant Growth

Several studies have reported techniques to determine plant growth. In a study by Zhang et al. [207] on potato plants, the plant's number of leaves, leaf area, and plant height was measured for five months. The ground truth for plant height and leaf was

collected using 2D image analysis. The number of leaves was counted manually. The correlation between measured values and ground truth shows a good estimation for plant height, number of leaves, and leaf area with R^2=0.97.

In another study, Li et al. [93] estimated the biomass for individual plant organs and aboveground biomass of rice using terrestrial laser scanning (TLS) for an entire growing season. The field experiments were conducted in 2017 and 2018, providing two different datasets. Three different regression models, random forest (RF), linear mixed-effects (LME), and stepwise multiple linear regression (SMLR), were calculated to estimate biomass with data gathered at multiple growth stages of rice. The models have calibrated with the 2017 dataset and validated on the 2018 dataset. The results show that SMLR was suitable for biomass estimation at pre-heading stages, and the LME model performed well across all growth stages, especially at the post-heading stage. In addition, the combination of TLS and LME is a promising method to monitor rice biomass at post-heading stages. Friedli et al. [46] measured canopy height growth of maize, soybean, and wheat by terrestrial laser scanning (TLS) over a period of 4 months, with ground measurements taken 1 to 3 times a day. A high correlation (R^2) between ground truth and TLS-measured canopy was achieved for wheat.

Reji et al. [152] demonstrated the potential of 3D TLS for the estimation of the crown area, the biomass of vegetable crops, and plant height at various growth stages. Three vegetable crops were considered in this study: eggplant, cabbage, and tomato. LiDAR point clouds were collected using a TLS at different growth stages for five months. Validation with ground truth illustrates a high correlation for plant height R^2=0.96, crown area R^2=0.82, and combined use of crown area and plant height helped estimate biomass with correlation R^2=0.92 for all the three crops throughout the growth stages. In a study by Guo et al. [57], plant height was measured as a function of the scanning position, a number of scanning sites, and scan step angle were evaluated in the field of the growth stages of wheat. The results demonstrated that TLS with H_{95} can be an alternative to assess crops like wheat during an entire growth stage, and the height at which TLS can precisely detect wheat was 0.18 m.

Han et al. [59] determined the growth of maize for three months. Plant height, canopy cover, normalized difference vegetation index (NDVI),the average growth rate of plant height (AGRPH), and the contribution rate of plant height (CRPH) traits were extracted and evaluated. A time series data clustering method called typical curve was proposed to evaluate these traits. The system performed well with the accuracy of the traits ranging from 59% to 82.3%.

Itakura et al. [71] observed changes in chlorophyll content of eggplants for five days under water stress conditions with images captured once a day. The chlorophyll was measured using a spectrometer (Jasco V570). A regression method is used to estimate the correlation between the points in the 3D model and ground truth, and a high correlation was achieved with R^2=0.81. Paturkar et al. [129] determined the plant growth over one month. Eight manual readings and images were captured twice a week over this period. The ground truth of plant height is measured using a ruler, leaf area was measured using *ImageJ*, and the number of leaves was counted manually by moving around the plant. The correlation between the ground truth values and measured values demonstrates a strong estimation of leaf area, plant height, and the number of leaves with R^2=0.98.

2.8.1 Key Takeaways

The plant growth is determined over a specific period of time based on the plant type. Various ground truth readings and measured values from 3D models or surface models are collected over this time period. This time series data is then correlated using a regression model. R^2 is the most common metric used in the literature to assess performance. However, other metrics can also be used along with R^2, such as mean average percentage error (MAPE) and root mean squared error (RMSE).

2.9 Current Challenges and Research Directions

The literature shows that passive techniques, especially structure-from-motion, appear to be the most promising method for 3D acquisition because of their high point cloud resolution at a lower cost. SfM can be used for plant growth monitoring applications because of its economic and non-destructive nature. However, there are a few challenges that need to be addressed, such as:

1. **Illumination Effects:** Passive techniques, to be specific, SfM gives a good quality point cloud [129]. However, changes in the illumination while capturing the plant images can result in missing information such as blank patches in the 3D model of the plant surface and leaves. Active illumination techniques are more immune to changes in ambient lighting, although sensors can be swamped by strong sunlight.

2. **Movement due to Wind:** Because of plant displacement in two consecutive images due to wind, there can be many feature matching errors resulting in a poor 3D model. The resulting 3D model will have important missing details in the stem area of the plant with some half reconstructed leaves. Techniques which use only single images or capture multiple images simultaneously (e.g. stereo) are less sensitive to wind, although longer exposure times can result in motion blur.

3. **Computational Time:** Active techniques give a point cloud rapidly, but not all sensors contain colour information. However, using passive techniques, such as SfM, requires a certain number of images to reconstruct the plant in 3D. The computation cost of a reconstructed 3D model largely depends on the number of input images and the selection of the views. It is not necessary that every image will contribute equally to the overall quality of a 3D model. It is difficult to select the number of images because generating an accurate plant model with a limited number of images is difficult. Although the computation time is less, fewer images can generate false points in the 3D point cloud because of the larger change between images. In contrast, a large number of images will process redundant information which will inevitably increase computation time [128]. To get an appropriate number of images for precise 3D reconstruction, prior information or manual measurements of plants are required to compare to the corresponding measurements from the 3D model. Therefore, there is a need to find a way to get an appropriate number of images for precise 3D reconstruction and thus to reduce the computation time.

4. **Robust Segmentation:** There is no standard method that can be applied for segmentation because of the wide variations in plant architecture. There is a need for a robust segmentation method that can work on most plant architectures.

5. **Robust Plant Trait Measurements:** As discussed earlier, naturally, plant leaves and stems can curl, and because of this, not all approaches will provide accurate results. Cylinder fitting will be optimal if the stem is straight to calculate stem height. Calculating internode distance will not be sufficient to measure leaf length and width if the leaf is curled. Therefore, there is a need for a robust measurement approach that could be applied on curly and straight leaves and stems.

One domain in which more progress can be expected for 3D plant monitoring, especially for plant trait segmentation, is neural networks. The fundamental obstacle to using neural networks in plant monitoring applications is the requirement of large ground-truth training data. Manual segmentation of plant images is time consuming, prone to error, and tedious. To date, a limited number of benchmark databases for plant phenotyping with labels have been published publicly [30, 113, 188]. With more benchmark databases for 3D plant phenotyping being made publicly available, the neural network will pursue its success in other domains.

Neural networks can also be used in 3D: 3D convolutional neural networks can deal with voxel grids, while numerous neural network architectures are developed to deal with point clouds [147, 149, 55, 213, 148].

2.10 Summary

This chapter conducted a comprehensive survey of the acquisition techniques, possible representations and analysis techniques as applied to 3D plant physiognomic analysis and identified the open issues and future directions. This chapter also investigated and discussed the current studies where researchers have proposed promising techniques and applications for segmentation and clustering plants. Furthermore, we have also discussed the various plant traits to consider for plant physiognomic analysis. These plant traits can be at the plant organ level or canopy level. Some exciting technological advancements, such as the use of deep learning algorithms, are also discussed in this chapter with their current disadvantages.

MASSEY UNIVERSITY
TE KUNENGA KI PŪREHUROA
UNIVERSITY OF NEW ZEALAND

GRADUATE RESEARCH SCHOOL

STATEMENT OF CONTRIBUTION
DOCTORATE WITH PUBLICATIONS/MANUSCRIPTS

We, the candidate and the candidate's Primary Supervisor, certify that all co-authors have consented to their work being included in the thesis and they have accepted the candidate's contribution as indicated below in the *Statement of Originality*.

Name of candidate:	Abhipray Paturkar
Name/title of Primary Supervisor:	Professor Gourab Sen Gupta
In which chapter is the manuscript /published work:	Chapter 3

Please select one of the following three options:

(●) The manuscript/published work is published or in press

- Please provide the full reference of the Research Output:

A. Paturkar, G. Sen Gupta and D. Bailey, "Non-destructive and cost-effective 3D plant growth monitoring system in outdoor conditions." Multimedia Tools and Applications, vol 79, no. 47, pp. 34955, 2020.

( ) The manuscript is currently under review for publication – please indicate:

- The name of the journal:

- The percentage of the manuscript/published work that was contributed by the candidate: 90.00

- Describe the contribution that the candidate has made to the manuscript/published work:

Experimental setup, data acquisition, data processing, methodology development, data analysis, manuscript writing, figure generation.

( ) It is intended that the manuscript will be published, but it has not yet been submitted to a journal

Candidate's Signature:	Abhipray Paturkar Digitally signed by Abhipray Paturkar Date: 2022.03.09 13:23:22 +13'00'
Date:	09-Mar-2022
Primary Supervisor's Signature:	Gourab Sen Gupta Digitally signed by Gourab Sen Gupta DN: cn=Gourab Sen Gupta, c=NZ, o=Massey University, ou=School of Food and Advanced Technology, email=g.sengupta@massey.ac.nz Date: 2022.03.10 10:37:32 +13'00'
Date:	10-Mar-2022

This form should appear at the end of each thesis chapter/section/appendix submitted as a manuscript/ publication or collected as an appendix at the end of the thesis.

MASSEY UNIVERSITY
TE KUNENGA KI PŪREHUROA
UNIVERSITY OF NEW ZEALAND

GRADUATE RESEARCH SCHOOL

STATEMENT OF CONTRIBUTION
DOCTORATE WITH PUBLICATIONS/MANUSCRIPTS

We, the candidate and the candidate's Primary Supervisor, certify that all co-authors have consented to their work being included in the thesis and they have accepted the candidate's contribution as indicated below in the *Statement of Originality*.

Name of candidate:	Abhipray Paturkar
Name/title of Primary Supervisor:	Professor Gourab Sen Gupta
In which chapter is the manuscript /published work:	Chapter 3

Please select one of the following three options:

(●) The manuscript/published work is published or in press

- Please provide the full reference of the Research Output:

A. Paturkar, G. Sen Gupta and D. Bailey, "3D reconstruction of plants under outdoor conditions using image-based computer vision." In International Conference on Recent Trends in Image Processing and Pattern Recognition, pp. 284-297. Springer, Singapore, 2018.

( ) The manuscript is currently under review for publication – please indicate:

- The name of the journal:

- The percentage of the manuscript/published work that was contributed by the candidate: 90.00

- Describe the contribution that the candidate has made to the manuscript/published work:

Experimental setup, data acquisition, data processing, methodology development, data analysis, figure generation, manuscript writing.

( ) It is intended that the manuscript will be published, but it has not yet been submitted to a journal

Candidate's Signature:	Abhipray Paturkar Digitally signed by Abhipray Paturkar Date: 2022.03.09 13:21:11 +13'00'
Date:	09-Mar-2022
Primary Supervisor's Signature:	Gourab Sen Gupta Digitally signed by Gourab Sen Gupta DN: cn=Gourab Sen Gupta, c=NZ, o=Massey University, ou=School of Food and Advanced Technology, email=g.sengupta@massey.ac.nz Date: 2022.03.10 10:38:18 +13'00'
Date:	10-Mar-2022

This form should appear at the end of each thesis chapter/section/appendix submitted as a manuscript/ publication or collected as an appendix at the end of the thesis.

Chapter 3

3D Reconstruction of Plants using Smartphone's Camera in Outdoor Conditions

This chapter demonstrates the proposed easy and cost-effective set-up for 3D reconstruction of plant models and discusses the effects of adverse outdoor scenarios. The work in this chapter was initially published in a book chapter and subsequently expanded in a journal version as follows:

1. A. Paturkar, G. Sen Gupta and D. Bailey, "3D reconstruction of plants under outdoor conditions using image-based computer vision." *In International Conference on Recent Trends in Image Processing and Pattern Recognition*, Communications in Computer and Information Science, vol. 1037, pp. 284-297. Springer, Singapore, 2018. DOI: 10.1007/978-981-13-9187-3_25

2. A. Paturkar, G. Sen Gupta and D. Bailey, "Non-destructive and cost-effective 3D plant growth monitoring system in outdoor conditions." *Multimedia Tools and Applications*, vol 79, no. 47, pp. 34955-34971, 2020. DOI: 10.1007/s11042-020-08854-1

3.1 Introduction

Building a 3D model is extremely useful for many practical applications where inferring measurements about the shape or size of an object is a requirement. In biological science, building 3D models can help analyse different properties of objects. For example, building a 3D model of a plant can be useful in plant phenotyping, an important aspect of precision agriculture. It helps scientists and researchers collect valuable information regarding plant structure, which is inevitably a basic requirement to enhance plant discrimination and selection [114]. 3D models of the plant help evaluate plant growth and yield over time, which permits management of the plant to be more extensive [92]. 3D plant models could be used to describe leaf features, discriminate between weed and crop, estimate the plant's biomass, and for growth monitoring.

3.1.1 Overview of 3D Reconstruction Techniques

With the rapid acceleration of hardware capability in terms of CPU power, storage and 3D scanners, we can now capture huge amounts of data, and the fidelity

FIGURE 3.1: Testing site

of the resultant models is constrained by the quality of merging/reconstruction algorithms. Due to recent advancements of imaging technologies, building semi-automated or automated systems is becoming possible for plant science and agricultural applications, where a major task is to build a 3D model of the plant to analyse different biological properties (like growth, etc.). As discussed in chapter 2, cutting-edge and non-destructive technologies have great potential to revolutionize phenotyping capabilities. However, they often come at a cost, and each technique has some merits and demerits [130]. Depending on the requirements of the experiment, there can be low-cost alternatives to high-end, high resolution instruments, such as using a smartphone camera to capture the images instead of using a high-resolution single lens reflex camera, or a Kinect gaming sensor can be used to measure crop architecture features [210].

3.1.2 Research Contribution

To address the problem of expensive and destructive sensors, we propose using a smartphone's rear camera to capture the images and later use computer vision methods to stitch the images together to form a 3D model. The idea behind using a smartphone camera is that most people have a smartphone with good camera specifications nowadays.

The advantages of using a smart-phone camera over expensive laser scanning sensors are: it does not need a bulky set-up to capture the plant data, it is easy to use, the user needs no prior training, it is highly flexible and can be moved anywhere around the plant, and most importantly it is cost-effective. This allows us to capture plant images from multiple viewpoints. This chapter describes the proposed setup and discusses the effects of adverse outdoor scenarios.

3.2 Methods and Materials

3.2.1 Testing Site

We had access to a polyhouse located in Hokowhitu, Palmerston North, New Zealand in 1000-square-feet area for this research. Figure 3.1 shows the polyhouse and the working area.

3.2.2 Types of Plant

In this research, we selected five types of plants, namely, chilli, cauliflower, lettuce, maize, and tomato. These are high-value plants, with some having consistent demand throughout the year in the New Zealand market. In addition, these would also allow us to test the proposed system on a variety of different plant architectures (complex recursive structures). We considered five samples for each plant to ensure the system's robustness. This gave a variety of plant architectures to work with and test the framework.

3.2.3 Plant Settings

Plants were planted in a row with a distance of 90cm in between plants. This is because our study aimed at modelling individual plants. As a result, other plants did not hinder the development of the model, and only one plant was monitored at a time.

3.2.4 Imaging Sensor

In this research, we captured the plant images using Apple iPhone 6s+, which uses a Sony RGBW IMX315 sensor with 12-megapixel camera, $f/2.2$ aperture, focal length of 29mm (standard), sensor size of 1/3", pixel size of 1.22 μm, auto image stabilization, and backside illumination sensor which helps to perform better in low-light.

3.2.5 Image Acquisition Scheme

Images were taken under outdoor conditions. The images were captured sequentially following a circular path with respect to the plant axis. Seven to ten such paths were followed at various angles, heights and distances from the plant. At least 15 images were captured on each path by revolving around the plant with a mobile phone's rear camera, capturing at every 10° to 15° of the perimeter. The distance between plant and camera was not kept constant. The camera positions were chosen to ensure that the plant was entirely in the field of view, and the images were of good quality (not blurred etc.). The image acquisition process produced more than 100 images with 95% overlap between successive images. This gives us a variety of images to work with. The image acquisition scheme and samples of the captured images with different view angles of the chilli plant are shown in figures 3.2 and 3.3, respectively.

3.2.6 Number of Samples Generated

As mentioned in section 3.2.2, 5 plants of each species were monitored, with each plant captured 9 times over a 4 week period. This produced 9 point clouds of each sample to work with. In total, we generated 225 point clouds at various growth stages for 5 plants with 5 samples each. This gave us a variety of plant architectures to work with and to test our methods.

We also performed non-destructive manual (ground truth) measurements of the plant features while we captured the plant images. For the physical estimation of the number of leaves, we simply counted manually, and for leaf area, we took images of the leaves against a white background without plucking them and used ImageJ [2] to calculate leaf area during the growth period. We selected a ruler scale to measure the plant height, leaf length, and leaf width manually.

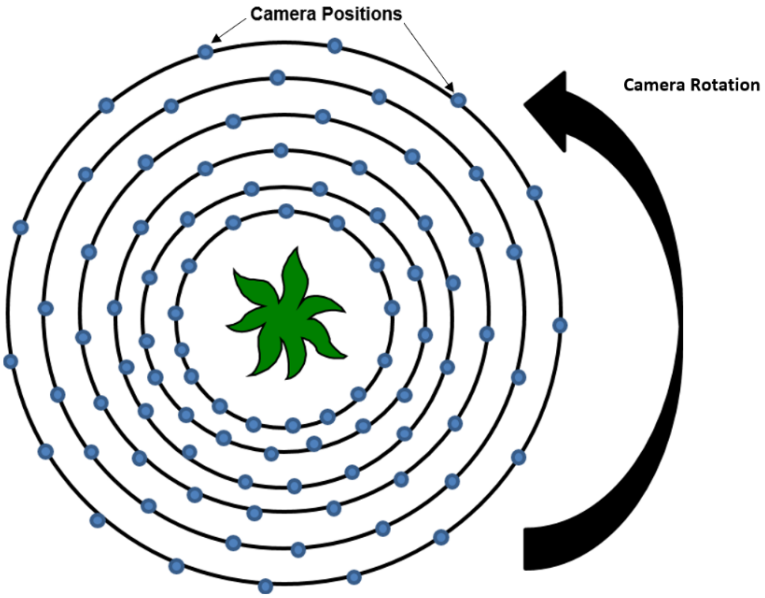

FIGURE 3.2: Illustration of image acquisition scheme

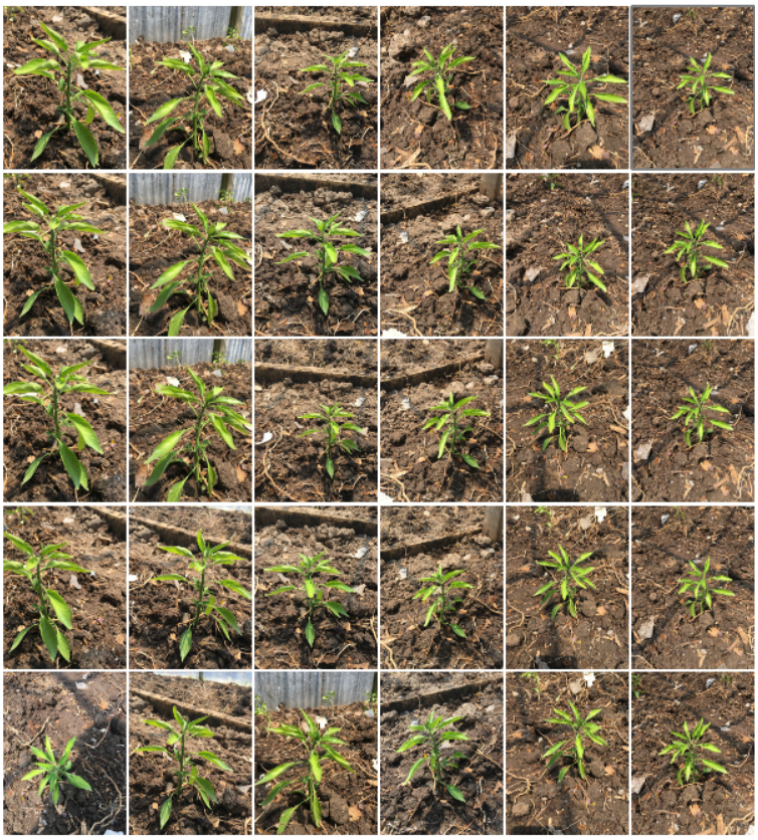

FIGURE 3.3: A sample of the captured images with different view angles and distances of a chilli plant

3.2.7 Structure-from-Motion Work-flow

The key issue that SfM addresses is the identification of the 3D location of the matching features in numerous images captured from various heights, angles, and distances. SfM is a widely used technique for 3D reconstruction [122], [19], [89], [187], [107].

First, distinctive keypoints on the plant must be found in each image. The matching of these keypoints from one view to another enables a 3D model to be constructed. The scale-invariant feature transform (SIFT) [101] is used for this because the resulting keypoints are invariant to image scaling, rotation, change in illumination, and translation. The important steps in SIFT are as follows:

1. **Scale-space extrema detection:** The primary step of SIFT searches over all image locations and scales using a difference-of-Gaussian function to detect promising keypoints that are orientation and scale invariant.
2. **Localisation of keypoints:** Keypoints are filtered to remove those with poor stability. Stability is a measure of the sensitivity of keypoints to changes in position and scale.
3. **Orientation assignment to the keypoints:** The orientation of every keypoint is determined from local image gradient directions. These are calculated based on the detected scale to give scale invariance.
4. **Keypoint descriptor:** The pattern of local image gradients at the chosen scale in each keypoint area is used to form a (hopefully unique) descriptor. Gradients provide invariance to changes in illumination and are relatively insensitive to shape distortion.
5. **Keypoint matching:** These keypoints are matched between pairs of images acquired from various angles and views. Bundle adjustment is used to form a sparse 3D point cloud of the plant and simultaneously retrieve camera positions and intrinsic parameters.

3D Reconstruction

VisualSFM [196] is used to generate 3D point clouds of the plants. VisualSFM uses a combination of SfM and multi-view stereo to generate the 3D models.

Post-Processing

Once a sparse 3D model is generated, it is then filtered. Significant outliers and artefacts (e.g. erroneous peaks and troughs resulting from keypoint descriptor mismatches) and any unnecessarily reconstructed surrounding topography are manually removed at this stage. Later, the estimated camera parameters, orientations, and positions are used to build a dense 3D point cloud. Here, we used a cross-correlation matching approach. A pixel in one image is matched with the corresponding pixel in the next image on the epipolar line for an overlapped image pair [165]. This process is repeated for every pair of images considering that the keypoint's estimated position is less noisy.

Finally, the free open source software *Meshlab* [24] is used for post-processing. The unstructured dense 3D models are remeshed and filtered to reduce geometric

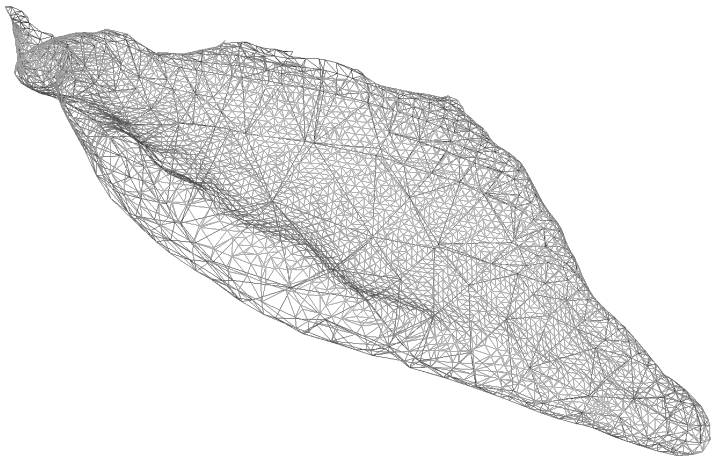

FIGURE 3.4: Leaf mesh consisting different sizes of triangular polygons

complexity. Once we generate a structured 3D model after filtering, mesh generation and texturing is done. This mesh consists of different sizes of triangular polygons (see fig. 3.4). The polygonal mesh is a combination of edges, faces, and vertices that define the plant's size and shape. There are several methods for building a polygonal mesh model, but the method by Kazhdan et al. [154] called Poisson surface reconstruction is widely used to get a polygonal mesh of the plant from the point cloud because of its efficiency. Then, a mesh optimization step is performed (this optimises the point distribution) to achieve a clean triangulated mesh. In order to recover the visible texture from the plant images, firstly, the mesh is parametrised to determine which camera view has the best view of each face of the model. These views give the best texture of the plants to produce a texture map. This texture map consists of texture for each face from one image. A detailed 3D model is generated using the developed texture map. This reconstructed 3D model is later used to extract the different plant growth and structure parameters such as plant height, leaf length, leaf width, number of leaves, and leaf area.

3.3 Results

3.3.1 3D Reconstruction of Chilli Plant

To illustrate this method for generating the 3D model, here we demonstrate results only for the chilli plant. The process of 3D modeling generates a sparse point cloud. Fig 3.5 shows a sparse point cloud of a chilli plant with 143,706 points in the point cloud. A dense point cloud is achieved after removing noise from the sparse point cloud and performing detailed correspondence matching. Fig. 3.6 shows the corresponding dense point cloud with 855,624 points. The dense point cloud is more accurate than the sparse point cloud. Fig. 3.6 shows the high quality reconstructed 3D model of the chilli plant from different views.

3.3.2 3D Reconstruction of all the Plants

The range of plants we considered for this research has a variety of architecture complexity which is defined as the amount of occlusion the plant has, the formation

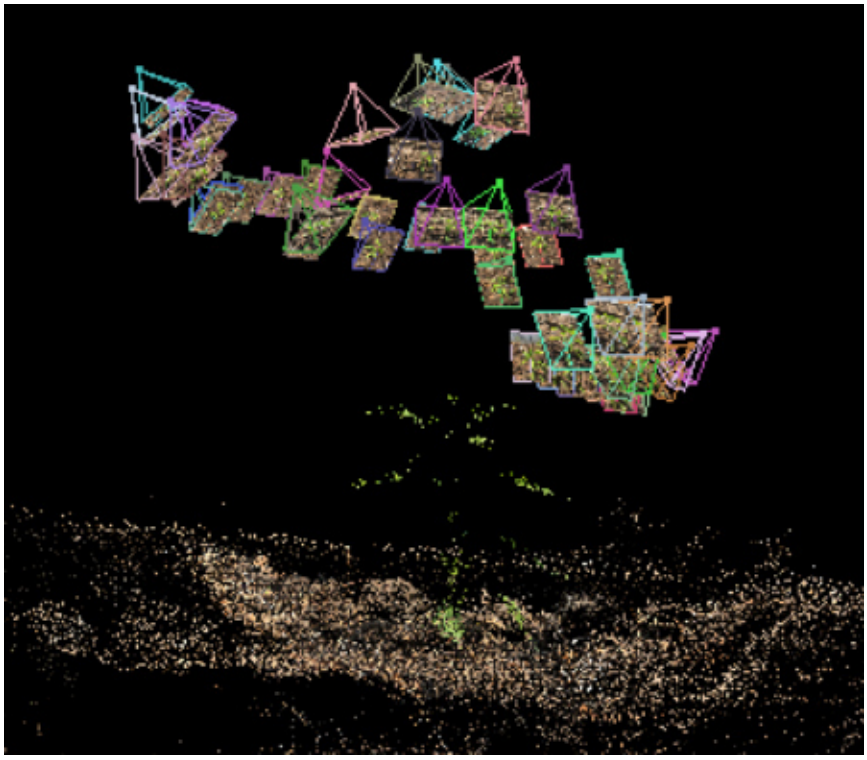

FIGURE 3.5: Sparse 3D point cloud of the plant. The triangles in the image represent the viewpoint of the plant

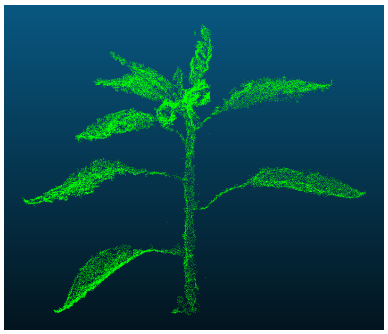

(A) 3D model (Side View)

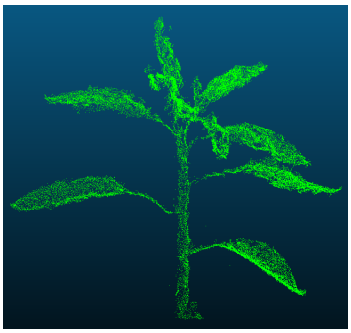

(B) 3D model (Side View)

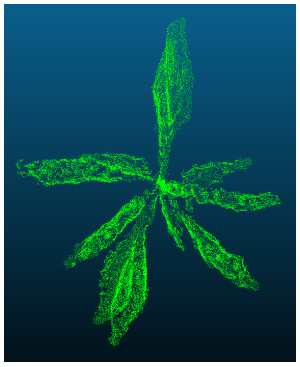

(C) 3D model (Top View)

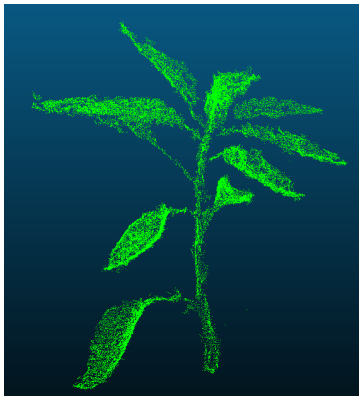

(D) 3D model (Side View)

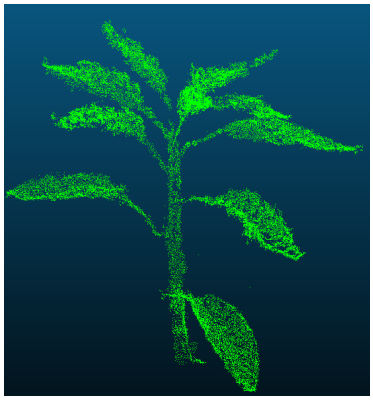

(E) 3D model (Side View)

FIGURE 3.6: 3D Models of chilli plant

of leaves (some plants have curly leaves and some have straight), and the growth stage. Figures 3.7 to 3.11 shows 3D reconstructed models at different growth stages of tomato, cauliflower, lettuce, chilli, and maize plants. The number of images used to reconstruct these 3D models has varied from 20 images to 90 images depending on the growth stage and plant type. Similarly, the number of points in the point cloud and computation time to process these images also differ based on the plant architecture's complexity (growth stage and plant type). More complex architectures, more images to generate a 3D model; hence an increase in computation time.

The tomato plants have a less complex architecture in the initial vegetative growth stage. However, the tiny fern-like structure on the plant makes the architecture complex in the advanced vegetative growth stage. This can be seen in fig 3.7, where there is distortion in the 3D model due to these ferns. In addition, the occlusion of leaves also makes the plant architecture complex. The cauliflower plants have relatively simple architecture during the initial vegetative growth stage. However, it gets complex in the advanced vegetative stage because of the occlusion of leaves (see fig 3.8). The lettuce plants have curly leaves with heavy occlusion right from the initial vegetative stage. Due to the occlusion in the advanced growth stage, the 3D models do not generate an exact plant geometry (see fig 3.9). In contrast, chilli plants have a relatively easy architecture compared to other plants, and the leaves have less occlusion in all growth stages. The complexity of maize plants varies because the leaves sometimes stick to each other, making it difficult for precise 3D modeling.

After visually comparing our reconstructed 3D plant model with the actual plant, all the leaves and stems of the actual plants are reconstructed according to the described 3D model. During the reconstruction process, the position of a few points in the point cloud are situated marginally lower or higher than adjacent points in the model. These points do not reconstruct any actual characteristics of the plant. In essence, we have a variety of plants with different levels of architecture complexity to work with.

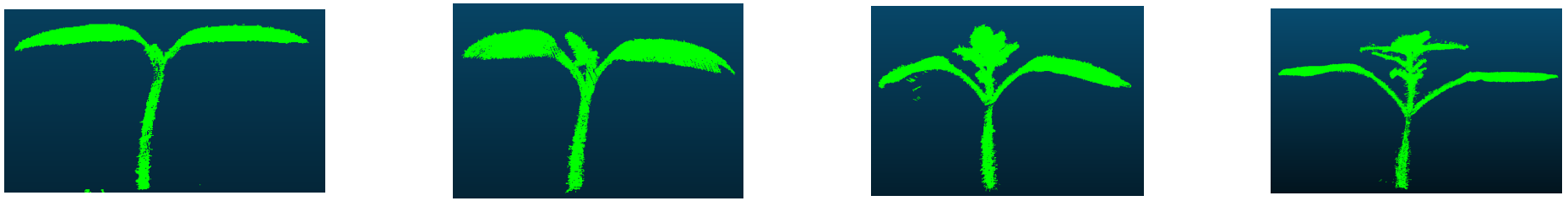

FIGURE 3.7: 3D models of tomato plant at different growth stages

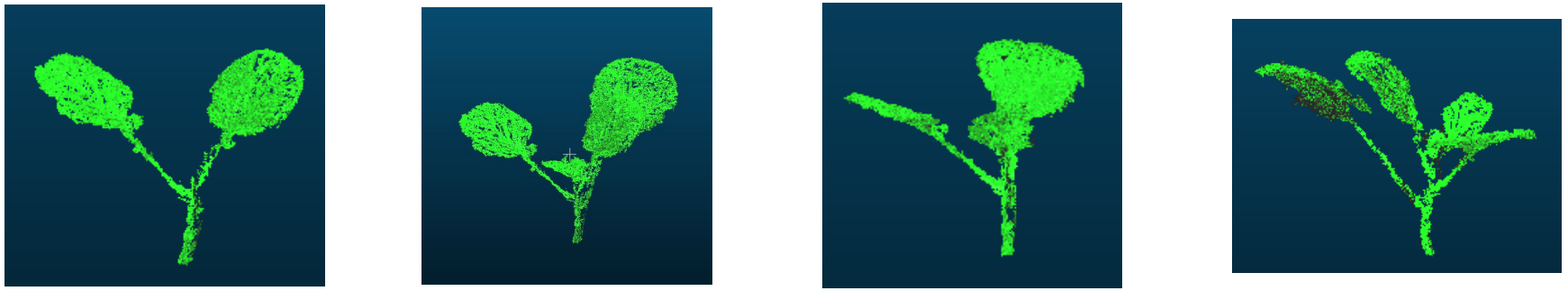

FIGURE 3.8: 3D models of cauliflower plant at different growth stages

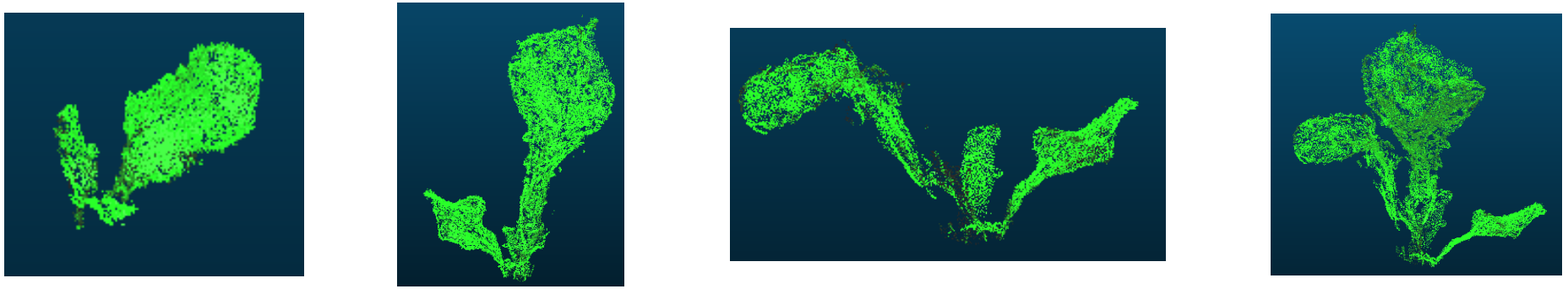

FIGURE 3.9: 3D models of lettuce plant at different growth stages

FIGURE 3.10: 3D models of chilli plant at different growth stages

FIGURE 3.11: 3D models of maize plant at different growth stages

TABLE 3.1: Mean squared error for stem height and number of leaves

Plant	Mean Squared Error	
	Stem height (cm)	Number of leaves
Tomato	0.09	0
Cauliflower	0.08	0
Lettuce	0.1	0.5
Chilli	0.09	0
Maize	0.02	0

3.3.3 Quality Assessment of the 3D Models

To assess the quality of the generated 3D models, features extracted from the model are compared with ground truth data (manually measured values of the actual plant). Two plant features: stem height and number of leaves, are extracted from the 3D model. The stem height is calculated by calculating the distance between the marked point on the stem tip and bottom in the reconstructed 3D model. These points are selected visually by the user. Fig 3.12 shows the marked points on the plant and the distance between the marked points. Similarly, the number of leaves can be estimated by zooming and rotating the reconstructed 3D model manually by the user.

Fig 3.13 compares measurements from the model with the ground truth during the growth stages for each plant variety. Only one sample for each plant species is shown. For instance, fig. 3.13 (A) shows that the height of the chilli plant grew from 5 cm to 31 cm during the measurement period. Table 3.1 shows excellent agreement between manual stem height measurement and the measured stem height from the 3D model. Similarly, the tomato, cauliflower, and maize plants have shown excellent relation between manual height measurement and the measured height. However, the lettuce plant differs between the manual and measured stem height because of the more complex architecture. Because of the high degree of occlusion, measuring the stem height in the reconstructed 3D model is difficult. The plant height growth change is more complex than other growth parameters. This is because the plant height depends on different factors, e.g. light competition, wind speed, and so on [127]. Fig. 3.14 (A) represents the number of leaves produced during the growth period of the chilli plant increased from 3 to 11 leaves. It also clearly shows how close the manual and measured measurements are. Similar results were achieved for the tomato, cauliflower, and maize plants. However, the lettuce plant results were less promising as it is difficult to reconstruct the heavily occluded plant, and therefore, it failed to reconstruct some of the inner leaves accurately.

3.3.4 Discussion

The image acquisition process was conducted manually with a user capturing images by a smartphone's camera without using a tripod, making this process easy, economical, and adaptable. The SfM algorithm automatically estimates the intrinsic camera parameters, saving time by avoiding the need to calibrate the camera separately. The time required for image acquisition is 2-3 min and this time increases with the plant's growth as more images are required. The invested time per plant for post-processing takes 10-12 minutes for generation of the point cloud, 7-12 minutes for removing outliers and filtering. The proposed 3D reconstruction system is a cost-effective approach as we are using a smartphone's camera, a standard SfM

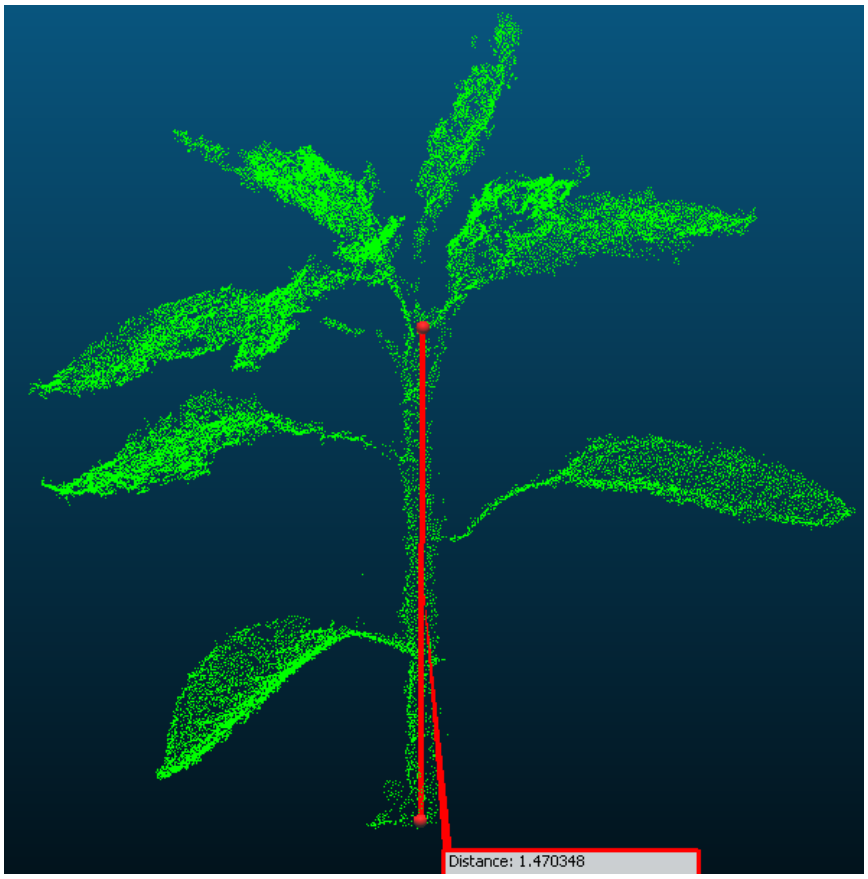

FIGURE 3.12: The approximate calculation of stem height from the reconstructed 3D model

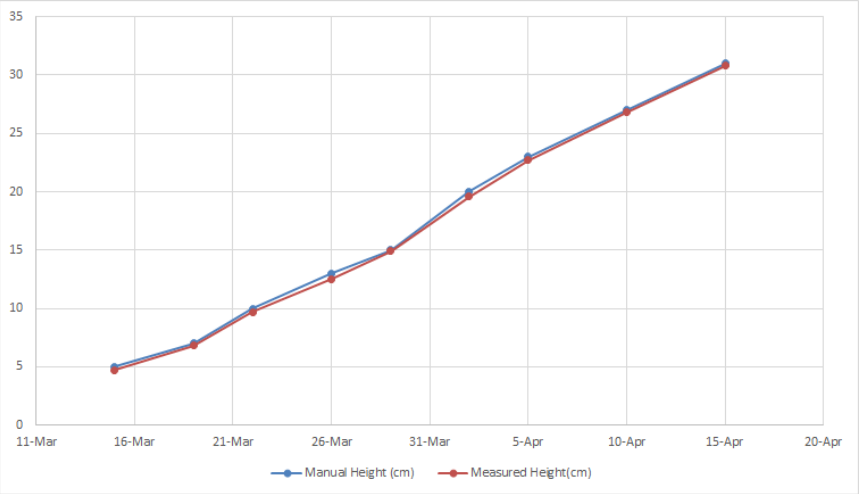

(A) Chilli plant stem height (cm)

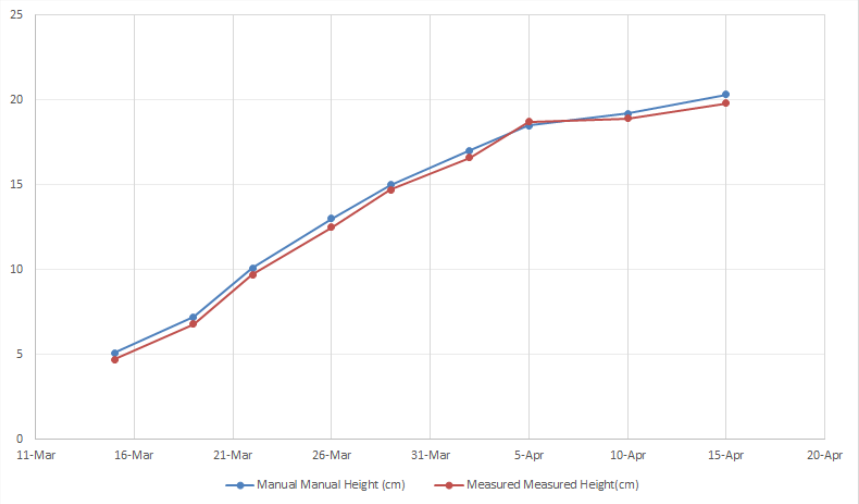

(B) Tomato plant stem height (cm)

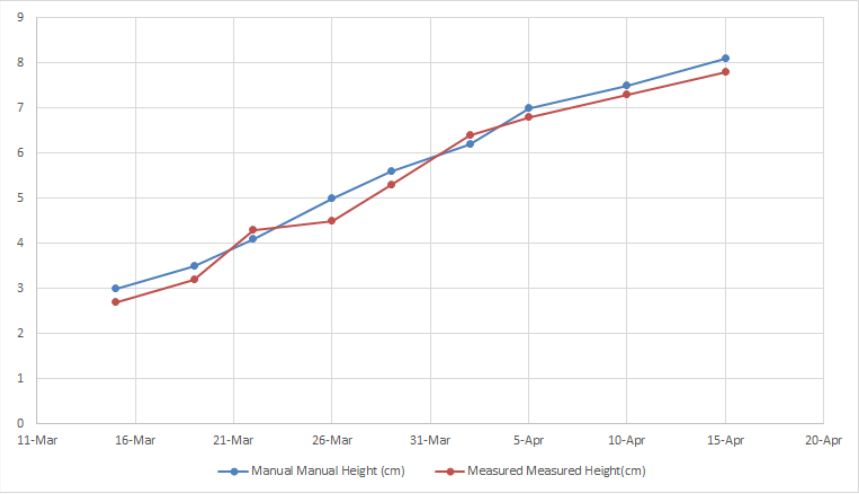

(C) Cauliflower plant stem height (cm)

FIGURE 3.13: Comparison of manual and measured measurements of the plants

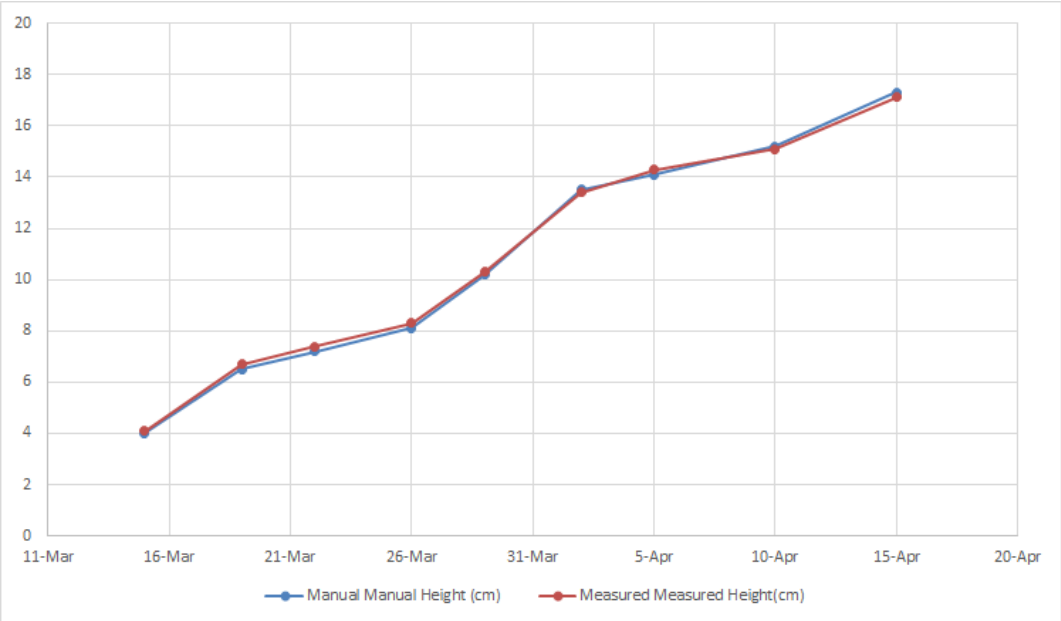

(D) Maize plant stem height (cm)

FIGURE 3.13: Comparison of manual and measured steam height measurements of the plants

algorithm to model the plants in 3D, and open source point cloud software is used to process the point cloud, which makes this system cost-effective. In comparison, the commercial software Pix4DMapper for processing the images and point clouds used in [155] is expensive, around $7200, and a camera used in [208] costs around $2000. Laser scanning systems (LiDAR) costs around $111k.

The quality of the generated 3D models has been assessed. All the plants except lettuce were reconstructed in 3D, which shows that the proposed system has the potential to replace the expensive sensors for the image acquisition process. The reason that the lettuce plant was not reconstructed accurately is due to its complex architecture. Because of the heavy occlusion of leaves, it is difficult to reconstruct the lettuce plant's inner leaves, which is a limitation of an image-based computer vision technique. However, more work needs to be done on the reconstruction of high-value lettuce plants as few studies considered this plant when working on the reconstruction of plants in 3D.

In general, the quality of the 3D model depends on the number of images used for 3D reconstruction. However, more images require more computation time to process the 3D model. Therefore, it is very important to develop a method to determine the appropriate number of images required for a good quality 3D reconstruction [21],[82].

In addition, based on our outdoor experimentations, we identified some scenarios that still cause problems and need more attention. When it is windy, the displacement of the plant due to wind gives many feature matching errors resulting in a poor 3D model. One possible solution for this is to detect inconsistent matches between the images because of the wind and filter those images from the set used to construct the 3D model. The resulting 3D model was missing important details in the stem area of the plant with some half reconstructed leaves.

To conclude, this study demonstrated that our proposed system has the potential to reconstruct the plants in 3D in outdoor conditions. The image acquisition process

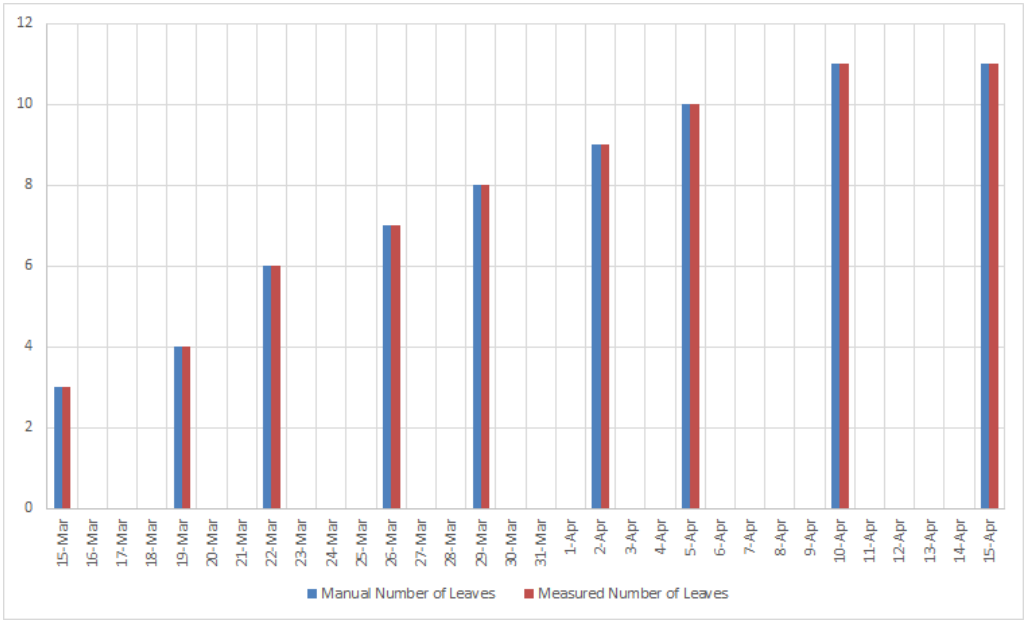

(A) Chilli plant number of leaves

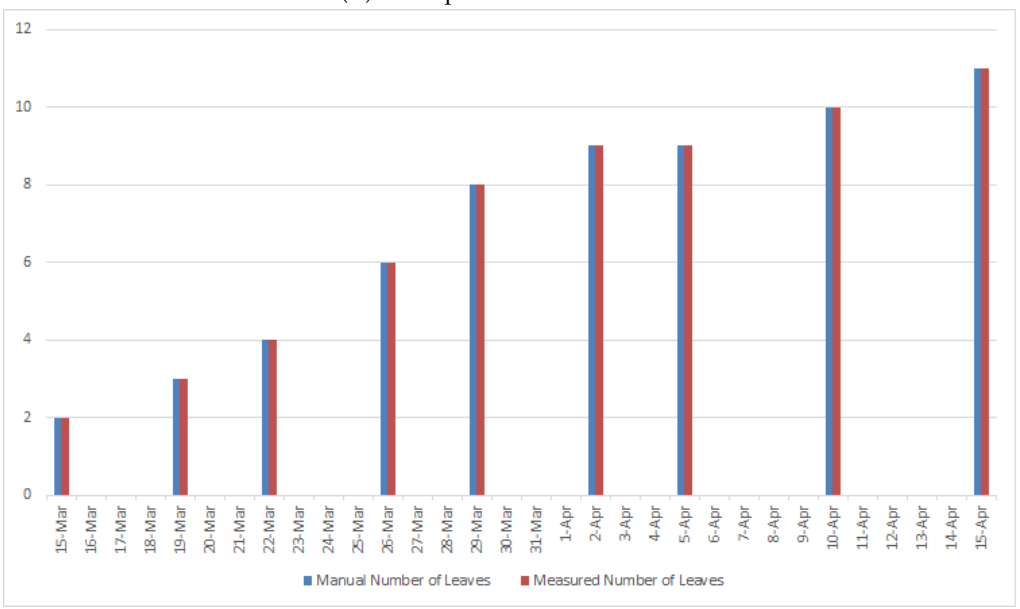

(B) Tomato plant number of leaves

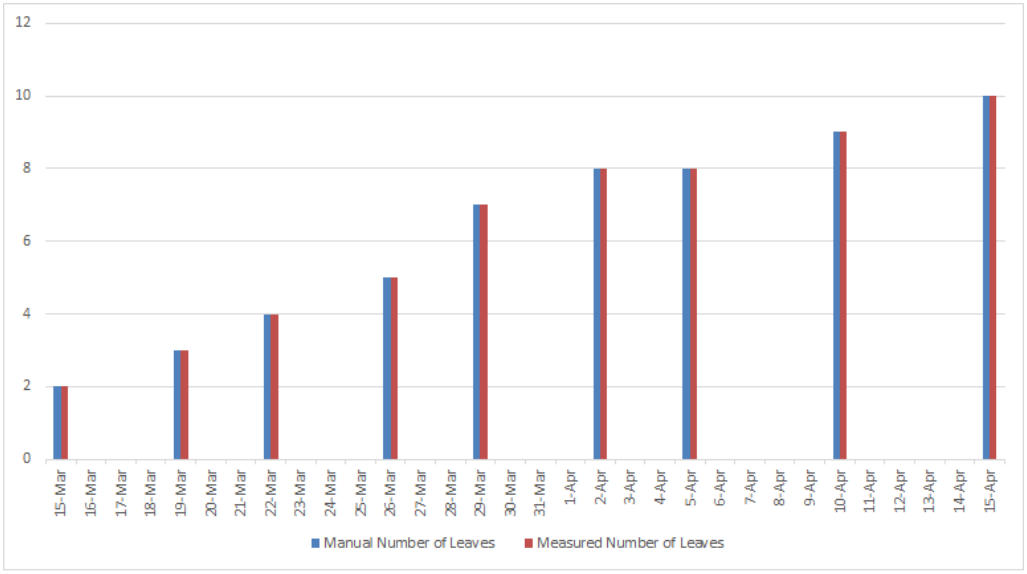

(C) Cauliflower plant number of leaves

FIGURE 3.14: Comparison of manual and measured measurements of the plants

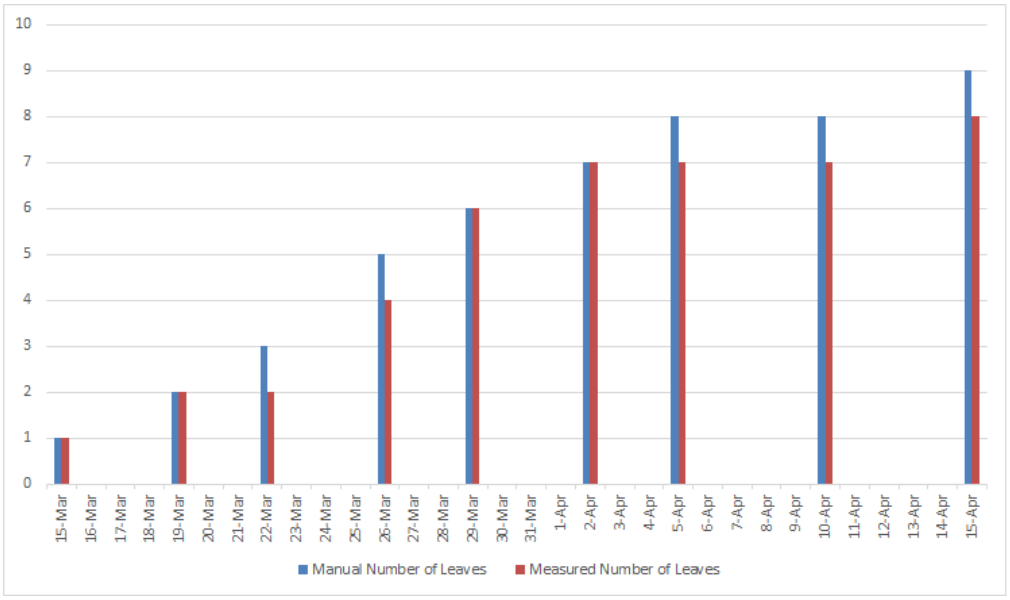

(D) Lettuce plant number of leaves

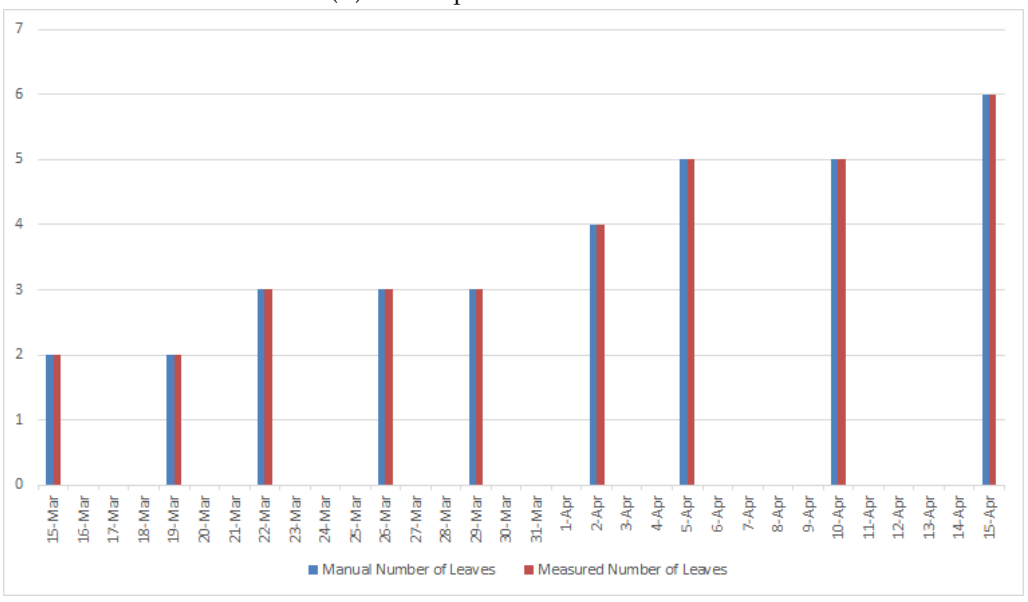

(E) Maize plant number of leaves

FIGURE 3.14: Comparison of manual and measured measurements of the plants(cont.)

is simple and cost-effective and does not require expert knowledge. Hence, this system is an appropriate alternative to costly state-of-the-art systems.

MASSEY UNIVERSITY
TE KUNENGA KI PŪREHUROA
UNIVERSITY OF NEW ZEALAND

GRADUATE RESEARCH SCHOOL

STATEMENT OF CONTRIBUTION
DOCTORATE WITH PUBLICATIONS/MANUSCRIPTS

We, the candidate and the candidate's Primary Supervisor, certify that all co-authors have consented to their work being included in the thesis and they have accepted the candidate's contribution as indicated below in the *Statement of Originality*.

Name of candidate:	Abhipray Paturkar
Name/title of Primary Supervisor:	Professor Gourab Sen Gupta
In which chapter is the manuscript /published work:	Chapter 4

Please select one of the following three options:

(●) The manuscript/published work is published or in press

- Please provide the full reference of the Research Output:

A. Paturkar, G. Sen Gupta and D. Bailey, "Effect on Quality of 3D Model of Plant with Change in Number and Resolution of Images Used: An Investigation." In Advances in Signal and Data Processing, pp. 377-388. Springer, Singapore, 2021.

( ) The manuscript is currently under review for publication – please indicate:

- The name of the journal:

- The percentage of the manuscript/published work that was contributed by the candidate: 90.00

- Describe the contribution that the candidate has made to the manuscript/published work:

Methodology development, data processing, data analysis, manuscript writing, figure and table generation.

( ) It is intended that the manuscript will be published, but it has not yet been submitted to a journal

Candidate's Signature:	Abhipray Paturkar Digitally signed by Abhipray Paturkar Date: 2022.03.09 13:26:35 +13'00'
Date:	09-Mar-2022
Primary Supervisor's Signature:	Gourab Sen Gupta Digitally signed by Gourab Sen Gupta DN: cn=Gourab Sen Gupta, c=NZ, o=Massey University, ou=School of Food and Advanced Technology, email=g.sengupta@massey.ac.nz Date: 2022.03.10 10:38:47 +13'00'
Date:	10-Mar-2022

This form should appear at the end of each thesis chapter/section/appendix submitted as a manuscript/ publication or collected as an appendix at the end of the thesis.

Chapter 4

Reducing Computation Cost for Accurate 3D Modelling

This chapter investigates the effect on 3D models of different parameters. This investigation enables an appropriate number of input images and resolution of the images to be determined for a precise 3D model. This work resulted in the following book chapter:

1. A. Paturkar, G. Sen Gupta and D. Bailey, "Effect on Quality of 3D Model of Plant with Change in Number and Resolution of Images Used: An Investigation." *In Advances in Signal and Data Processing*, Lecture Notes in Electrical Engineering, vol. 703, pp. 377-388. Springer, Singapore, 2021. DOI: 10.1007/978-981-15-8391-9_28

4.1 Introduction

Precise reconstruction of an object from multiple images is an ongoing problem. In the past few years, advancements in reconstruction techniques have been made. However, these techniques have been applied to simpler objects e.g. human faces, vases, buildings, or round objects. Objects with more complex architectures, such as plants, pose more challenges and issues to precisely reconstruct in 3D. Complex architectures are subject to significant occlusion, where a leaf is not visible from the current view, and the parallax effect, where plant appearance differs from view to view, makes reconstructing plants more difficult than convex objects. Reconstruction of plants is difficult because of high self-occlusion, the presence of many leaves, shiny surfaces, and texture-loss in some camera views, making feature matching more difficult. In addition, plants are very sensitive to changes in the environment, from small changes such as foliage reorganisation to life-long growth patterns.

Consequently, plants have a complex architecture that changes over time, making it complicated to reconstruct, especially by fixed, standard camera phenotyping systems. To reduce this complication and contribute to the solution of this problem, we proposed an easy and cost-effective 3D plant reconstruction system in the previous chapter. However, we determined that some more parameters need attention to reconstruct a precise 3D model, such as the number of input images used for reconstruction and the resolution of the images. The computation time and quality of a reconstructed 3D model largely depend on the number of input images and the selection of the views. It is not necessary that every image will contribute equally to the overall quality of a 3D model. It is difficult to select the number of images because it is difficult to generate an accurate plant model with a limited number of images. Because of matching errors, fewer images might generate false points in the 3D point cloud. In contrast, a large number of images will result in processing

redundant information, which will inevitably increase computation time [70, 95]. To determine an appropriate number of images for precise 3D reconstruction, prior information or manual measurements of plants are required to compare to the corresponding measurements from the 3D model.

Clearly, there is a need to consider the number of input images and their resolution for the reconstruction process. These parameters have not yet been discussed in this area of plant phenotyping. In this work, we investigate these two parameters.

4.1.1 Overview of Structure-from-motion

Structure from motion is widely used for the 3D reconstruction of plants in the literature. SfM uses a single camera to capture the images. SfM automatically calculates the intrinsic and extrinsic camera parameters, which saves time. However, the computation time and quality of the 3D model depend on the number of images used to generate the 3D model. Therefore, it is important to know what is the appropriate number of input images to generate accurate 3D models in less computation time. However, many studies use SfM for the 3D reconstruction of plants [150, 178], only a couple of studies look at the change in the number of input images used for 3D modeling. Rossi et al. [156] looked at the change of input images as well as resolution. However, only single set of images with different resolution was used. Various plant traits such as plant height, branch height, stem diameter, and leaf area were measured to assess quality of reconstructed point cloud. Only three plants were considered in this study. Zhou et al. [212] considered changed in number of images to analyse the effect on reconstructed point cloud. However, only single plant was considered in this study. Some of the studies mentioned the need to develop a method to get an appropriate number of images [95], [96], [121], [166]. Clearly, there is a need of a robust method to analyse the effects on reconstructed point cloud with change in input images and resolution.

After the successful generation of 3D models of various plants at different growth stages, in this chapter, we investigate reducing the computing cost for accurate 3D modeling using an appropriate number of input images.

4.1.2 Research Contribution

This chapter proposes a robust method to reconstruct the 3D model using limited input images and resolution. The contributions are 1. To analyse the effect of using a different number of input images on extracted plant features, such as stem height and number leaves in 3D using images of five different plants, each at five different growth stages. These extracted 3D values are compared to manual measurements to determine an appropriate number of images for reconstruction. 2. To analyse the effect of image resolution on the quality of the 3D data.

4.1.3 Materials and Methods

Computer Platform and Software

We used a personal computer (Intel Core i5-4570 CPU at 3.20 GHz and 8GB RAM). To generate the 3D models, VisualSFM [196] is used.

TABLE 4.1: Total number of captured images for each plant in the advanced vegetative growth stage

Plant	Total number of captured images
Tomato	93
Cauliflower	96
Chilli	90
Lettuce	84
Maize	68

Dataset

For this experiment, we used the same image dataset as chapter 3. We considered the image dataset for the plants in the advanced vegetative growth stage because the plant architecture is complex in this stage compared to the early growth stage. In addition, early growth stage plants require fewer input images for reconstruction and, therefore, less computation time.

The total number of images captured is different for each plant species in their respective advanced vegetative growth stages. Table 4.1 shows the number of images available for each plant.

Investigating Parameters

This investigation considers two different parameters which have not been discussed yet in the literature. For illustration, the results for a chilli plant in the advanced vegetative growth stage are shown here. The results of other plants are provided in Appendix A.

1. **Change in the number of input images for 3D modeling:** The 3D modeling method explained in chapter 3 will be repeated on different subsets of randomly selected images for a particular set of input images. The size of the subset for this chilli plant is varied from 25 images through to 78 images. The experiment is repeated five times for each subset size, selecting a different random subset. The quality of the reconstructed 3D model was determined by comparing the features extracted from the model with ground truth data (manually measured values of the actual plant). Plant features, such as stem height and the number of leaves were extracted. By exploring the correlation of extracted features with ground truth values, the number of images required to accurately reconstruct the chilli plant was determined.

2. **Change in image resolution:** Once the appropriate number of images for reconstruction is determined, the effects of image resolution on the 3D data was analysed. This will provide information about the best image resolution for the reconstruction of the chilli plant.

4.1.4 Measurement of plant features from the reconstructed 3D model

Two plant features: stem height and number of leaves, are extracted manually from the 3D model. The stem height is calculated by the method explained in chapter 3. Similarly, the number of leaves can be estimated by zooming and rotating the reconstructed 3D model manually by the user.

(A) All 90 images (B) 78 images (C) 65 images

(D) 50 images (E) 35 images (F) 25 images

FIGURE 4.1: Example 3D reconstructions of a chilli plant with different numbers of input images

4.1.5 Results and Discussion

3D Modeling

For illustration purposes, here, the result of only one plant is discussed. The results for other plants are provided in Appendix A. Detailed 3D modeling was performed as described in chapter 3. The experiment uses five different subsets of randomly selected images from the set of input images. Using from 5 to 20 input images give poor 3D models. A small number of images do not cover enough plant views to provide sufficient images for an accurate reconstruction. The quality of the 3D model is directly proportional to the number of views and images [95]. Fig 4.1 (A) shows a reconstructed 3D model using all 90 captured images. This model has replicated the actual plant very well when compared visually.

Fig. 4.1 (B) shows the 3D model derived from 78 images. While there are some differences with fig. 4.1 (A), these are minor. With fewer images, some details start to get lost, such as leaf stalks and the stem. Consequently, features of the plant derived from the 3D model become less accurate. As leaves become disconnected from the stem, fig. 4.1 (D), the number of leaves decreases, and as the stem becomes more broken (fig. 4.1 (D) to 4.1 (F)), the measured stem height decreases. With fewer images, the number of points detected on the leaf surfaces decreases, distorting the shape and size of the leaves.

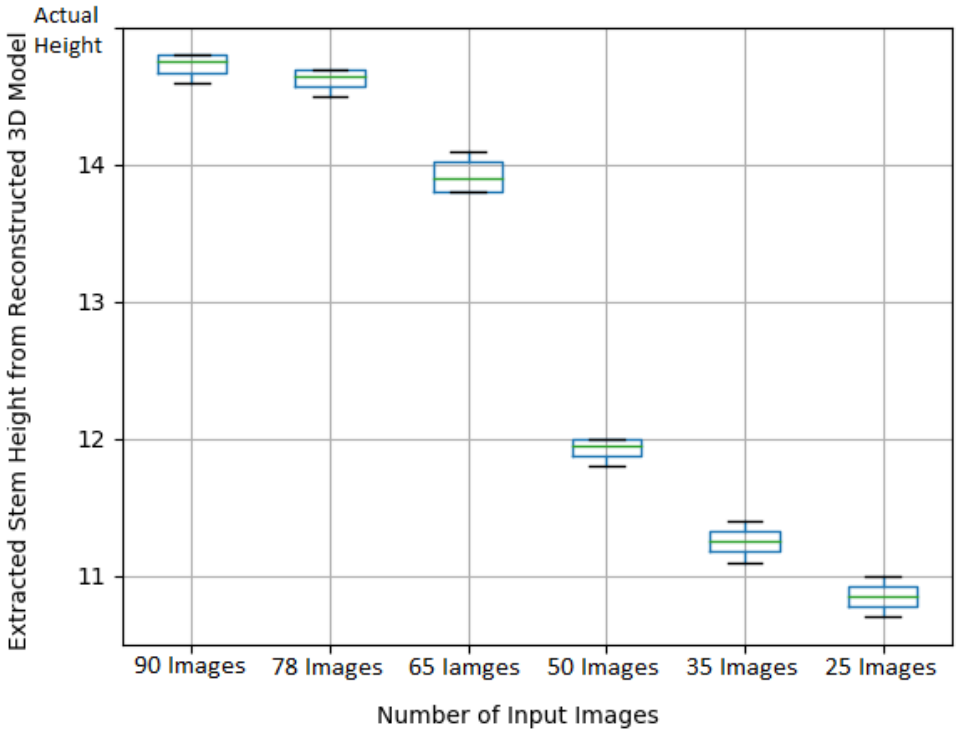

FIGURE 4.2: Extracted stem height from reconstructed 3D model with change in number of input images for chilli plant

4.1.6 Investigation Parameters

Change in number of input images for 3D modeling

For each subset size, the median, range, and interquartile range are represented by a box-whisker-plot. This clearly shows the variations from different random selections (see fig. 4.2), and gives a clear idea of the accuracy of the extracted stem height for different subsets of input images. Similarly, fig. 4.3 shows the number of leaves extracted from the 3D model with the change in the number of input images.

Using fewer images provides less information about the plant features as they do not cover enough plant views. Due to insufficient plant views, the features from one image are not matched efficiently to another image. This causes feature matching errors, resulting in unwanted outliers and loss of information. Because of the loss of information, the plant features, such as plant leaves, are not reconstructed accurately, with parts of the leaf missing. Consequently, the leaf becomes disconnected from the stem, so fewer leaves are counted on the reconstructed plant compared to the actual plant. Similarly, the plant stem is not reconstructed accurately with fewer input images. This gives an inaccurate stem height from the reconstructed model.

Consequently, the feature matching error and amount of information loss reduce with more input images as the input images cover sufficient plant views. It is important to use sufficient plant views to reconstruct the plant precisely. When input images with sufficient plant views where considered, the error between extracted values from the 3D model and ground truth values reduced. The 3D model with 78 input images provided a good correlation between the extracted 3D values and ground truth values for this chilli plant. From this experiment, it is clear that, instead of using all images, we can extract plant features precisely using fewer images which will inevitably save computation time and memory.

TABLE 4.2: Execution time taken based on number of images used for 3D reconstruction

Plant	Number of Input Images	Execution Time (Minutes)
Tomato	93	8.3
	75	7.4
	60	6.5
	50	5.3
	35	4.2
	25	3.2
Cauliflower	96	9
	80	7.5
	65	7
	50	6.3
	35	4.5
	25	3.2
Chilli	90	7.5
	78	6.4
	65	6
	50	5.1
	35	4.5
	25	3
Lettuce	84	8.5
	70	7.5
	60	7
	50	6.4
	35	4.2
	25	3.1
Maize	68	6.5
	55	5.4
	45	5
	40	4.3
	35	3.4
	25	2.5

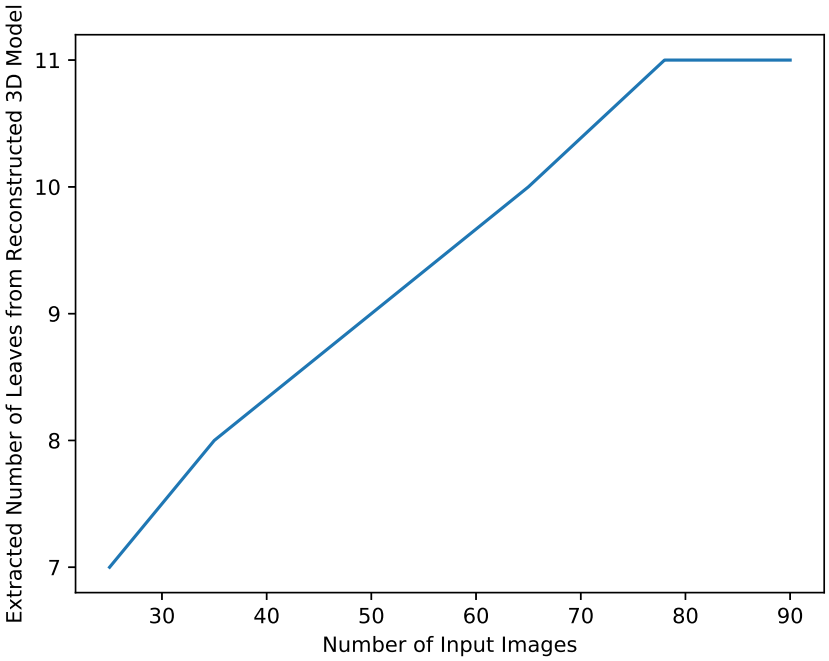

FIGURE 4.3: Extracted number of leaves from reconstructed 3D model with change in number of input images for chilli plant

We repeated the same experiment for the remaining plants and achieved similar results. The results for the remaining plants are provided in Appendix A. From the overall results, we analysed that the tomato, cauliflower, chilli, and maize plant results were reconstructed accurately with fewer images. In contrast, due to its complex architecture, the lettuce plant was difficult to reconstruct accurately using fewer images. The majority of the lettuce plant was missing when fewer images were used.

Table 4.2 lists the execution time for the number of input images used for each plant. It can be seen that the execution time reduces significantly with fewer input images. There is at least one minute difference between the execution time taken for all images and the second subset. Therefore, in terms of the chilli plant, where 78 images provided a good quality 3D model with an execution time of around 6.4 minutes which is far less than using all the images for 3D reconstruction.

Change in Image Resolution

The experiment in the previous section provided an approximate minimum number of images for accurate 3D reconstruction. In this section, the effect of changing image resolution will be explored. The original resolution of each image was 2016×1512 that gave 143,706 data points on average for the sample plant. These were sufficient to generate a precise 3D model. However, when the image size is reduced, there is a significant reduction in the number of 3D points detected, as shown in fig. 4.4. We observed a similar effect on the rest of the plants. The results for the remaining plants are provided in Appendix A.

Although these data points are sufficient to reconstruct a 3D model, the quality of the model is poorer with fewer data points. When the resolution is further reduced, the number of data points is also reduced to 107,313. The reduction in resolution tends to result in inefficient feature detection and matching. Detecting fewer

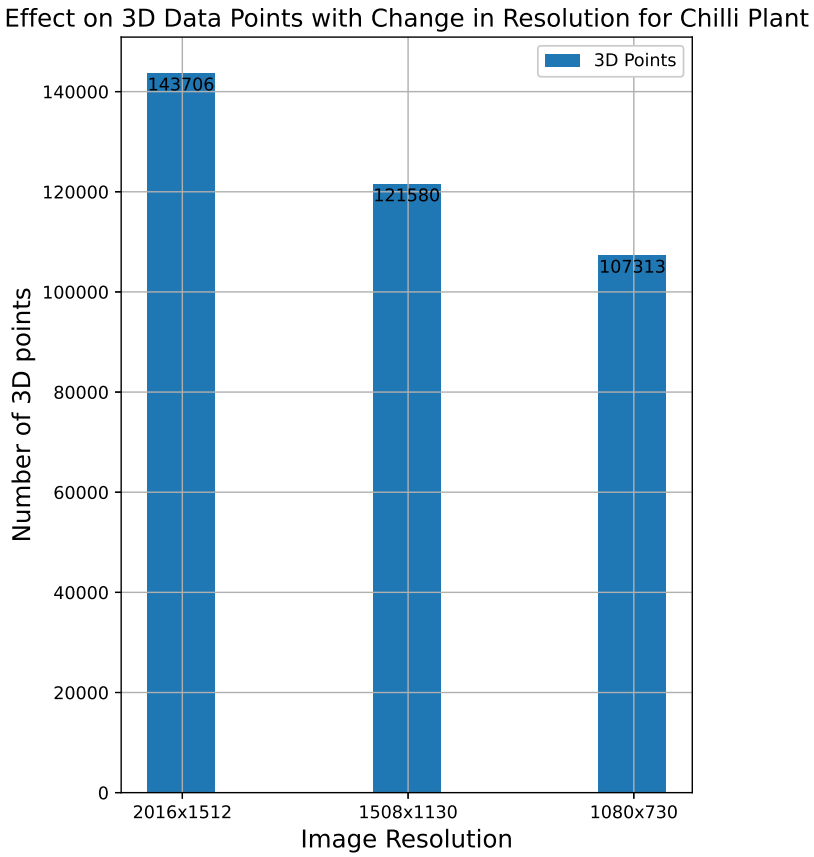

FIGURE 4.4: Number of 3D data points detected for different image resolutions for chilli plant

features leads to feature matching errors responsible for creating unwanted outliers or distortions resulting in a poor quality 3D model. Thus, the better the resolution of the images, the more 3D data points are detected.

4.1.7 Conclusion

The results of the experiments showed that 3D reconstruction of the plants and extracting plant features using fewer images is possible, which inevitably reduces the computation time. However, the number of input images required for precise 3D reconstruction depends strongly on plant architecture. If the plant architecture is complex, more input images will be required for 3D reconstruction. Similarly, if plant architecture is simple, fewer images are sufficient for precise 3D reconstruction.

The contributions to the knowledge are (1) Investigation of the effect on 3D model when there is a change in the number of input images. (2) Proposed a possible way to determine the selection of an appropriate number of images for accurate 3D resolution. (3) Investigation of the effect on 3D data when there is a change in image resolution.

The proposed method needs considerable development in future, including how to select random images in a subset and image resolution.

MASSEY UNIVERSITY
TE KUNENGA KI PŪREHUROA
UNIVERSITY OF NEW ZEALAND

GRADUATE RESEARCH SCHOOL

STATEMENT OF CONTRIBUTION
DOCTORATE WITH PUBLICATIONS/MANUSCRIPTS

We, the candidate and the candidate's Primary Supervisor, certify that all co-authors have consented to their work being included in the thesis and they have accepted the candidate's contribution as indicated below in the *Statement of Originality*.

Name of candidate:	Abhipray Paturkar
Name/title of Primary Supervisor:	Professor Gourab Sen Gupta
In which chapter is the manuscript /published work:	Chapter 5

Please select one of the following three options:

(●) The manuscript/published work is published or in press

- Please provide the full reference of the Research Output:

A. Paturkar, G. Sen Gupta and D. Bailey, "Plant Trait Segmentation for Plant Growth Monitoring." In 2020 35th International Conference on Image and Vision Computing New Zealand, (IVCNZ), pp. 1-6., 2020.

( ) The manuscript is currently under review for publication – please indicate:

- The name of the journal:

- The percentage of the manuscript/published work that was contributed by the candidate: 90.00

- Describe the contribution that the candidate has made to the manuscript/published work:

Algorithm development, data processing, data analysis, manuscript writing, figure and table generation.

( ) It is intended that the manuscript will be published, but it has not yet been submitted to a journal

Candidate's Signature:	Abhipray Paturkar Digitally signed by Abhipray Paturkar Date: 2022.03.09 13:29:18 +13'00'
Date:	09-Mar-2022
Primary Supervisor's Signature:	Gourab Sen Gupta Digitally signed by Gourab Sen Gupta DN: cn=Gourab Sen Gupta, c=NZ, o=Massey University, ou=School of Food and Advanced Technology, email=g.sengupta@massey.ac.nz Date: 2022.03.10 10:39:21 +13'00'
Date:	10-Mar-2022

This form should appear at the end of each thesis chapter/section/appendix submitted as a manuscript/ publication or collected as an appendix at the end of the thesis.

Chapter 5

Plant Trait Segmentation for Plant Growth Monitoring

This chapter presents a novel plant point cloud segmentation algorithm. This work resulted in the following conference publication:

1. A. Paturkar, G. Sen Gupta and D. Bailey, "Plant Trait Segmentation for Plant Growth Monitoring." *In 2020 35th International Conference on Image and Vision Computing New Zealand*, (IVCNZ), pp. 193-198., 2020. DOI: 10.1109/IVCNZ51-579.2020.9290575

5.1 Introduction

3D point cloud segmentation is an important step for plant phenotyping applications. The segmentation should be able to separate the various plant components such as leaves and stem robustly to measure traits. Also, the segmentation method needs to work on a range of plant architectures with good accuracy and computation time.

These 3D models represent the plant traits accurately. For further analysis, to measure plant traits accurately, there is a need for a robust segmentation algorithm to differentiate the plant components irrespective of the plant's growth stage and architecture.

The segmentation process clusters points in the point cloud with similar features into homogeneous regions. In a recent study [51], the segmentation methods are divided into two types: First, machine learning methods based on feature descriptors such as surface feature histograms (SFH), point feature histograms (PFH), and fast point feature histograms FPFH [143] to differentiate the various classes of the object and classify the data based on the resultant model. Second, methods based on geometrical interpretation and mathematical models such as model fitting [130], DBSCAN [137], K-means [37], region growing [50], and so on. Most of these methods perform exceptionally well on man-made objects that are completely uniform in shape. However, plants have complex architectures because of self-occlusion and lack of texture for feature matching [207]. Also, reconstructing the branching region of a plant is an issue addressed by [91]. This complexity changes from species to species. These aforementioned methods are time consuming and sometimes require prior knowledge for segmentation.

Paulus et al. [143] presented a method for plant segmentation based on a point feature histogram descriptor (relationships between the points in the k-neighbourhood and their estimated surface normals). This descriptor was selected into a surface feature histogram to segment leaves and stem efficiently. This new descriptor is then used as a feature for support vector machine (SVM) classification. However,

SVM is a supervised approach for classification which needs labelled data. In this method, for training the classifier, a user has to label the point cloud and indicate what leaves and stem, which is very tedious. Gelard et al. [153] also proposed a method in which the stem was detected first by fitting a geometric structure and then removing these points from the point cloud. It allowed them to then segment the leaves. Petioles were then inserted for every leaf. This process provided good segmentation results but still requires prior knowledge about the plant and user interaction for segmentation. However, this method struggles with plants with complex architecture and is time-consuming. Some methods use intensity data [155] or geometric distance data [155]. Luo et al. [181] used a spectral clustering approach on the graph between a 3D model's points. In another study, Yin [133] was required cutting and scanning the leaves individually to get the plant data. The aforementioned methods are not straightforward, particularly when the leaves are overlapping. These methods are time consuming and struggle on large point clouds or need to cut the plant leaves, which inevitably hampers the plant growth.

Another method uses the 3D mesh generated from the point cloud [27]. To achieve a plant mesh, they used commercial software named 3DSOM. A coarse segmentation is applied with a constrained region growing algorithm, which helps to recognise the plant stem and leaves. Tubular shapes are fitted for accurate stem segmentation and petiole detection. However, this process not only requires strong prior knowledge about the plants but also has a long computation time. Other approaches, such as Poisson reconstruction [154] and ball pivoting [60], do not provide desired results, possibly because of the complex plant architecture.

In the literature, in the context of 3D plant phenotyping, only one deep-learning-based technique [136] exists which results in the segmentation of plant's individual traits from a 3D point cloud. In general, the 3D point cloud segmentation into individual plant traits using deep-learning is a new field. Some general techniques exist, which can be divided into two classes. One class of techniques is point-based which directly works with unordered 3D point clouds. This consists of techniques such as, SGPN [38], PointNet [147], PointNet++ [190], and 3DmFV [128]. These techniques process the 3D point cloud as input and provide class labels for each point as an output. However, these architectures have the drawback that they are limited to the number of points in each model. If the size of the point cloud is large, there is no reliable solution for the network training and interface.

The other class of techniques is based on multi-view geometry, which generates numerous 2D projections from the 3D point cloud and then uses deep-learning based segmentation techniques on the produced 2D images, later connecting the various projections into a 3D point cloud segmentation. For example, SnapNet [168] was applied for semantic segmentation of a 3D model by producing a number of virtual geometry-encoded RGB images of the 3D object, training these images on a network, and then back-projecting the predicted labels to the 3D model to provide each point with a label. The important limiting factor to using neural networks in plant phenotyping applications is that it requires a large ground-truth training data, which is time-consuming and tedious to produce.

Table 5.1 illustrates the comparative analysis of various clustering methods. Clearly, there is a need for a fast and robust segmentation method for various plant architectures.

TABLE 5.1: Comparative analysis of clustering algorithms

Algorithms	Advantages	Disadvantages
K-means	-Fast and easy to implement. -Scalable for a reasonable number of clusters. -Less complexity compared to baseline algorithms.	-Number of cluster has to provided by the user. -Struggles with plant data. -Different run produces different outcome because of it random initialisation
DBSCAN	-Does not require number of cluster information. -Effective in detecting noise/outliers. -Performs well on cluster with homogeneous density.	-Struggles with plant data. -Struggles in high dimension data.
Machine learning	-Robust against the outliers. -Fast and easy to implement. -Performs well on cluster with homogeneous density.	-Needs labelled data. -Tedious.
Hierarchical clustering	-Number of clusters information is not required. -Choice of distance is not critical.	-Best for hierarchical data. -Struggles with the outliers, noise. -Slow

5.1.1 Research Contribution

This chapter focuses on processing the 3D model of the plant reconstructed using a passive 3D imaging technique called structure-from-motion (SfM). Our contribution lies in proposing and investigating the practicality of a fast and robust point cloud segmentation of plants with different architectures. Here, we propose a segmentation method using Euclidean distance. The proposed algorithm requires no prior information about the point cloud.

5.1.2 Materials and Methods

Computer Platform and Software

We used a personal computer (Intel Core i5-4570 CPU at 3.20 GHz and 8GB RAM). To generate the 3D models, VisualSFM [196] is used.

Dataset

For this experiment, we used the point cloud dataset generated using smartphone's camera and structure-from-motion in chapter 3. A total of 225 point clouds was used to test the practicality and robustness of the proposed algorithm.

Once a dense 3D point cloud of the plant is generated, it requires some preprocessing before segmentation.

Point cloud down-sampling:

In general, the generated 3D model is detailed and dense; processing it, is a memory and time-consuming. Lu et al. [104] suggested down-sampling the point cloud by merging close vertices with 0.5% to 10% of the diagonal length of the plant's bounding box, which consists of selected 3D points. Nonetheless, down-sampling the point cloud may lose important information about the plant, such as parts of the leaf or stem. Therefore, depending on the plant species, architecture, and quality of the 3D model, one should select the down-sampling rate. If it is not essential to down-sample the point cloud, one can simply skip this step. In this study, we have not downsampled the point clouds as it was not necessary.

5.1.3 Plant Point Cloud Segmentation

The goal of a segmentation algorithm is to divide an un-organized point cloud P into various parts for further operations and also to reduce the computation time for processing P. The majority of the straightforward methods are based on spatial decomposition, which finds boundaries and subgroups to allow the points to be grouped closely based on a proximity measure. This measure is a Minkowski norm; important examples are Manhattan and Euclidean distance.

A basic segmentation technique in Euclidean space can be performed by using an octree structure (3D grid subgroup of a space based on fixed width boxes). An octree representation is important for cases where a volumetric representation of the contained space is required and is also fast to build. This octree representation can be applied for specific applications which needs equal spatial sub-groups. We need a robust method in some scenarios where the cluster size changes. In the context of 3D plants models, the cluster size changes from region to region. For instance, the leaf cluster may have a different point cloud size than the stem cluster.

To solve this problem, the algorithm should understand what a leaf cluster is and what makes it different from a stem cluster. Mathematically, a cluster is defined as follows.

Let P be the set of points in the point cloud being segmented with a radius threshold r_{th}. Two points, $p_i, p_t \, \epsilon \, P$ are adjacent if:

$$min \mid\mid p_i - p_t \mid\mid < r_{th} \tag{5.1}$$

Points $p_i \, and \, p_j$ are in the same cluster C_i if they are connected by a path of adjacent points. Consequently, points are in different clusters if there is not such a path, i.e. :

$$min \mid\mid p_i - p_j \mid\mid \geq r_{th}, \forall \; p_i \, \epsilon \, C_1, \; p_j \, \epsilon \, C_2 \tag{5.2}$$

However, from an implementation perspective, it is necessary to know how the minimum distance threshold between two clusters can be calculated.

Algorithm 1 Plant Point Cloud Segmentation

Input: Point cloud ***P, Value of*** r_{th}
Output: Segmented point cloud

```
while P ≠ ∅
select one p_i ϵ P              *Seed Point for new cluster
    move p_i from P to Q        *Q is points being processed
    create new cluster C_n
    while (Q ≠ ∅)               *Growing region
    select one p_j ϵ Q
        move p_j to C_n from Q
        find all (p_k ϵ P)      *Adjacent points
                where || p_k − p_j || < r_th
                move p_k from P to Q
    end while
end while
```

However, the question to be asked here is, what is a suitable value of r_{th} in order to get accurate segmentation? A very small value of r_{th} will give multiple clusters, which may not be the desired result. In contrast, a very high value of r_{th}, will cluster the leaves and stem as a single cluster. So, the value of r_{th} has to be selected after a detailed analysis to check what value gives a better result. The value of r_{th} will change according to the plant architecture and growth stage. This also limits this algorithm from being automatic. Algorithm 1 shows the pseudo code of the proposed radius search algorithm. To deal with the noise present in the point cloud and prevent wrong segmentation, a cluster with fewer than 10 points is considered noise and discarded. Fig. 5.1 illustrates the results of our proposed algorithm of different plants at various growth stages.

5.1.4 Results

We tested the proposed algorithm on 225 point clouds of 5 different species at various growth stages. This allowed us to assess our algorithm for accuracy, sensitivity, and reliability on the range of plant architectures from easy to complex. Fig. 5.1 shows a few segmentation results to examine the performance over the growth period. MATLAB is used to implement the other baseline algorithms. In most cases,

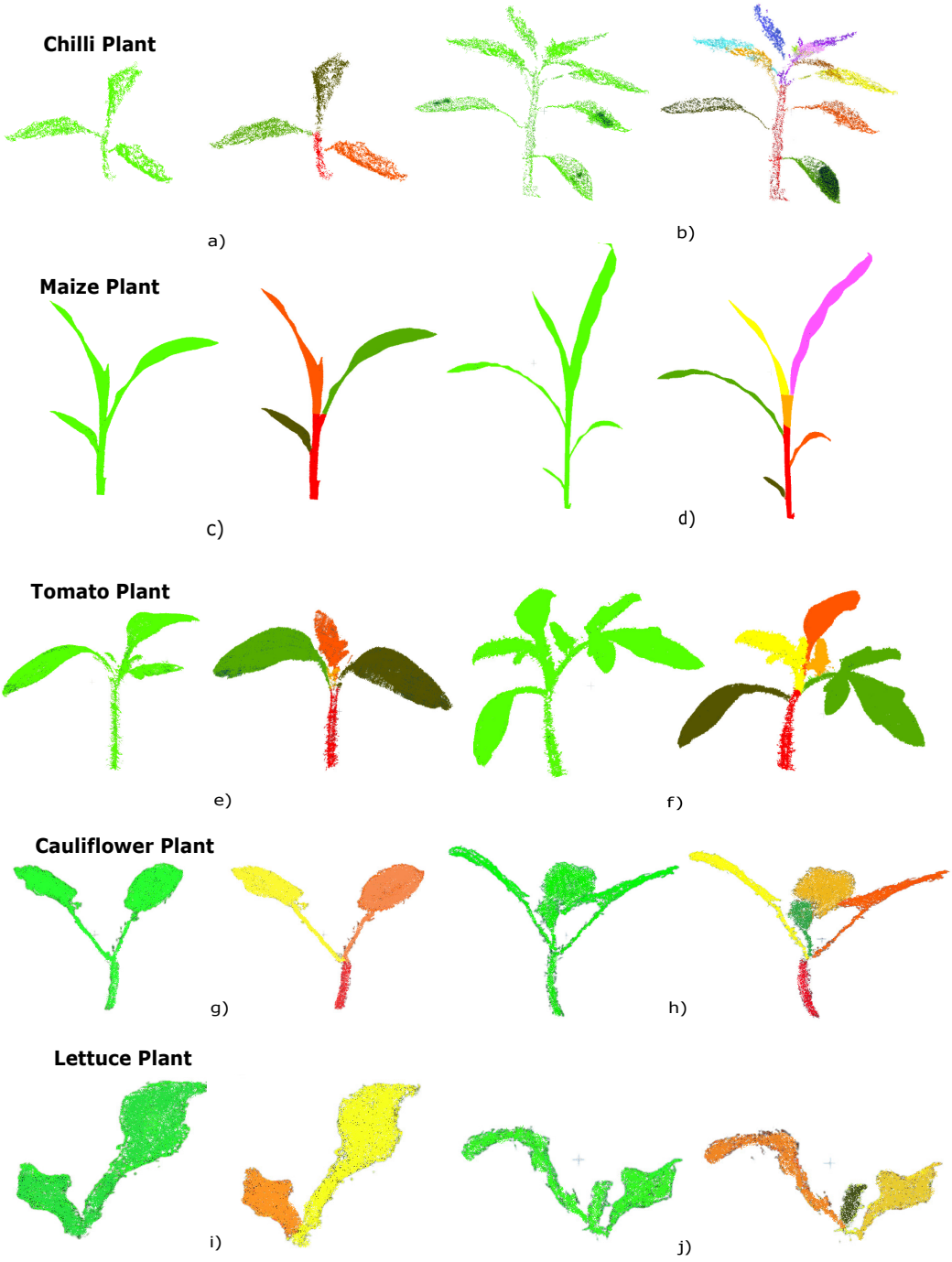

FIGURE 5.1: Results of the proposed algorithm of different plants at various growth stages

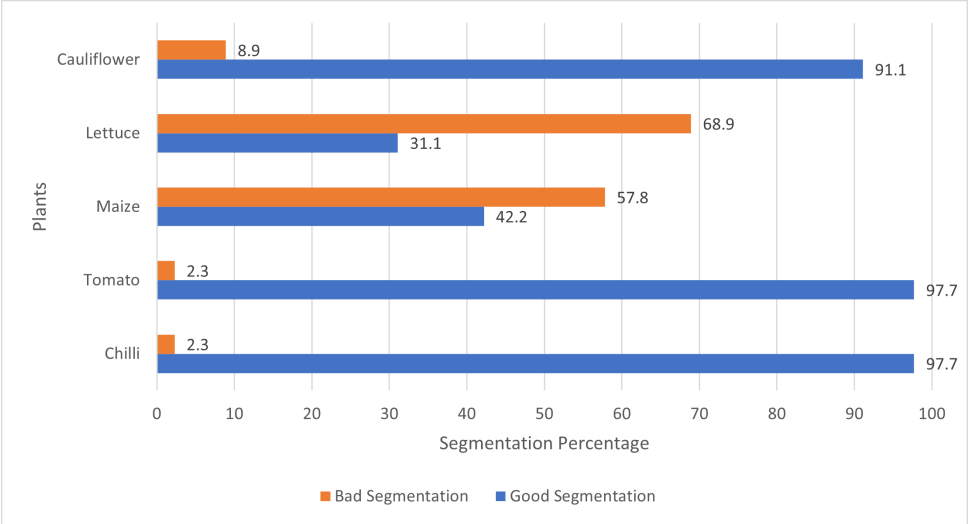

(A) Performance of the proposed algorithm

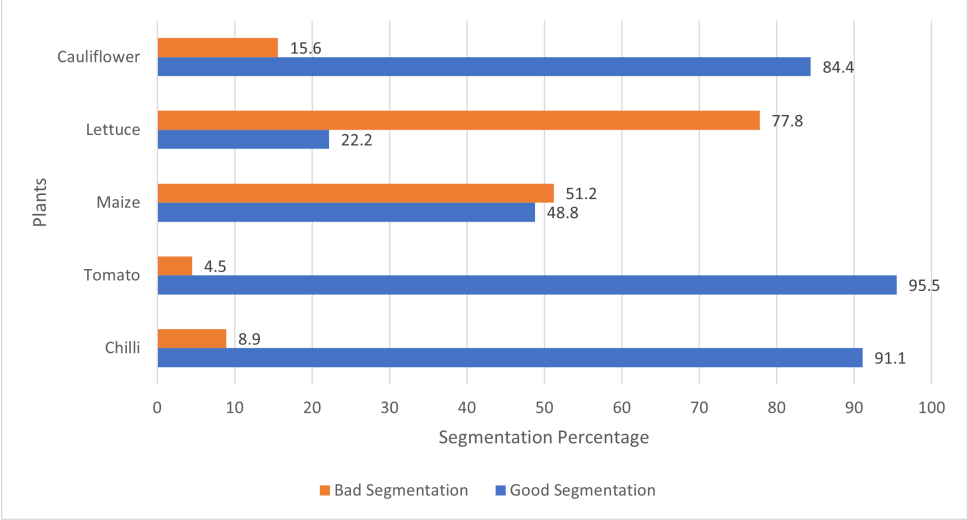

(B) Performance of k-means algorithm

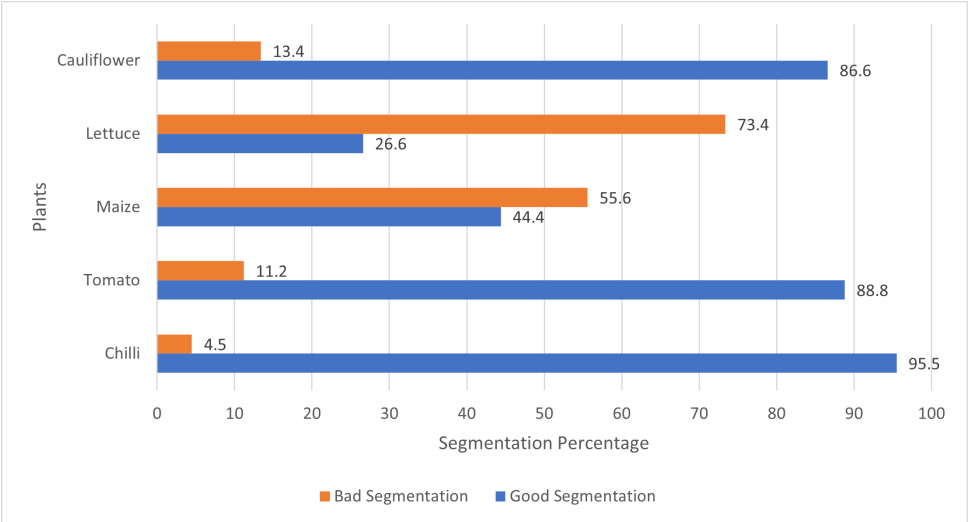

(C) Performance of DBSCAN algorithm

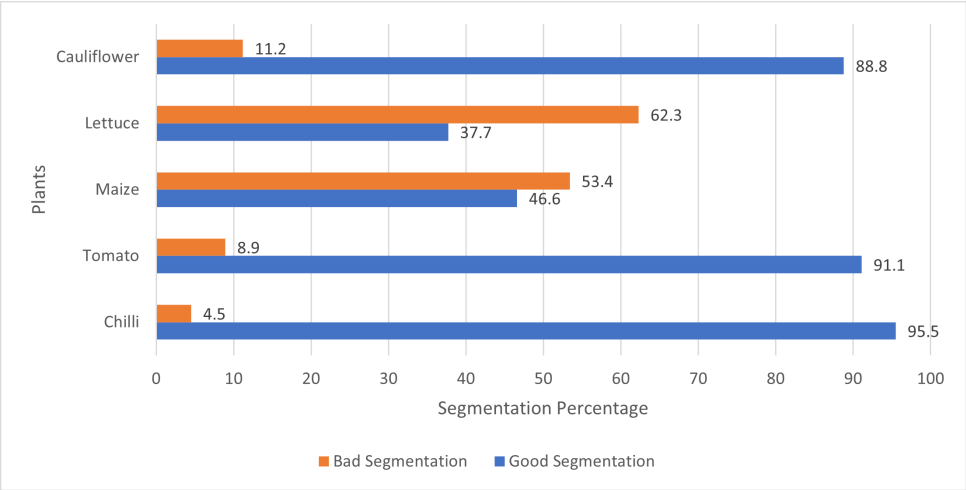

(D) Performance of ML(SVM) algorithm

FIGURE 5.2: Comparison of overall performance of the proposed and standard algorithms

plants were successfully segmented into leaves and stem, 63 point clouds were not well segmented. 31 out of these 63 point clouds belonged to lettuce plants. The reason for the unsuccessful segmentation of the lettuce plant was the heavily occluded architecture. In some cases, the lettuce leaves were occluded and stuck to each other, making them very difficult to separate. In addition, the problematic point clouds are from a more advanced vegetative growth stage. A further 26 point clouds belonged to maize plants. The maize leaves were sticking to each other, resulting in unsuccessful segmentation. The majority of the unsuccessful segmentation was reported in the advanced vegetative growth stage. As shown in Fig. 5.1 (c), when the maize plant is at an early growth stage, the segmentation is better than the advanced growth stage segmentation Fig. 5.1 (d). The remaining six unsuccessful cases belong to four cauliflower, one chilli plant and one tomato plant. The reason was the crown of small leaves at the top, which made the segmentation difficult.

Apart from these cases, as shown in Fig. 5.1 (a) and 5.1 (b), the proposed algorithm successfully segmented leaves and stem at different growth stages. Fig. 5.1 (a) shows an early growth stage of the chilli plant, and Fig. 5.1 (b) shows a month old chilli plant. Similarly, the algorithm has shown good performance for the tomato plant and provided successful segmentation irrespective of the growth stage. Fig 5.2 illustrate the overall performance of the proposed and standard algorithms. Table 5.2 provides the ratio of good segmentation and bad segmentation of proposed and standard algorithms for all the plants. Here, good segmentation refers to the meaningful segmentation of the plants (leaves segmented as leaves and stems as stems), in contrast, bad segmentation refers to inaccurate segmentation (leaves segmented as stems or stems as leaves). From fig 5.2 and table 5.2, it can be derived that all the algorithms struggle to segment the lettuce and maize plant. K-means algorithm has performed well on maize plants compared to all other algorithms. At the same time, the proposed algorithm has performed well on chilli and tomato plants. Moreover, the SVM-based machine learning algorithm has performed well on lettuce and cauliflower. In essence, these algorithms did not perform well on plants with complex architectures.

Table 5.3 compares different algorithm run times on the plant point clouds. The computation time varies according to the size of the point cloud, and the size of the

TABLE 5.2: Plant and algorithm wise performance assessment

Plant and Algorithm	Good Segmentation(%)	Bad Segmentation (%)
Proposed Algo.		
Chilli	**97.7**	2.3
Tomato	**97.7**	2.3
Maize	42.2	57.8
Lettuce	31.1	68.9
Cauliflower	91.1	8.9
K-means Algo.		
Chilli	91.1	8.9
Tomato	95.5	4.5
Maize	**48.8**	51.2
Lettuce	22.2	77.8
Cauliflower	84.4	15.6
DBSCAN Algo.		
Chilli	95.5	4.5
Tomato	88.8	11.2
Maize	44.4	55.6
Lettuce	26.6	73.4
Cauliflower	86.6	13.4
ML(SVM) Algo.		
Chilli	95.5	4.5
Tomato	91.1	8.9
Maize	46.6	53.4
Lettuce	**37.7**	62.3
Cauliflower	88.8	11.2

TABLE 5.3: Comparative analysis of standard algorithms

Plant	Point Cloud Data	Computation Time			
		K-Means	DBSCAN	Proposed	ML(SVM)
Chilli	387,845	1m.30s	3m.1s	30s	43s
Maize	487,768	1m.46s	3m.57s	35s	1m.4s
Tomato	413,639	1m.30s	3m.34s	41s	56s
Cauliflower	407,547	1m.42s	3m.21s	33s	48s
Lettuce	368,652	1m.21s	2m.44s	28s	39s

point cloud depends on the plant's growth stage. Here we provided the computation time of plants with advanced vegetative growth stages. K-means is reasonably fast, but it requires an exact number of clusters as an input to perform the operation. DBSCAN, on the other hand, takes the longest as it is dependent on the point cloud size. Machine learning methods, once trained, take much less time to give the output. However, to train the model, we require a lot of labelled data which is a time consuming process. The proposed algorithm has outperformed other segmentation methods by taking less than a minute to execute the segmentation operation. The computation time, as well as complexity of the proposed algorithm, is less than other algorithms. However, immunity to the noise points is satisfactory. We compared our proposed algorithm with machine learning methods, K-means, and DBSCAN. It is tricky to assess the quality of the segmentation algorithm as it may depend on the application's purpose.

5.1.5 Performance Evaluation

Hubert et al. [203] and Rand [45] have demonstrated methods and metrics to evaluate the similarity of results from two different segmentation methods. Here, we are using adjusted rand index (ARI) (commonly used indices to compare clustering results) proposed by Hubert et al. [203] for quantitative analysis. In this study, the point cloud dataset is manually segmented using TerraScan software by TerraSolid Inc. to use as a reference for performance evaluation. The segmented point cloud from the algorithm is compared with the manually segmented point cloud by measuring the ARI. The highest value of ARI between the segmentation methods shows the best performing algorithm. Table 5.4 shows the performance of the algorithms based on ARI.

TABLE 5.4: Algorithm performance based on ARI

Algorithm	**ARI**
K-means	0.8890
DBSCAN	0.9181
Proposed	0.9342
ML(SVM)	0.9254

It is seen that the proposed algorithm has performed better than other algorithms on plant data with reference to ARI. Therefore, the proposed method can be a potentially beneficial algorithm for segmenting plant point clouds.

5.1.6 Determination of Best (r_{th}) Value

In order to get the best r_{th} value, the same ARI metric is used. Experiments are conducted on each plant in the dataset with various r_{th} values. The same manual segmentation process is used to compare with the segmented point clouds using ARI. A similar approach is used to select the best parameters for the other baseline algorithms. The r_{th} value was varied from 0.003 to 0.08 throughout the experiments for various species. The highest ARI value achieved for each of the r_{th} values provides with the best r_{th} value. This process is repeated for all species and growth stages.

We have three important findings from the result:

1. The proposed algorithm performed well and showed potential when compared to the standard algorithms in terms of computation time and performance.

2. The proposed algorithm does not need down-sampling and can be applied directly on the point cloud.

3. The proposed algorithm performed well on the various plant architectures irrespective of plant species when compared to reference point clouds using ARI.

However, it is very difficult to achieve precise and meaningful segmentation every time, especially in the heavily occluded areas. As Fig. 5.1 (d) illustrates, it is very difficult to segment the maize leaves as some of the leaves might be sticking to each other. However, the algorithm still segments the point cloud, but it is not accurate and meaningful.

5.1.7 Conclusion

This chapter proposed a plant point cloud segmentation algorithm based on Euclidean distance for various plant species and demonstrates the results on different 3D point clouds generated using structure-from-motion. We implemented and evaluated our approach on five different plant species, and provided comparisons to other existing techniques. Furthermore, we supported all claims made in this chapter through our evaluation. For evaluation purpose, ARI has been used in this study. Addition metrics such as F-measure or mean intersection-over-union can also be used. Compared to the other segmentation algorithms, the proposed algorithm has shown potential advantages:

1. Irrespective of point cloud size, plant growth stage, and architecture, the algorithm did not take more than 50 seconds.

2. The proposed algorithm does not require any prior knowledge of the plant for segmentation like we need in k-means and machine learning methods.

Despite these encouraging results, there is further space for improvements. The proposed algorithm could be further developed and the main limitation of the algorithm is that it does not perform well on the high resolution point clouds generated using active image acquisition techniques. As the high resolution point clouds have points close to each other, this algorithm struggles to provide good results. In addition, the segmentation is not meaningful in all cases. Deep neural networks are

one domain where more progress can be expected for plant trait segmentation. The fundamental obstacle to use neural networks in plant phenotyping applications is the requirement of large ground-truth training data. In future, the complexity of the algorithm should be examined to compare with other baseline algorithms.

MASSEY UNIVERSITY
TE KUNENGA KI PŪREHUROA
UNIVERSITY OF NEW ZEALAND

GRADUATE RESEARCH SCHOOL

STATEMENT OF CONTRIBUTION
DOCTORATE WITH PUBLICATIONS/MANUSCRIPTS

We, the candidate and the candidate's Primary Supervisor, certify that all co-authors have consented to their work being included in the thesis and they have accepted the candidate's contribution as indicated below in the *Statement of Originality*.

Name of candidate:	Abhipray Paturkar
Name/title of Primary Supervisor:	Professor Gourab Sen Gupta
In which chapter is the manuscript /published work:	Chapter 6

Please select one of the following three options:

○ The manuscript/published work is published or in press

- Please provide the full reference of the Research Output:

◉ The manuscript is currently under review for publication – please indicate:

- The name of the journal:

BMC Plant Methods

- The percentage of the manuscript/published work that was contributed by the candidate: 90.00
- Describe the contribution that the candidate has made to the manuscript/published work:

Methodology development, mathematical modeling, data processing, data analysis, manuscript writing, figure and table generation.

○ It is intended that the manuscript will be published, but it has not yet been submitted to a journal

Candidate's Signature:	Abhipray Paturkar Digitally signed by Abhipray Paturkar Date: 2022.03.09 13:33:02 +13'00'
Date:	09-Mar-2022
Primary Supervisor's Signature:	Gourab Sen Gupta Digitally signed by Gourab Sen Gupta DN: cn=Gourab Sen Gupta, c=NZ, o=Massey University, ou=School of Food and Advanced Technology, email=g.sengupta@massey.ac.nz Date: 2022.03.10 10:40:06 +13'00'
Date:	10-Mar-2022

This form should appear at the end of each thesis chapter/section/appendix submitted as a manuscript/ publication or collected as an appendix at the end of the thesis.

Chapter 6

Plant Traits Measurement in 3D

This chapter presents the novel formulas to measure leaf length and leaf width even when curled. This work is currently under review in the plant methods journal as follows:

1. A. Paturkar, G. Sen Gupta and D. Bailey, "Plant traits measurement in 3D for growth monitoring", *Plant Methods* 18, article 59 (2022). DOI: 10.1186/s13007-022-00889-9

6.1 Introduction

Plant-phenotyping is a set of protocols and techniques used to precisely calculate plant architecture, composition, and growth at different plant growth stages. Plant phenotyping provides vital information about plants for crop production and plant breeding programs which is helpful to farmers in their decision-making process. Conventional phenotyping is manual, which is tedious, prone to errors, and labour intensive [130]. Popular plant traits for growth monitoring include stem height, stem diameter, leaf area, leaf length, leaf width, number of leaves or fruits on the plant, and biomass [47].

Plant-phenotyping is implemented by combining several techniques, such as spectroscopy, non-destructive imaging, and high performance computing [47]. Plant traits are measured at different scales, e.g. at the level of organs, plants, and canopies. Different types of sensors are used for each of these scales [157]. Traits can be measured using 2D or 3D imaging techniques. 3D imaging techniques produce a full geometric model of the plants, enabling the extraction of plant features. Some existing non-destructive phenotyping systems use 2D hyperspectral imaging [9], or methods for calculating structural parameters of the plant [12, 63].

Image-based 2D methods can also help to extract plant traits. Systems often consist of a single camera mounted above the plant to produce a top view, occasionally combined with one or two more cameras to produce side views to calculate the leaf area or biomass of the plant [53]. However, the calculation of biomass of a plant using 2D images has limited accuracy because these techniques depend on the camera's position relative to the plant. Precise leaf measurements can be achieved if the camera inspects a view perpendicular to the leaf. Nonetheless, this cannot be guaranteed in practical set-ups, providing inaccurate leaf measurements.

2D Systems For Plant Measurement

A semi-automatic phenotyping system [184] uses 2D images to monitor plant rosette growth rate and expansion of size during its vegetative stages. This system constantly rotates the pots' positions within the greenhouse environment to reduce the

effect of micro-environmental conditions. In the initial growth stage of the plant, 2D images can monitor the growth efficiently as the plant architecture is simple [177]. However, as the plant architecture becomes more complex, 2D images cannot reliably monitor the growth. The system presented in [61] uses images taken from two different views (side and top view) for growth monitoring. Different plant traits are measured, such as plant height and width. The measurements from this system were inaccurate as it could not handle the occlusion efficiently. Walter et al. [199] presented a system in which the growth and leaf area was calculated using a camera mounted above the plants. The limited information about the plant is achieved as the camera provided only one view. A growth monitoring system is presented in [140], which helped to calculate traits of plants growing in different pots. This system captures images from two views (side and top view) to calculate plant width, height, and leaf area.

Clearly, 2D image-based methods have limitations such as the inability to handle occlusion, not providing sufficient information about plant traits, plant measurements depending on the orientation of the camera and leaf. These limitations lead to inaccurate plant trait measurements. To overcome these issues, 3D image-based methods have been used and documented in the literature [127].

3D Systems For Plant Measurement

Image-based 3D methods can be divided into active and passive techniques, with the major approaches being LiDAR [67], structured light [125, 67, 100], structure-from-motion [127, 130], and stereo vision [158, 126, 183]. The advantage of using active techniques like LiDAR is that they are not only robust against sunlight but are also able to get depth information in dim light. However, LiDAR has several disadvantages, such as poor resolution, a warm-up time is required for stable measurement [67], it needs multiple captures to handle occlusion, and the sensor is costly [67, 130]. Structured light systems have struggled to perform well in outdoor conditions due to insufficient contrast of the projected patterns within bright sunlight [23]. In contrast, passive techniques can give high resolution, accurate measurement of plant traits and have a lower sensor cost. However, these require computationally more expensive processing. Computation time also depends on the complexity of the plant architecture. In brief, passive approaches are mainly used in applications where accurate measurements, occlusion handling, and obtaining high resolution 3D model are important [127].

The popular passive approaches for 3D modeling are structure-from-motion (SfM), stereo vision, and shape from texture/silhouette/focus/shading [124, 139, 209, 155, 119, 180]. Stereo vision is the most widely used technique for obtaining 3D information. It provides high resolution depth data from two different views; however, it is restricted due to the texture of plants and has a relatively high computation time. Shape-from texture/silhouette/focus/shading uses a single camera to capture images, making it simpler to set up than stereo vision but results in self-occlusion. SfM extends stereo imaging to construct a 3D model from a large number of input images, reducing problems related to self-occlusion and identifying correspondences between images. Nonetheless, SfM has several disadvantages, such as a large computation time, and the quality of the 3D model can depend on the number of input images. SfM is a reliable technique for 3D modeling of plants with resolving occlusion, self occlusion, identifying correspondences between images, and providing high resolution structural information.

In recent years, computer vision researchers have predominantly used SfM to generate high-quality 3D models. SfM is implemented on a large collection of overlapped images to get sparse and dense point clouds and can be applied to a range of scales such as seedlings, plants, and trees. The potential of SfM was examined by Snavley et al. [171], who used Bundler software to reconstruct an object in 3D using hundreds of overlapping images acquired by a single camera. SfM detects and matches identical features in images acquired from different views. Distinctive features in each image are detected using a scale invariant feature transform (SIFT) [101]. This method has performed well in outdoor conditions.

Recently, many studies have been conducted on 3D plant reconstruction. Golbach et al. [52] used a shape-from-silhouette for the 3D reconstruction of plants. This study considered the plant traits, such as leaf length, leaf width, stem height, and leaf area. However, this study has several limitations; firstly, the system can not precisely measure leaf length and width if the leaf is curled. Secondly, this study considered only seedlings for measuring plant traits, making the 3D reconstruction and measurement process easier as the plant architecture is simple. Yu et al. [208] used SfM to reconstruct a sweet potato plant by capturing images from different views. This study considers various plant features for growth monitoring, such as leaf area, plant height, number of leaves on the plant, and leaf area index (LAI). A high correlation was achieved between ground truth measurements and extracted measurements from the 3D model. However, this study did not consider other important plant traits, like leaf length and leaf width, which are also important for plant growth monitoring.

Jay et al. [75] used SfM to reconstruct a crop row using a single camera mounted above the crop row having only one view (top view). This approach provided limited information about the crop, such as the number of leaves, leaf length, and leaf width. Santos et al. [163] used SfM and used a computer-vision based image acquisition approach by moving a single camera over the crop to get overlapping images from different views to solve the occlusion problem. This study achieved a good correlation between measured and ground truth values of the plant. However, this study needs to consider more plant traits like leaf length and leaf width. Rose et al. [155] also used SfM for 3D plant modeling and extracted plant features of a three-week-old tomato plant, such as plant height, convex hull, and leaf area. Overall this study reported a good correlation between ground truth values and measured values. Paturkar et al. [129] used smartphone's camera to capture the plant images and then used SfM for 3D modeling of the plants. This study measured various plant traits, including plant height, number of leaves, and leaf area index. However, this study did not consider measuring the stem height, leaf length, and leaf width when it is curled. This study demonstrated that it is possible to achieve good 3D modeling results using smartphone's camera.

There is a need to consider additional features to monitor plant growth, such as, leaf length and width, which have rarely been considered in the literature [132]. These features are important as the photosynthesis process is dependent on leaves, making leaf dimensions important traits in growth monitoring. Such measurements need to be robust even if the leaf is not flat (which is common). In this study, we will consider these plant traits (leaf length and width) along with other traits, such as the number of leaves and stem height. We will also look at leaf trait measurements when the leaf is curled.

6.1.1 Research Contribution

This chapter proposes a 3D plant trait measurement framework. The feasibility of the proposed method to measure leaf length, leaf width, leaf area, stem height, and the number of leaves was validated by evaluating the reliability and accuracy of measuring these traits at different plant growth periods in outdoor conditions. The overall aim is to extract accurate plant traits from the 3D model. The contributions include 1. Considering additional plant traits for growth monitoring, such as leaf length and width along with number of leaves, and stem height. 2. Investigating a novel approach to measure leaf length by calculating the distance between apex (tip) of the leaf through considering additional points in the middle region of the leaf to the stipule (point where leaf attaches to the stem). This way we can measure leaf length accurately even if the leaf is curled. 3. Investigating a novel approach to measure leaf width by measuring the widest part of leaf. The widest part is perpendicular to the leaf axis from apex to stipule.

6.1.2 Materials and Methods

For this experiment, we used the segmented point cloud dataset generated using using the proposed algorithm in chapter 5. Fig. 6.1 illustrates the flowchart of plant traits measurement.

After leaf and stem segmentation, important plant traits for growth monitoring are measured: leaf length, leaf width, number of leaves, and stem height. These traits are important as the leaf size plays a vital role in plant growth. In this study, we repeated these proposed measurements for all plant growth stages to validate the method's accuracy and reliability.

For illustration purposes, only chilli plant in advanced vegetative growth stage is considered in this chapter. The results for the remaining plants are provided in Appendix B.

Plant Trait Measurements

Leaf Length

Our definition of leaf length is the length along the midrib. The midrib is a strengthened vein along the middle of a leaf running from the apex (tip of the leaf) to the stipule (leaf's connection to the stem). The midrib is detected using the method proposed in [204], which converts the leaf into its principal component analysis (PCA) coordinates to find the apex and the stipule. The segmentation method has precisely segmented each leaf (as seen in the previous chapter). The apex of the leaf is defined as the point on the leaf which is furthest from the stipule. In contrast, the stipule of the leaf is defined as the point on the leaf furthest from the apex. These points are marked by black points a and s in fig. (6.2).

Our study also measured leaves that are curled, which makes the measurement challenging. If the leaf is straight, the Euclidean distance between apex and stipule will provide the leaf length. However, this approximation will underestimate the true length when the leaf is curled. Therefore, to tackle this challenge, we consider additional points in between apex and stipule, which will provide a close approximation of leaf length. We calculated the leaf length by considering 3 to 8 additional points between apex and stipule. However, the results from 5 to 8 points were identical, and therefore, we selected 5 points to reduce computation time. These five points are marked by red points (b-f) in fig. 6.2. The leaf length is measured using:

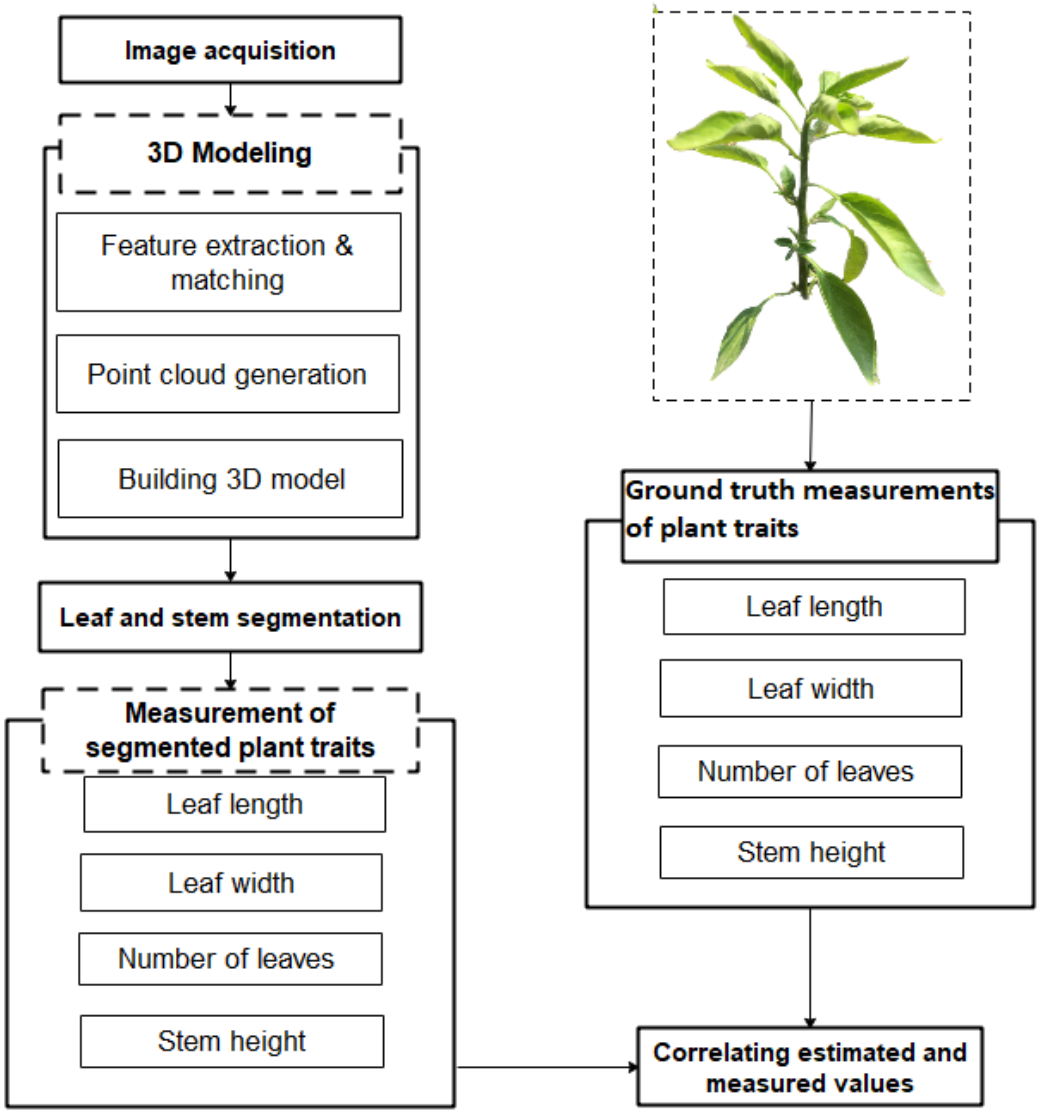

FIGURE 6.1: Flowchart of 3D plant reconstruction and plant trait measurements

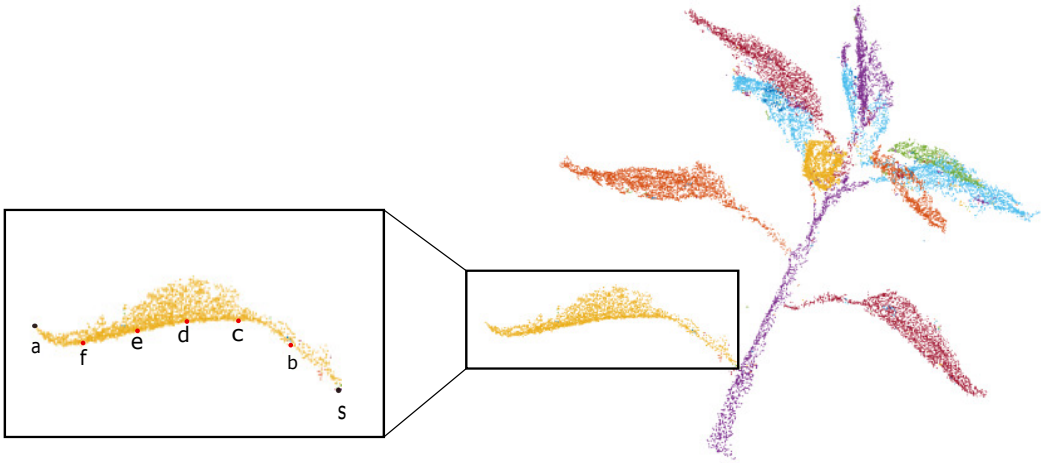

FIGURE 6.2: Leaf length measurement.

$$Leaf_{length} = \left\|s \vec{-} b\right\| + \left\|b \vec{-} c\right\| + \left\|c \vec{-} d\right\| + \left\|d \vec{-} e\right\| + \left\|e \vec{-} f\right\| + \left\|f \vec{-} a\right\| \tag{6.1}$$

Leaf Width

To measure the leaf width, the leaf's widest region, which is perpendicular to the axis through the apex and stipule, is found, marked by a black line in fig. 6.3. The widest region on the leaf is determined by the part where the Euclidean distance between the two red dots is maximum. However, finding the location of these red dots is difficult. To do that, for all points on the leaf, the orthogonal projection on the line from the apex to stipule is measured. The distance between the apex and stipule is divided into 25 equidistant segments. The leaf points having projection in a segment selected, shown in red dots (fig. 6.3). These red dots form a band across the leaf. The leftmost red point on the line, L_P and rightmost point on the line, R_P is used to approximate the width of that area. This step is repeated for all 25 segments; the leaf width is defined by the maximum of:

$$Leaf_{width} = max(\left\|L_P \vec{-} R_P\right\|) \tag{6.2}$$

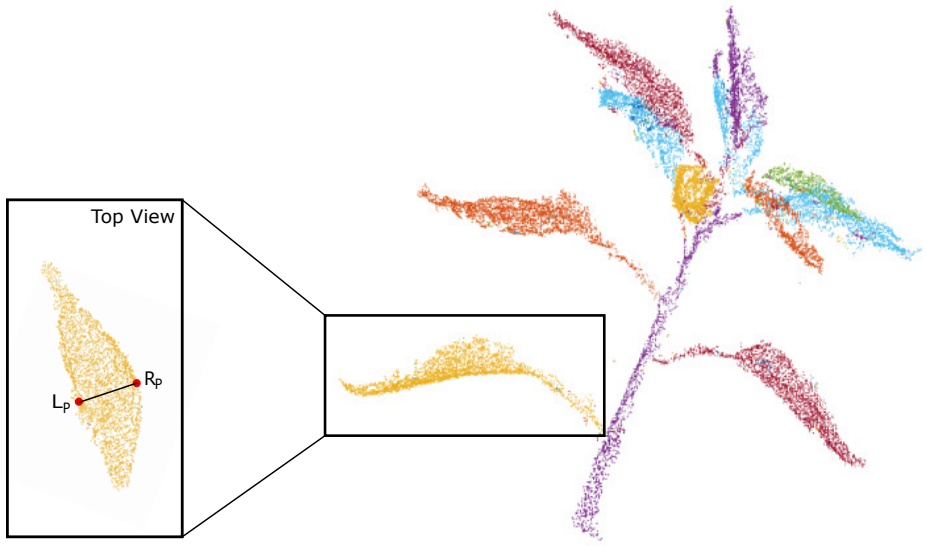

FIGURE 6.3: Leaf width measurement

Stem Height

We tried an approach used in [52] called mid-line tracking, which scans the number of points on the stem to measure stem height. However, we analysed that in some cases, at the initial growth stage of the plant, when the stem is very short, the stem is not detected. In addition, in natural conditions, the stem can be curved as well, and hence a close approximation of true stem height is also needed. To tackle this problem and measure stem height precisely, we selected three points on the plant stem since the measurements were approximately similar after selecting more than 3 points. Fig. 6.4 shows these three marked points at the bottom of the stem, one at the

middle and one at the point where the topmost leaf is connected. The stem height is measured by calculating the distance between these three points. The marked black points are selected by visual cues to measure stem height precisely.

FIGURE 6.4: Stem height measurement

Number of Leaves

The number of leaves is another important trait of the plant for growth monitoring. Plant growth mainly depends on the leaves as they photosynthesise. We have already derived the stipule of the leaves during the segmentation process. Therefore, counting the number of stipules in the model ultimately provides the information about the number of leaves.

Leaf Area

Meshlab allows the automatic calculation of the number of triangular polygons within the leaf mesh. The leaf area can be estimated from the area of the mesh. Fig. 6.5 shows the appearance of the triangular polygon in the leaf mesh of the chilli plant.

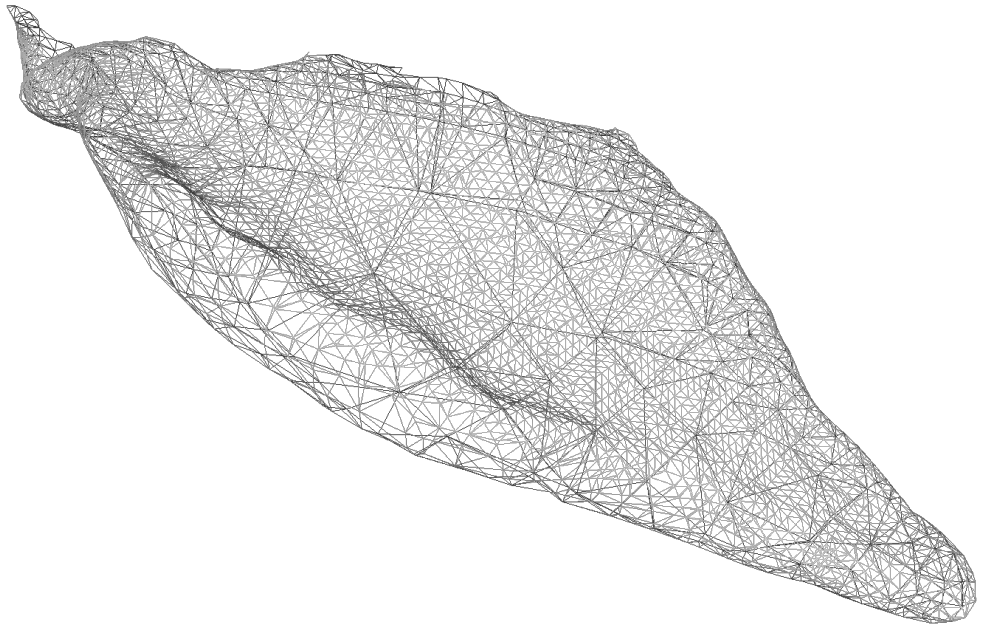

FIGURE 6.5: Leaf triangular polygonal mesh

6.1.3 Ground Truth Measurements

In this study, to establish the ground truth, we measured different plant traits, such as leaf length, leaf width, number of leaves on the plant, and stem height. The number of leaves varied over the growth period.

It is very easy and straight forward to count the number of leaves on the plant, simply by moving around the plant and carefully counting them. We used a conventional method of taking measurements with a ruler to measure leaf length, leaf width, and stem height [208].

For the manual (direct) measurements of leaf area, we captured images of the individual leaf with a white background without plucking it from the plant and used *ImageJ* to calculate leaf area for each measurement during the growth period. Fig 6.6 shows the captured image of the leaf and output window of *ImageJ*, respectively. Fig. 6.6 (A) illustrates an image of a plant leaf with a ruler. *ImageJ* uses this ruler to set a scale to calculate the leaf area of the thresholded area. The colour thresholding is performed to segment the leaf dimensions in the image and the leaf area, see fig 6.6 (B).

We define these measurements as the ground truth, although these measurements may not be accurate because of physical or human errors. For instance, some leaves are curled in such a way that it is difficult to measure accurately in the real world as the leaf may be damaged in the process of making it flat. However, careful measurements reduce these errors. In this study, we have considered these factors while calculating system accuracy.

6.1.4 Results

In this section, the system's accuracy is assessed based on regression between the ground truth values and measured values from the 3D segmented model at different growth stages. The correlation coefficient (R^2) indicated the quality of the fit. In addition, the mean absolute percentage error (MAPE) of the measured values from

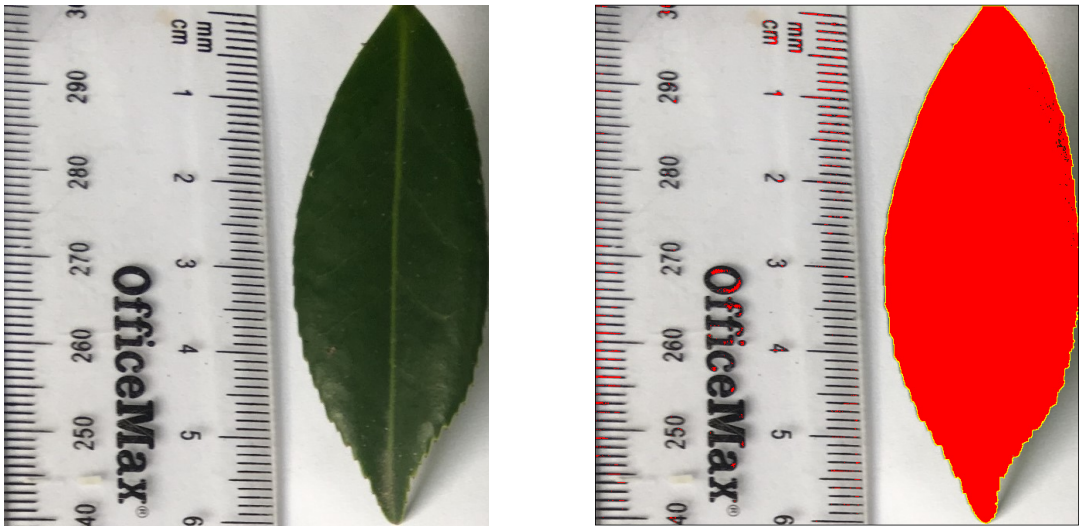

(A) Leaf area (captured image)

(B) Leaf area (output window)

FIGURE 6.6: Leaf area calculation using ImageJ

our 3D model, F_t and ground truth values, A_t is used to assess the accuracy:

$$M = \frac{100\%}{n} \sum_{t=1}^{n} \left| \frac{A_t - F_t}{A_t} \right| \tag{6.3}$$

Leaf Length

The length of each of the leaves was measured individually over one month. This gave a total 58 ground truth values and 58 measured values from the segmented 3D model for the leaf length. The leaf length varied from 1.6 cm to 6.5 cm throughout the experiment. Fig. 6.7 shows our proposed method performed well against the ground truth with a correlation coefficient of 0.97. The accuracy of the leaf length measurement method is determined by calculating RMSE, which is 0.2 cm. The mean absolute percentage error is 5.8%. The results for the remaining plants are provided in Appendix B.

Leaf Width

Fig. 6.8 shows a high correlation between the measured values and ground truth values of leaf width with a correlation coefficient of 0.96 with RMSE of 0.11 cm. The mean absolute percentage error is 8% which is higher than that for leaf length because the width is one-third of the leaf length. The results for the remaining plants are provided in Appendix B.

Stem Height

The stem height grew from 5 cm to 27 cm during the course of this experiment, with eight ground truth values and 3D model values. The measurements from our proposed method showed a high correlation with ground truth measurements, as shown in fig. 6.9(A). The correlation coefficient for stem height is 0.99 with an RMSE of 0.11 cm. The mean absolute percentage error is 2%. The results for the remaining plants are provided in Appendix B.

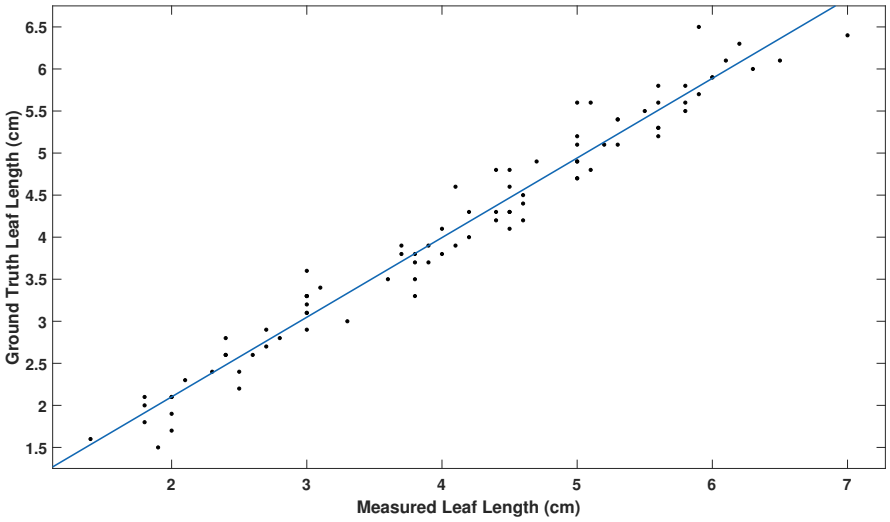

FIGURE 6.7: Correlation between Ground Truth and Measured Leaf Length

Number of Leaves

The segmentation algorithm has performed extremely well to segment the leaves from the plant. Therefore, it is easy to count the number of leaves. A high correlation between the measured number of leaves and the ground truth is achieved with a correlation coefficient of 1, as shown in fig. 6.9(B). The RMSE is zero as there is exact correspondence between measured and ground truth values.

Leaf Area

The leaf area ranged from 0.04 to 0.8 cm^2 during our experimentation duration. A good correlation between the measured leaf area and the ground truth is achieved with a correlation coefficient of 0.98, as shown in fig. 6.10. The mean absolute percentage error is 20%. The results for the remaining plants are provided in Appendix B.

6.1.5 Comparison with the State-of-the-art

This section compares the proposed plant growth monitoring system with different state-of-the-art systems. The detailed comparison is shown in table [6.1].

Golbach et al. [52] used shape-from-silhouette for the 3D reconstruction of plants. It also considered only seedlings for measuring plant traits, making the 3D reconstruction and measurement process easier as the plant architecture is simple. This study considered similar plant traits, such as leaf length, leaf width, stem height, and leaf area. However, their system can not measure leaf length and width precisely if the leaf is curled. The proposed method has overcome these drawbacks and performs well even if the plant leaf is curled.

Yu Zhang et al. [208] tested sweet potato in outdoor conditions and extracted different plant traits such as plant height, number of leaves, and leaf area from a 3D model. However, they did not consider other important leaf traits such as length and width. Our proposed system performed better in measuring plant height and number of leaves.

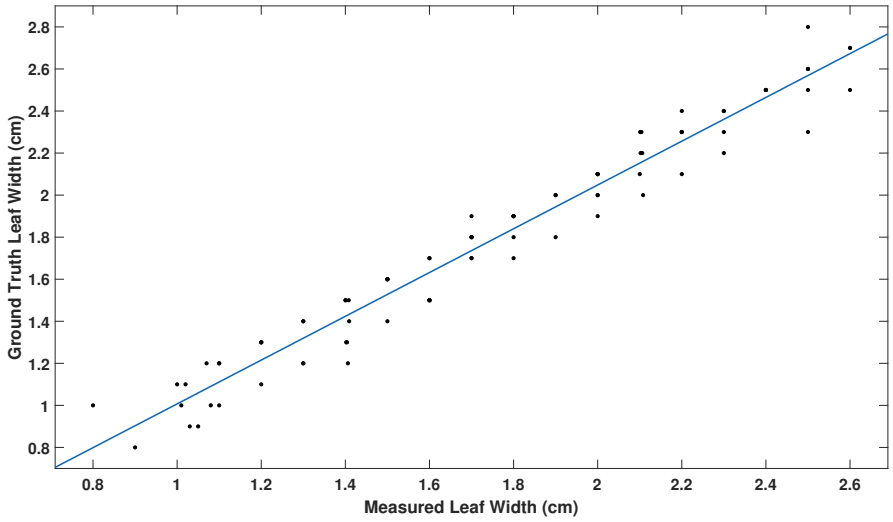

FIGURE 6.8: Correlation between ground truth and measured leaf width

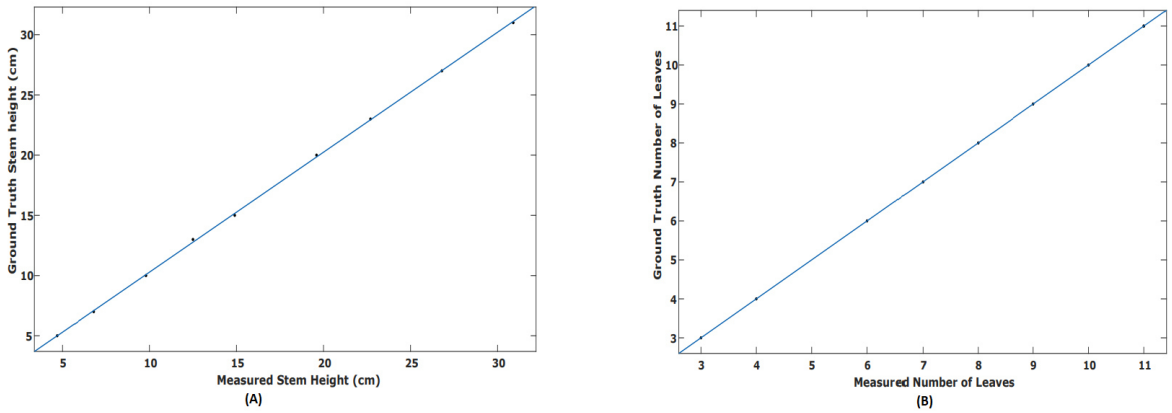

FIGURE 6.9: Correlation between ground truth and measured values for (A) stem height and (B) number of leaves

Hu et al. [70] used a Kinect sensor to monitor the growth of a leafy vegetable and extracted plant height, leaf area and volume. The results were highly correlated with manual measurements, but they did not test the system in outdoor conditions. The proposed approach achieves lower RMSE and a good correlation between the measured and the ground truth values compared to Hu's demonstrated system.

Rose et al. [155] proposed a photogrammetric method to precisely measure growth parameters of three-week-old tomato plants in the greenhouse. They demonstrated that all considered growth parameters are correlated with manual measurements. The proposed system achieved better correlation for plant height compared to their study. However, this study did not examine the system's performance in outdoor conditions.

Jay et al. [75] proposed an approach to extract leaf area and plant height for five different plants. These two parameters are highly correlated between calculated and manually measured values. Nonetheless, their approach did not deal with occluded leaves and did not have additional information to extract leaf length, leaf width, and the number of leaves.

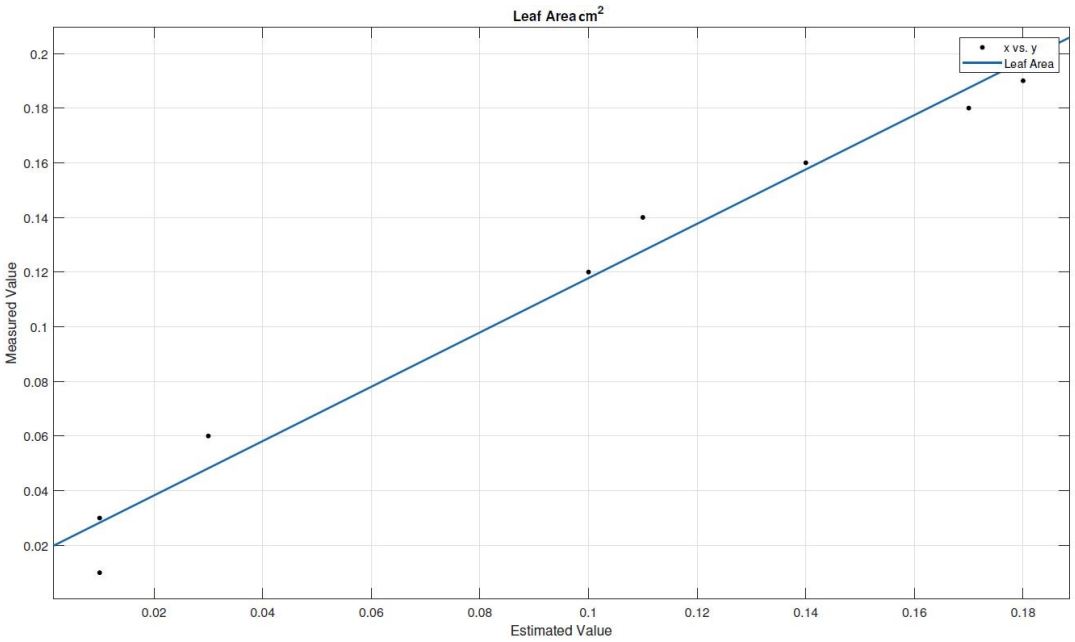

FIGURE 6.10: Correlation between ground truth and measured values for leaf area (cm^2)

TABLE 6.1: Comparative analysis of state-of-the-art systems

Method	**Stem Height**		**Leaf Length**		**Leaf Width**		**Number of Leaves**	
	RMSE	**(R^2)**	**RMSE**	**(R^2)**	**RMSE**	**(R^2)**	**RMSE**	**(R^2)**
Rose et al. [155]	0.14 cm	0.96	*NA*	*NA*	*NA*	*NA*	*NA*	*NA*
Jay et al. [75]	1.1 cm	0.99	*NA*	*NA*	*NA*	*NA*	*NA*	*NA*
Golbach et al. [52]	0.43 cm	0.87	0.43 cm	0.91	0.21 cm	0.85	*NA*	*NA*
Hu et al. [70]	0.29 cm	0.99	*NA*	*NA*	*NA*	*NA*	*NA*	*NA*
Yu et al. [208]	0.71 cm	0.97	*NA*	*NA*	*NA*	*NA*	4.03	0.99
Paturkar et al. [129]	0.13 cm	0.97	*NA*	*NA*	*NA*	*NA*	0.06	0.99
Our method	**0.11**cm	**0.99**	**0.2**cm	**0.97**	**0.11**cm	**0.96**	**0**	**1**

Paturkar et al. [129] which is a part of our previous work, measured stem height, number of leaves, and leaf area. However, this study did not address the issue of curled leaves and stem. The proposed method demonstrated that even a mobile phone can be used for image capture to reconstruct the plants in 3D, giving an $R^2 > 0.96$ for leaf length, leaf width and also, $R^2 > 0.99$ for stem height and the number of leaves.

6.1.6 Discussion and Conclusion

The proposed measurement and analysis methods are also applied to the remaining four plants, and the results are provided in Appendix B. Table 6.2 summarises the results of the remaining plants in detail. The leaf length, width, area, stem height, and the number of leaves show excellent correlation for cauliflower and tomato. However, the leaf area for lettuce did not show good correlation. To measure leaf width of maize plants was challenging, resulting in no records for maize plant. Similarly, it was impossible to measure the stem height for lettuce plants due to the heavy occlusion.

TABLE 6.2: Comparative analysis of of all the remaining plant

Plant	Leaf Area		Leaf Length		Leaf Width		Number of Leaves	
	RMSE	**(R^2)**	**RMSE**	**(R^2)**	**RMSE**	**(R^2)**	**RMSE**	**(R^2)**
Lettuce	0.02 cm	0.91	0.22 cm	0.98	0.31 cm	0.95	0	1
Cauliflower	0.02 cm	0.98	0.31 cm	0.93	0.11 cm	0.96	0	1
Maize	0.01 cm	0.99	0.8 cm	0.87	*NA*	*NA*	0	1
Tomato	0.01 cm	0.99	0.2 cm	0.96	0.1 cm	0.96	0	1

This chapter proposes methods to measure plant traits for growth monitoring based on the reconstruction of plants in 3D. Measured plant traits consist of leaf length, leaf width, number of leaves, leaf area, and stem height. These are the basic yet important phenotypic features of the plant. The proposed method is accurate for plant trait measurements. Structure-from-motion is used for the reconstruction of plants in 3D. The image acquisition process has been conducted in such a way that from every camera perspective, the plant is clearly visible. The image acquisition process was conducted manually with a user capturing images using a mobile phone camera without using a tripod or any other tools, making this process easy and adaptable. The time required for image acquisition is 2-3 minutes, and this time increases with the plant's growth as more images are required. The computation time per plant for post processing requires 10-12 minutes for generation of the point cloud 7-12 minutes for removing outliers and filtering. The segmentation time has varied from 3.2 seconds to 12.6 seconds and trait measurement time varied from 8.8 seconds to 17.5 seconds throughout the growth stages of the plant.

The generated 3D model of the plant is then accurately segmented into leaves and stem parts. These segmented parts are then used to calculate plant traits. Leaf length and leaf width can be measured with an absolute mean percentage error of 5.8% and 8%, respectively; error for stem height, leaf area, and the number of leaves is 2%, 20%, and 0%, respectively.

The advantages of the proposed method include reduced user involvement for plant segmentation and precise plant trait measurements.

The leaf length was measured precisely by considering 5 additional points in the middle region of the leaf from apex to stipule. This helped us calculate leaf length accurately even when the leaf was curled with a high correlation of 0.97 between ground truth and measured values. Similarly, leaf width is calculated by determining the widest part of the leaf with an RMSE of 0.11 cm and a correlation coefficient of 0.96. These methods helped to overcome the disadvantage associated with inaccurate measurement of curled leaves.

In conclusion, this study demonstrated that the methods proposed to calculate plant traits have the potential to monitor plant growth in outdoor conditions. Future work consists of applying this system to multiple plants to determine the robustness and reliability. Such a system can be potentially used to monitor commercial land, greenhouse, and agriculture production in the near future.

Chapter 7

Conclusion and Future Scope

7.1 Conclusion

In this thesis, we have focused on different problems related to plant growth monitoring in small scale (field) operations. We did not focus on applying this framework on a commercial scale at this stage, and therefore, considerable work is required to make this framework operative in a commercial field. We have shown the applicability of using a smartphone camera as a cost-effective and reliable image acquisition method. The feasibility to generate good quality point clouds has been demonstrated. The quality of the generated 3D models have been assessed. All the plants except lettuce were reconstructed in 3D, which shows that the proposed system has the potential to replace the expensive sensors for the image acquisition process. The reason that the lettuce plant was not reconstructed accurately is due to its complex architecture. Because of the heavy occlusion of leaves, it is difficult to reconstruct the lettuce plant's inner leaves, which is a limitation of an image-based computer vision technique. In future, to address this limitation, plant head can be measured instead of the number of leaves for lettuce. However, more work needs to be done on the reconstruction of high-value lettuce plants as few studies considered this plant when working on the reconstruction of plants in 3D.

We have also investigated a possible way to get an appropriate number of images to generate a good quality 3D model instead of using all images. The results of the experiments showed that 3D reconstruction of the plants and extracting plant features using fewer images is possible, which inevitably reduces the computation time. However, the number of input images required for precise 3D reconstruction depends strongly on plant architecture. If the plant architecture is complex, more input images will be required for 3D reconstruction. Similarly, if plant architecture is simple, fewer images are sufficient for precise 3D reconstruction. However, the proposed investigation needs further development, including selecting random images in a subset and image resolution.

The proposed point cloud segmentation algorithm can be used on a variety of plants. The proposed algorithm could be further developed, and the main limitation of the algorithm is that it does not perform well on the high resolution point clouds. As the high resolution point clouds have points close to each other, this algorithm struggles to provide good results. In addition, the segmentation is not meaningful in all cases. Deep neural networks are one domain in which more progress can be expected for plant trait segmentation. The fundamental obstacle to use neural networks in plant phenotyping applications is the requirement of large ground-truth training data. In future, the complexity of the algorithm should be examined to compare with other baseline algorithms.

Leaf length and width can additionally be considered to monitor plant growth. These plant features can also be measured when they are curled. This framework

can be used in both controlled or outdoor conditions. However, it struggles with the windy conditions since the images from the phone are distorted due to wind and resulting in poor image-pair matching and hence, the poor 3D model. Two possible solutions to address this limitation are developing a neural-network to classify between the good image and the distorted image, and another solution is using a plant canopy while capturing the plant images. We believe that the proposed non-destructive framework can be an excellent cost-effective alternative to expensive state-of-the-art methods for small scale (field) operations.

7.1.1 Performance of various stages in the framework on the considered plants

3D Reconstruction of Plants

In terms of plants, chilli, tomato, cauliflower, and maize plants have shown good relation between the measured height and manual height measurement. In contrast, the lettuce plant struggles between the manual and measured stem height because of the more complex architecture of the lettuce plant. Because of the high degree of occlusion, measuring the stem height in the reconstructed 3D model is difficult. For measuring the number of leaves, similar results were achieved for the tomato, cauliflower, and maize plants. However, the lettuce plant results were again less promising as it is difficult to reconstruct the heavily occluded plant, and therefore, it failed to reconstruct some of the inner leaves accurately.

Reducing Computation Cost

From the experiments, we analysed that the results for tomato, cauliflower, chilli, and maize plant were reconstructed accurately with fewer images. In contrast, due to its complex architecture, the lettuce plant was difficult to reconstruct accurately using fewer images. The majority of the lettuce plant was missing when fewer images were used. Based on the computation time, it can been seen that the execution time for lettuce and cauliflower is more compared to the other of the plants.

7.1.2 Plant Trait Segmentation

Based on the experiments, the lettuce and maize plant were difficult to segment because of their complex architecture. In contrast, the proposed segmentation algorithm showed better results on chilli, tomato, and cauliflower plants.

Plant Trait Measurement

The proposed measurement and analysis methods show that the leaf length, width, area, stem height, and the number of leaves show excellent correlation for cauliflower and tomato. However, the leaf area for lettuce did not show a good correlation. To measure the leaf width of maize plants was challenging, resulting in no records for maize plants. Similarly, it was impossible to measure the stem height for lettuce plants due to the heavy occlusion.

In essence, more work is needed on leafy vegetables with complex architecture. Very few prior studies have considered lettuce plants.

7.2 Future Scope

Due to the COVID-19 outbreak, the outdoor experiments were disrupted, resulting in a delay in analysis and experimentation on small plants. From the framework point of view, there are some limitations. The framework needs to be tested on tall plants (height > 1m). The segmentation algorithm works well with low-resolution point clouds which are generated using image-based or passive 3D reconstruction methods. So the future work can be to develop the algorithm further to work with high resolution point clouds. Leafy plants are also problematic for this framework, especially for 3D reconstruction and segmentation. However, having more images of leafy plants may resolve the problem for 3D reconstruction, although this would also increase the computation time. Although it has performed satisfactorily in this study, there is still scope for improvement for accurate 3D reconstruction and segmentation. However, there are very few studies reporting work on leafy plants, knowing the challenges they possess. The plant traits measurement can also be made robust by using visual cues for manual and 3D model measurements. These visual cues can be visible in the 3D model to understand the plant traits precisely, and this will help to analyse the performance of the methods. In commercial fields, potted plants can be monitored in future using this framework. To use in this environment, the potted plants will need to placed on a rotating platform, keeping the smartphone camera stationary. This way, image capturing can be done where the plants are planted closely. In the commercial environment, improvements are needed in the speed of the SfM. This proposed framework can also be used in horticulture or livestock farming in future.

Appendix A

Supplementary Material

A.1 Chapter 4: Reducing Computation Cost for Accurate 3D Modeling

Additional results for 3D reconstructions of remaining plants when using a different number of input images.

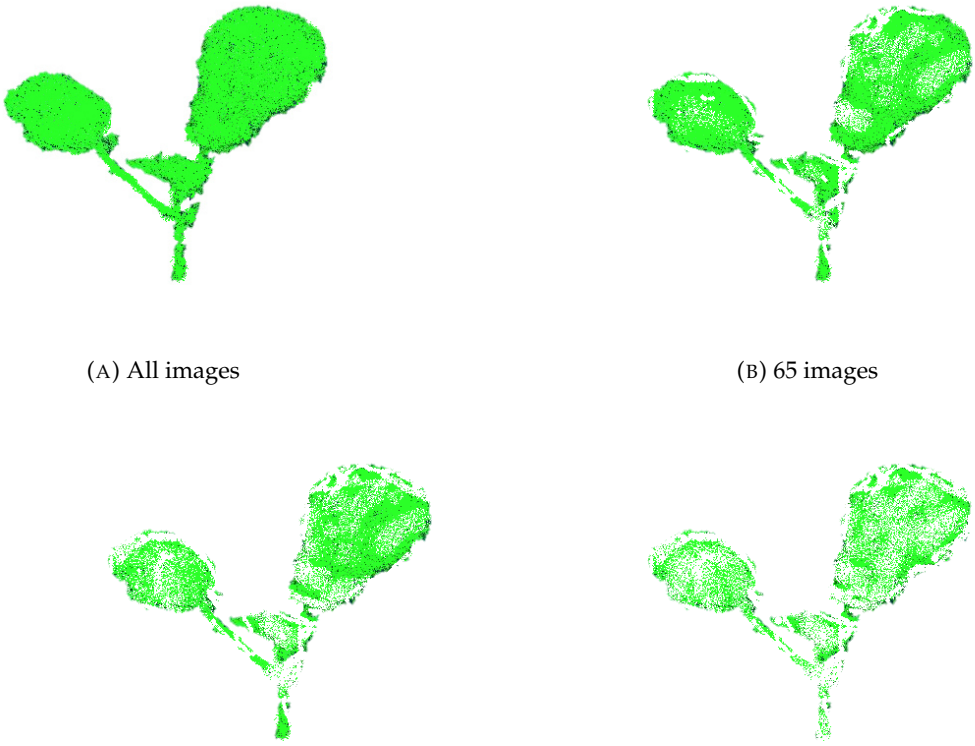

(A) All images

(B) 65 images

(C) 35 images

(D) 25 images

FIGURE A.1: Example 3D reconstructions of a cauliflower plant with different numbers of input images

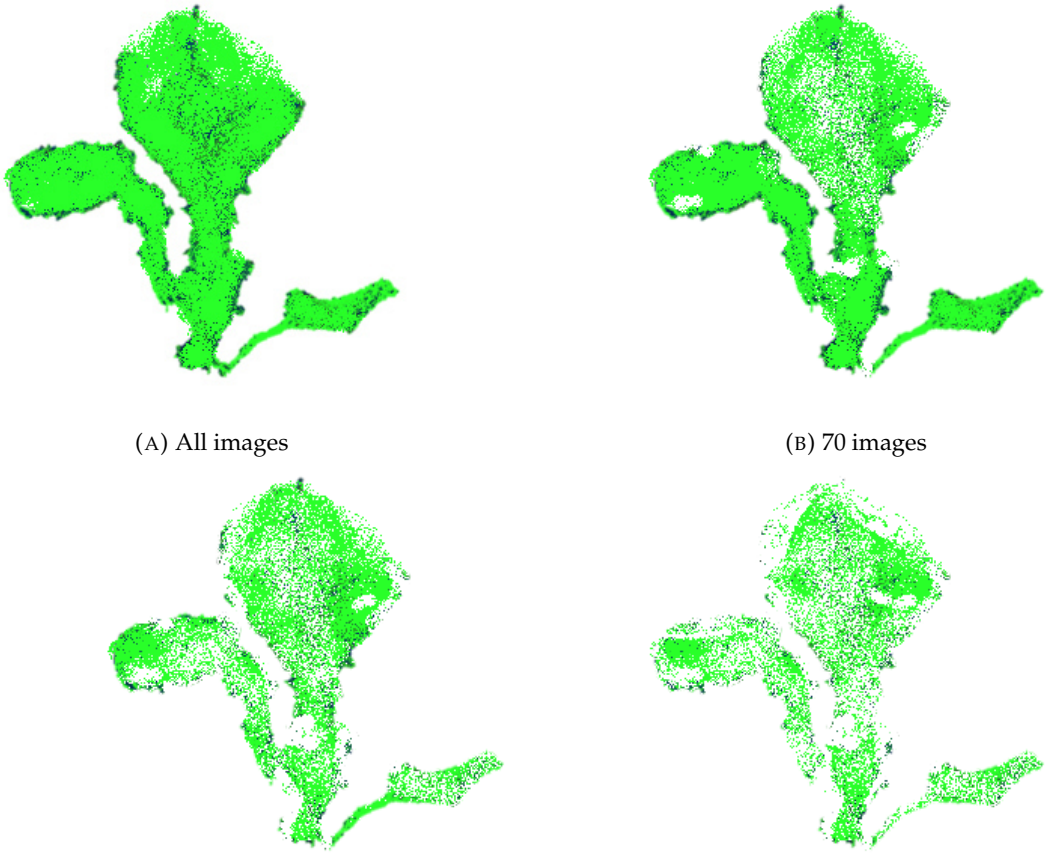

(A) All images (B) 70 images

(C) 50 images (D) 25 images

FIGURE A.2: Example 3D reconstructions of a lettuce plant with different numbers of input images

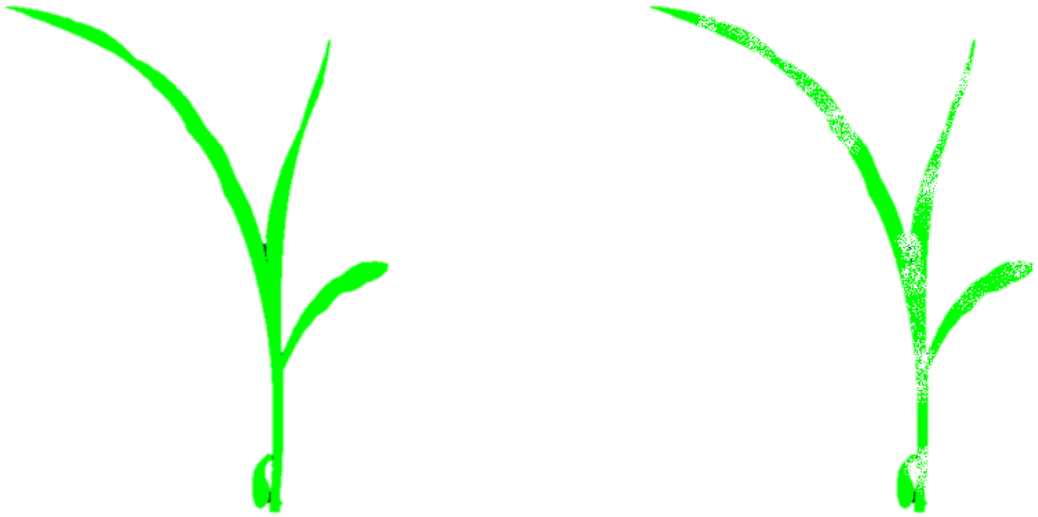

(A) All images

(B) 55 images

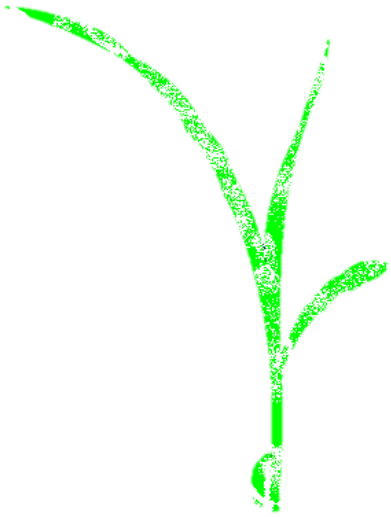

(C) 40 images

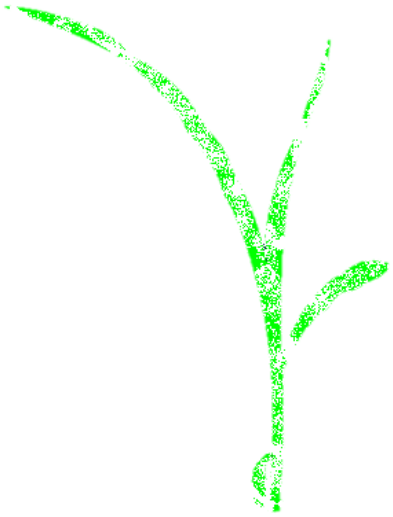

(D) 25 images

FIGURE A.3: Example 3D reconstructions of a maize plant with different numbers of input images

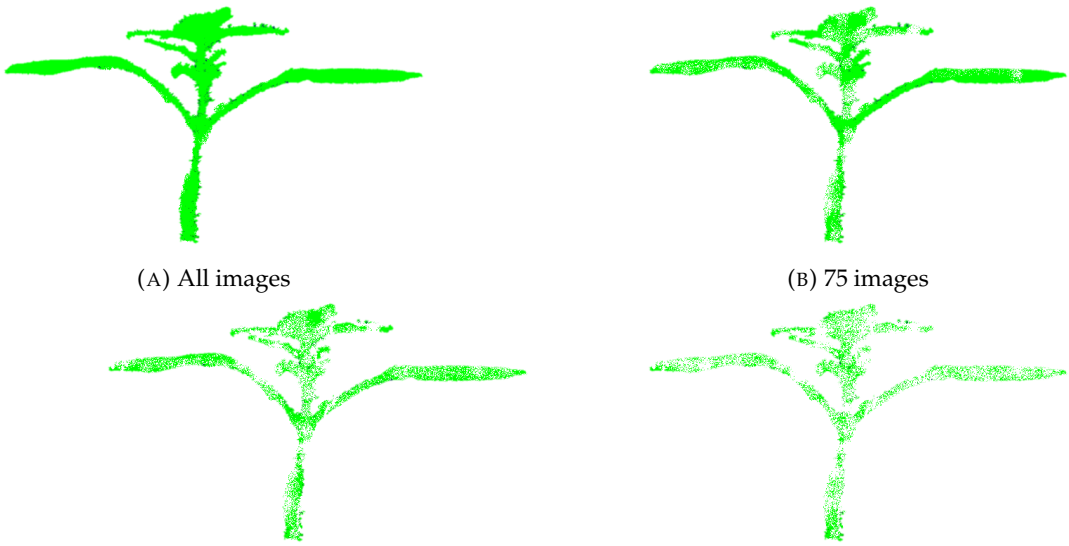

(A) All images (B) 75 images

(C) 50 images (D) 25 images

FIGURE A.4: Example 3D reconstructions of a tomato plant with different numbers of input images

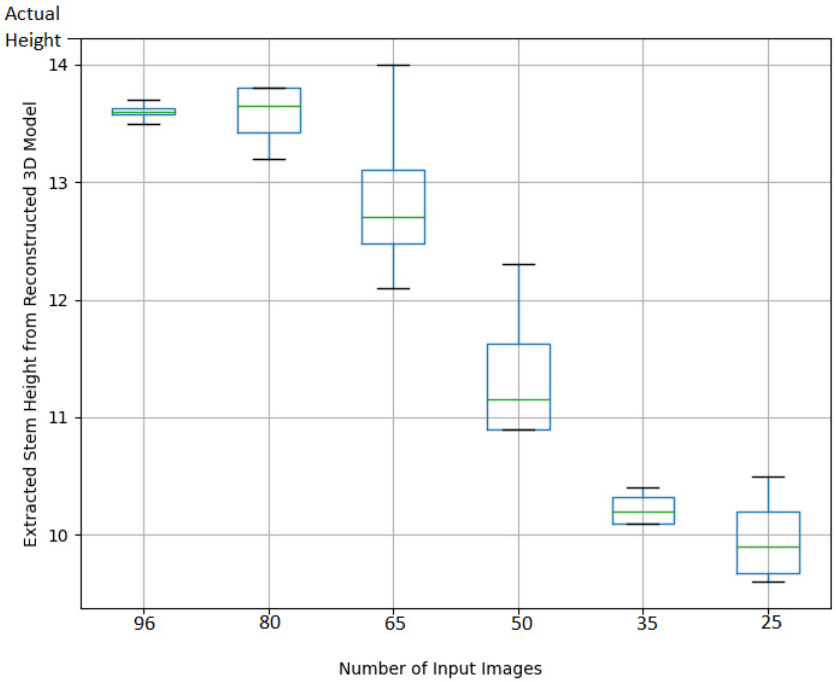

FIGURE A.5: Extracted stem height from reconstructed 3D model with change in number of input images for cauliflower plant

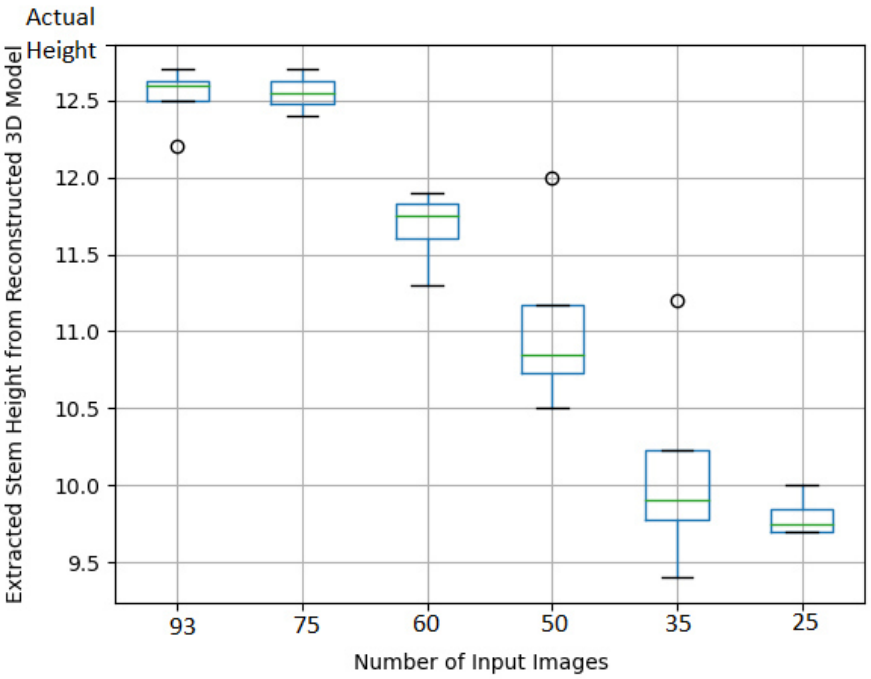

FIGURE A.6: Extracted stem height from reconstructed 3D model with change in number of input images for tomato plant

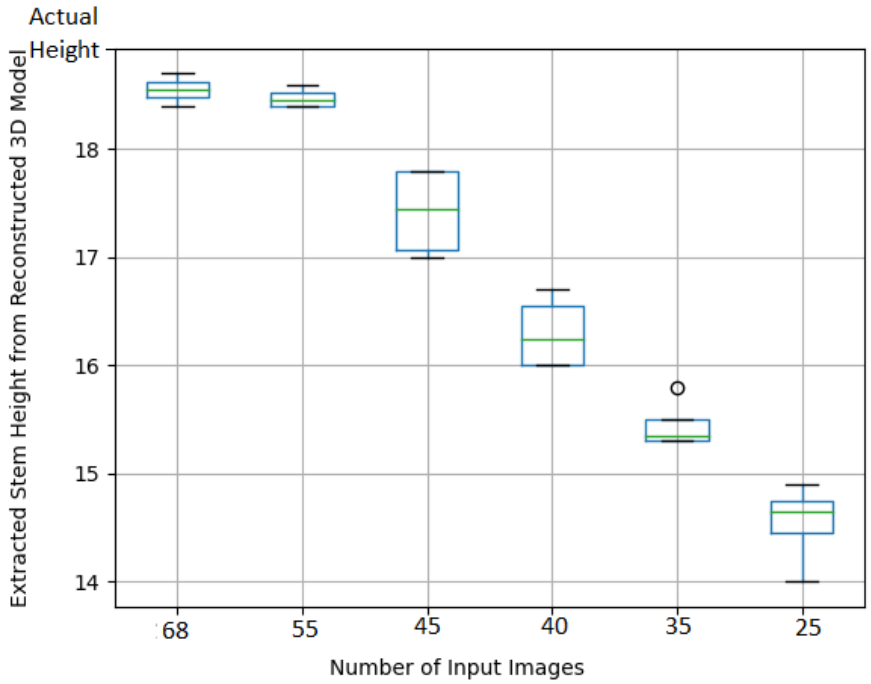

FIGURE A.7: Extracted stem height from reconstructed 3D model with change in number of input images for maize plant

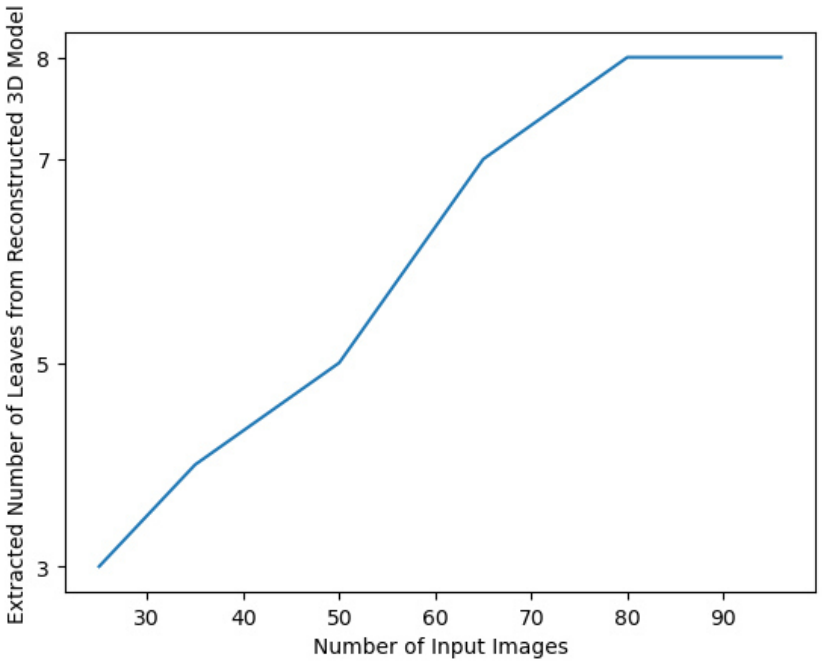

FIGURE A.8: Extracted number of leaves from reconstructed 3D model with change in number of input images for cauliflower plant

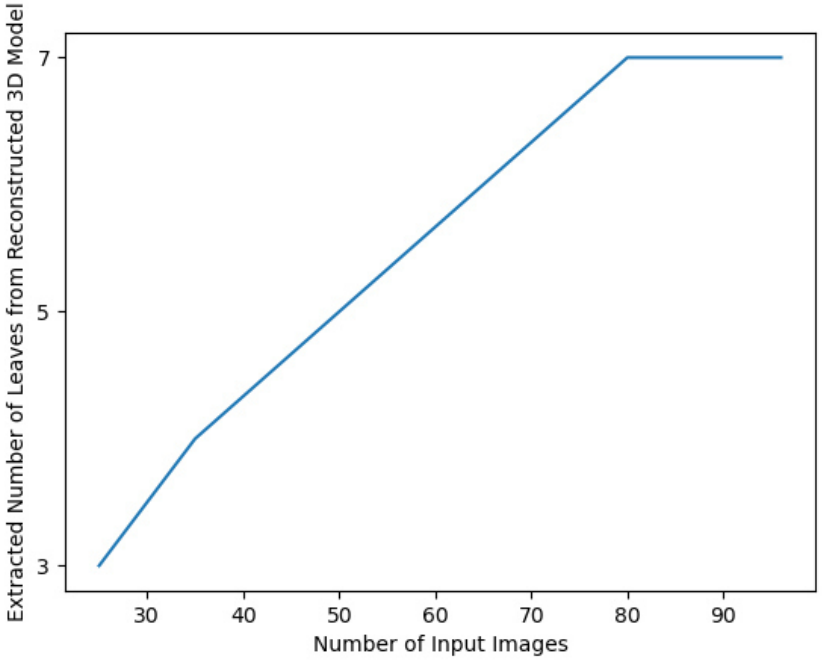

FIGURE A.9: Extracted number of leaves from reconstructed 3D model with change in number of input images for tomato plant

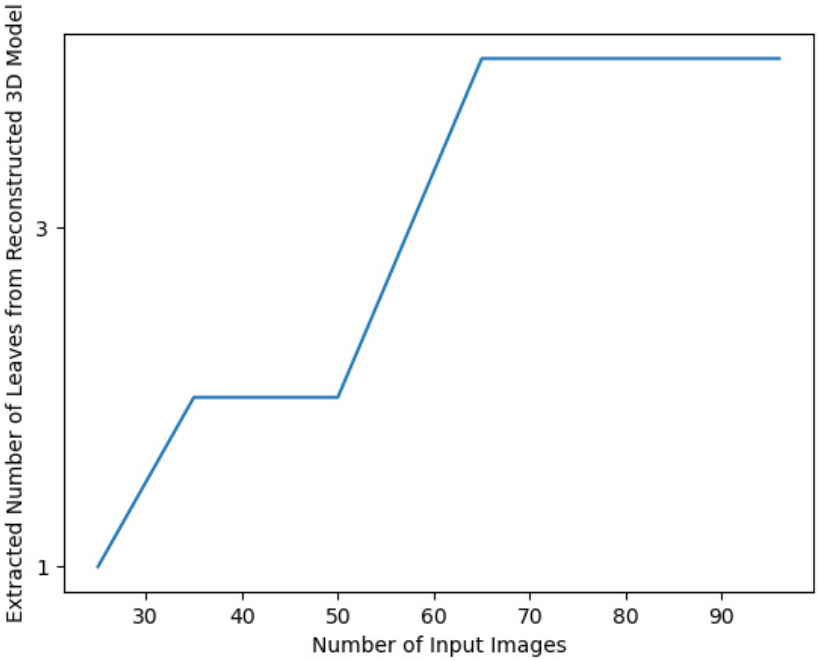

FIGURE A.10: Extracted number of leaves from reconstructed 3D model with change in number of input images for maize plant

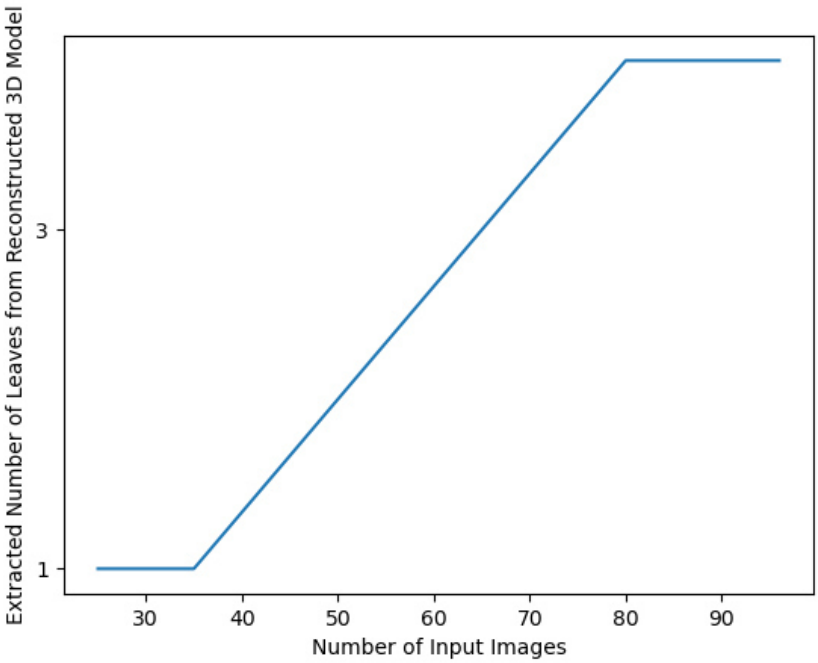

FIGURE A.11: Extracted number of leaves from reconstructed 3D model with change in number of input images for lettuce plant

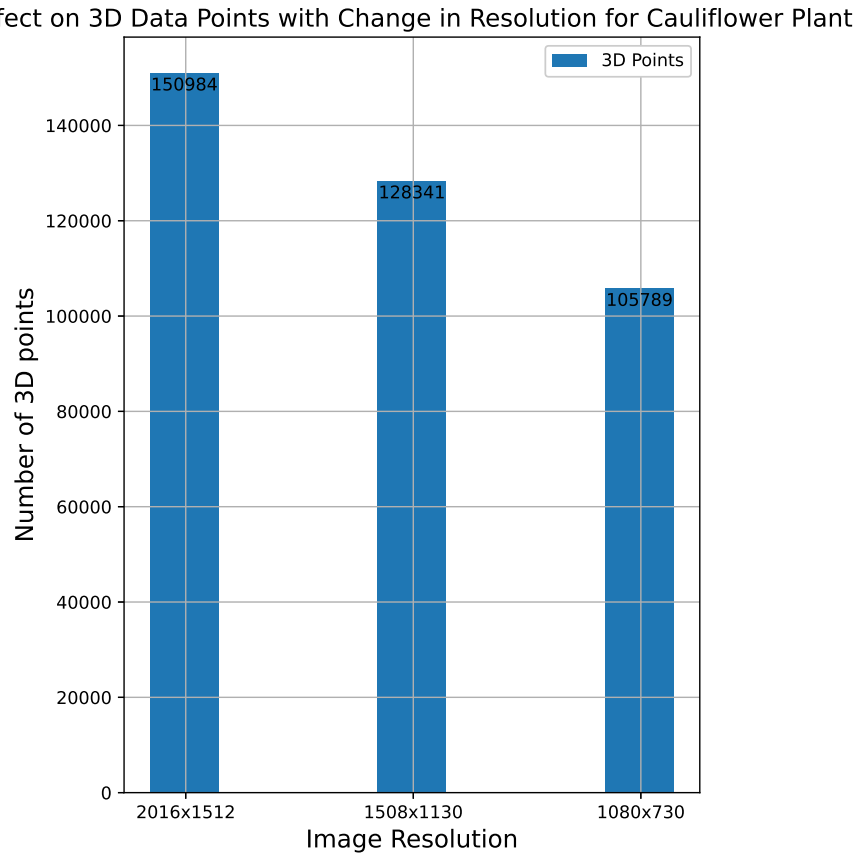

FIGURE A.12: Number of 3D data points detected for different image resolutions for cauliflower plant

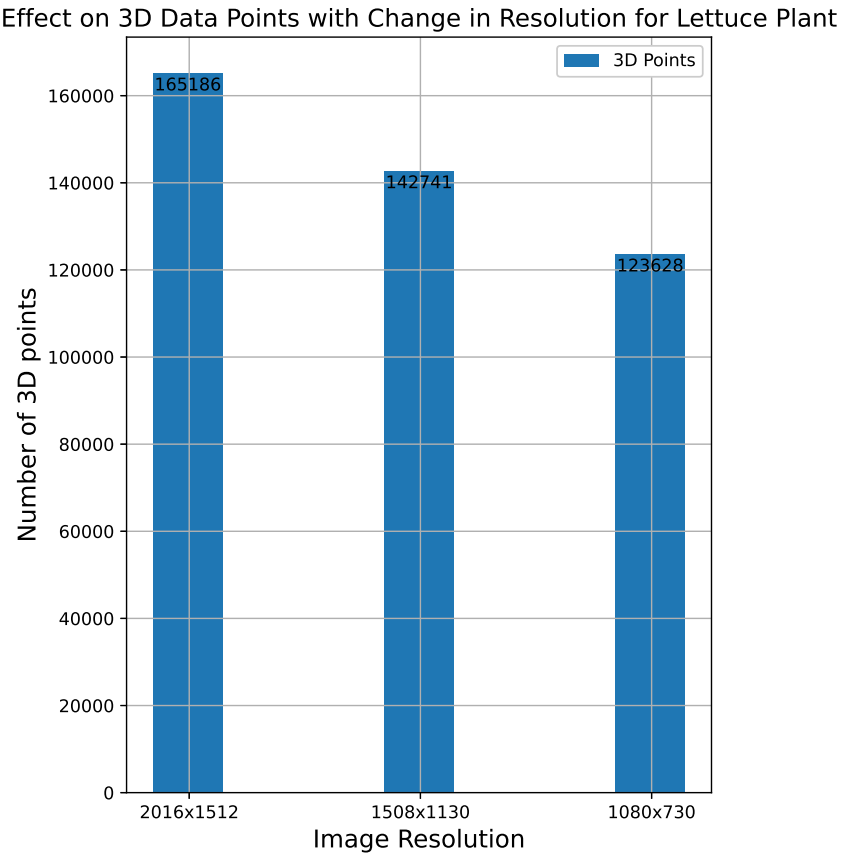

FIGURE A.13: Number of 3D data points detected for different image resolutions for lettuce plant

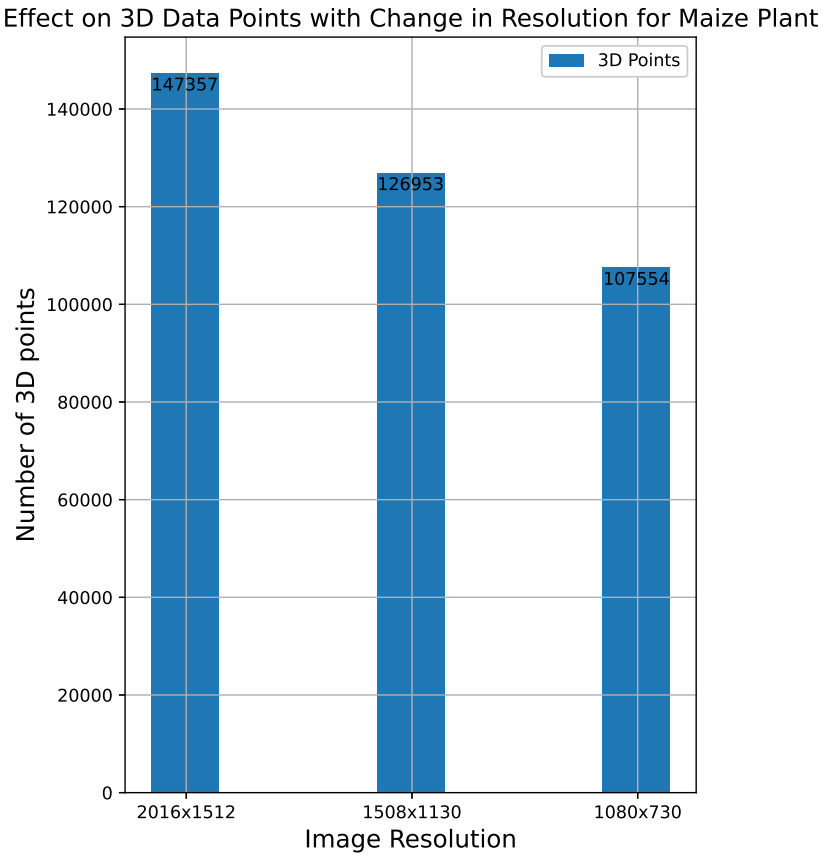

FIGURE A.14: Number of 3D data points detected for different image resolutions for maize plant

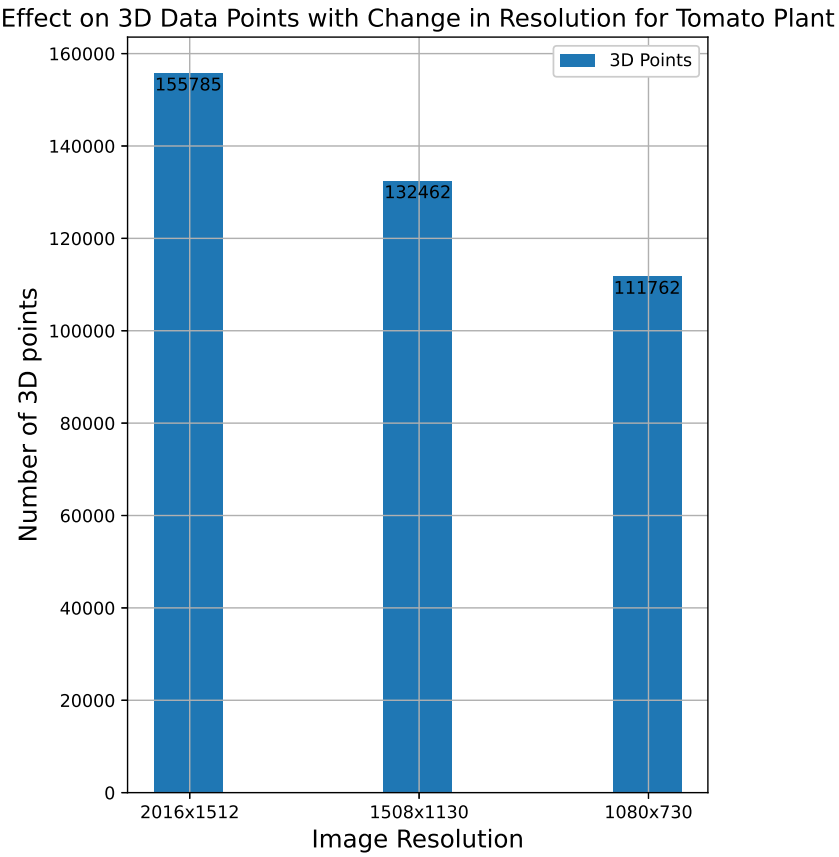

FIGURE A.15: Number of 3D data points detected for different image resolutions for tomato plant

Appendix B

Supplementary Material

B.1 Chapter 6: Plant Traits Measurement in 3D

Addition results of plant traits measurement for remaining plants.

B.2 Videos

The videos of various 3D modeling steps are provided on the following link: PhD Videos - Click Here

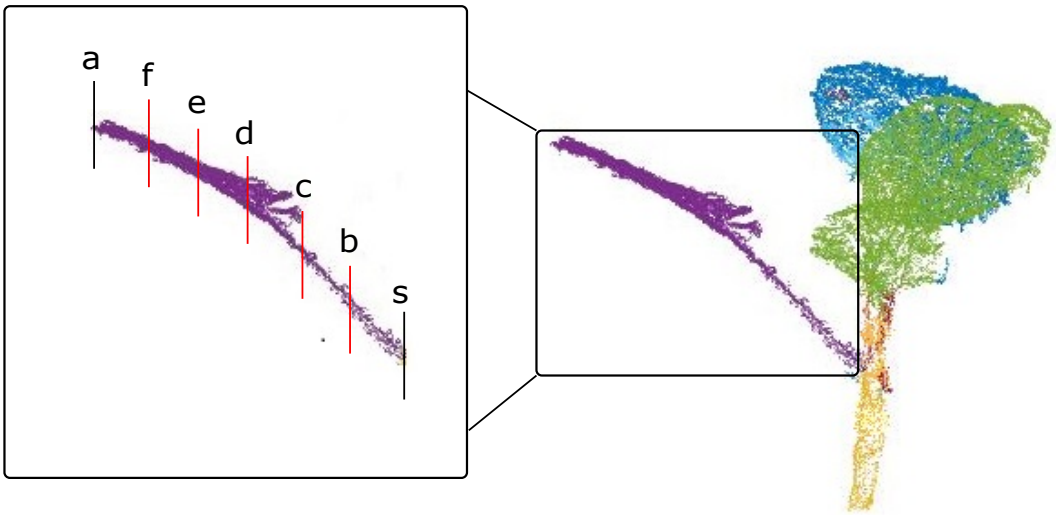

FIGURE B.1: Leaf length measurement for cauliflower

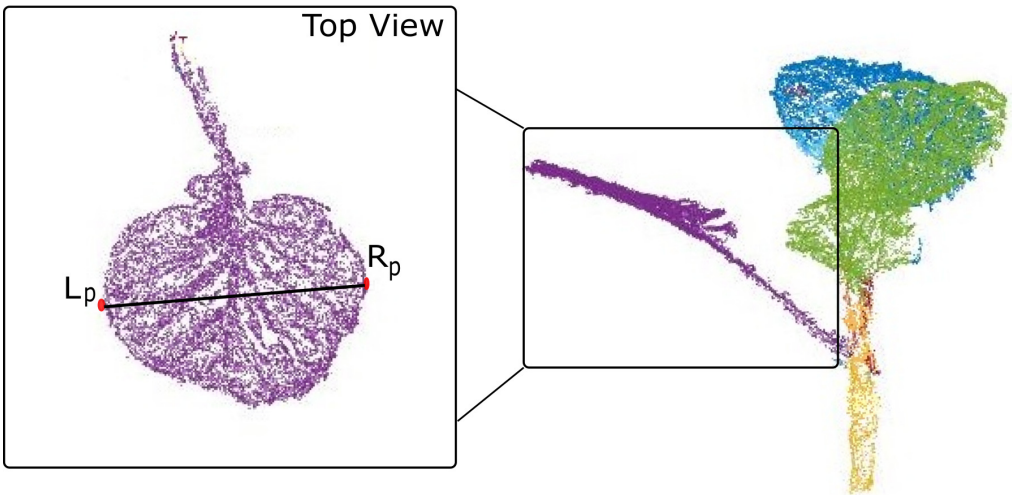

FIGURE B.2: Leaf width measurement for cauliflower

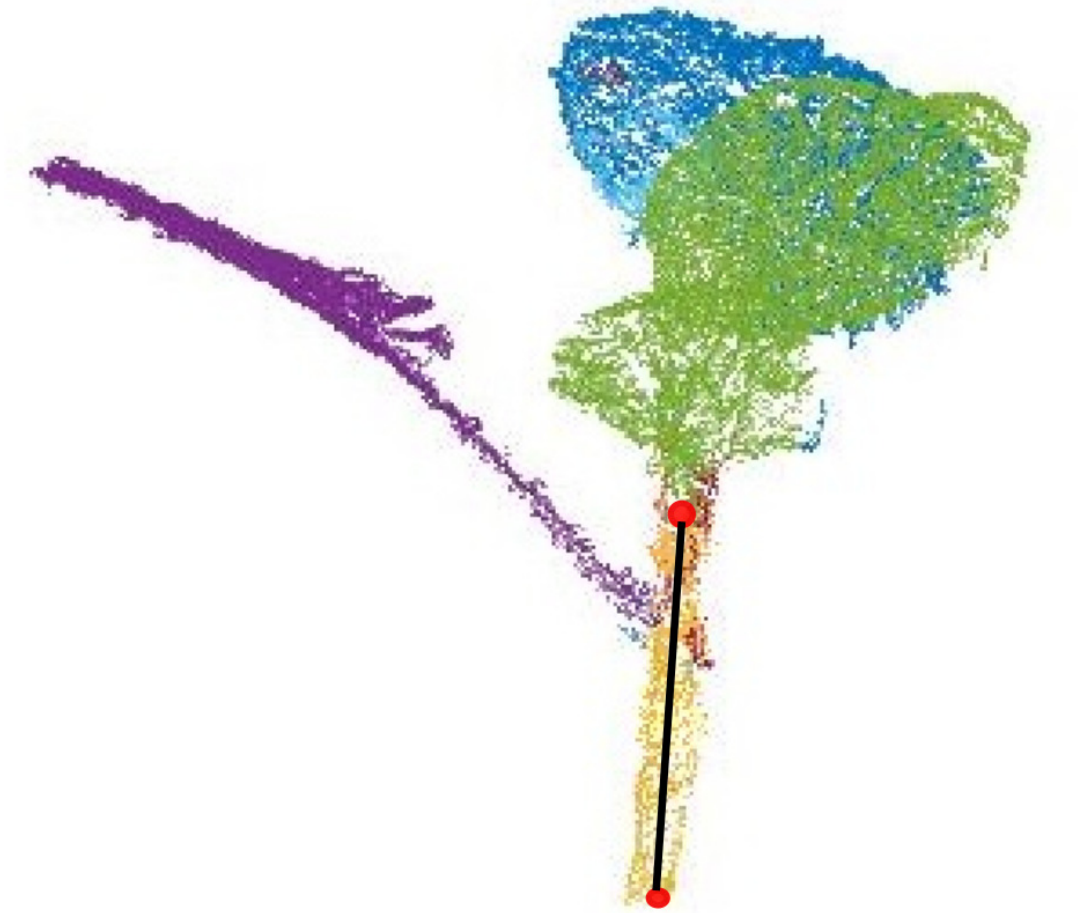

FIGURE B.3: Stem measurement for cauliflower

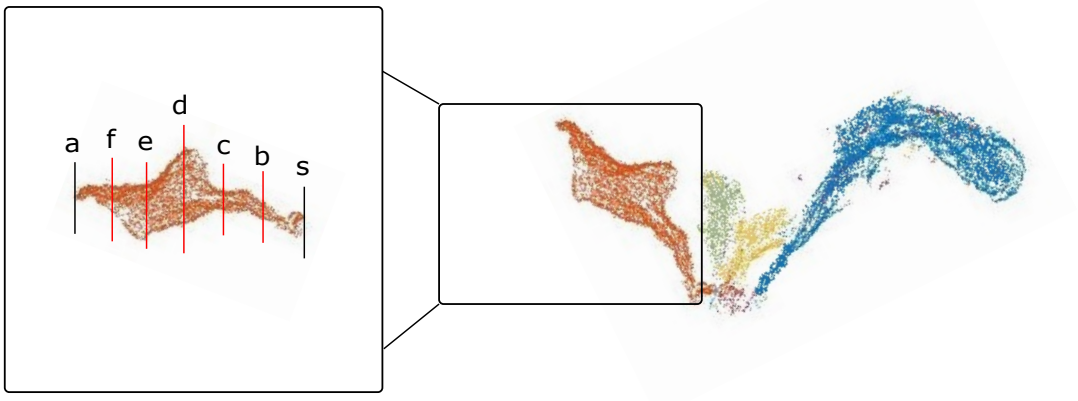

FIGURE B.4: Leaf length measurement for cauliflower

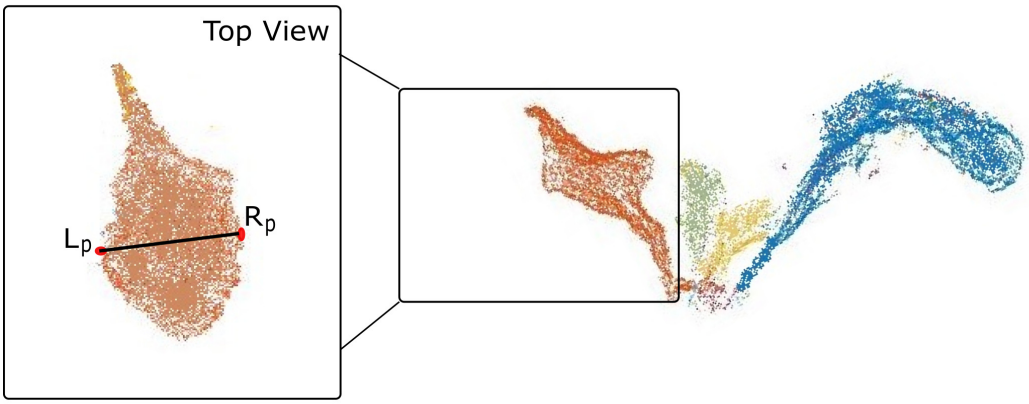

FIGURE B.5: Leaf length measurement for cauliflower

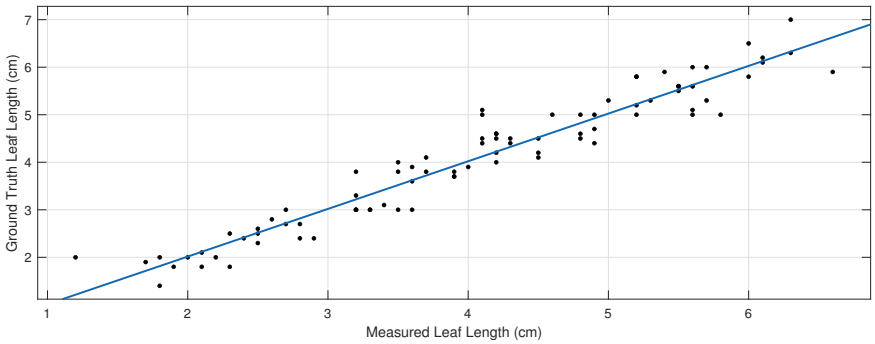

FIGURE B.6: Correlation between ground truth and measured leaf length for Cauliflower plant

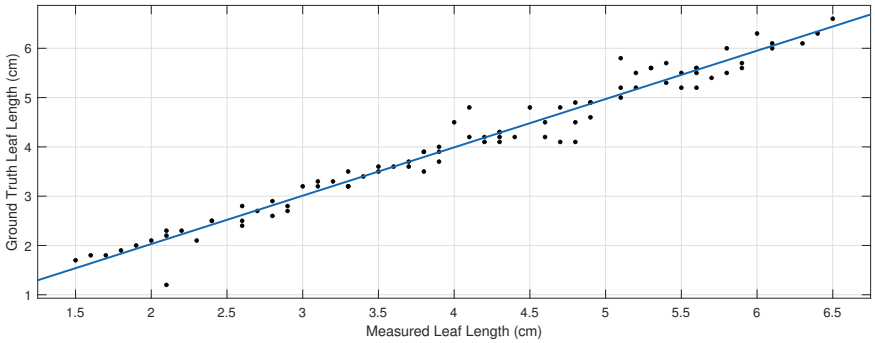

FIGURE B.7: Correlation between ground truth and measured leaf length for Tomato plant

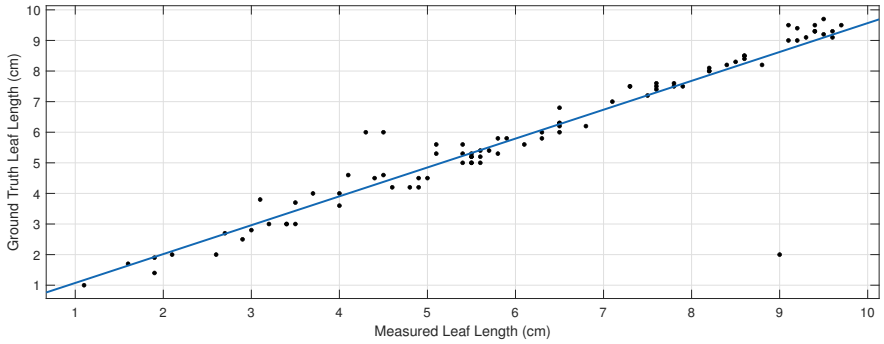

FIGURE B.8: Correlation between ground truth and measured leaf length for Maize plant

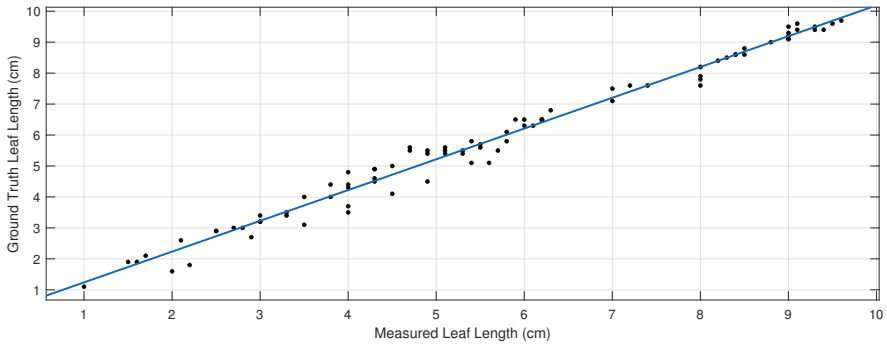

FIGURE B.9: Correlation between ground truth and measured leaf length for Lettuce plant

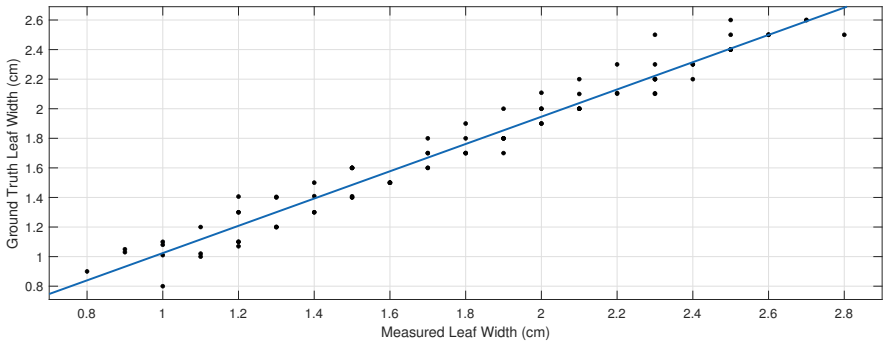

FIGURE B.10: Correlation between ground truth and measured leaf width for Cauliflower plant

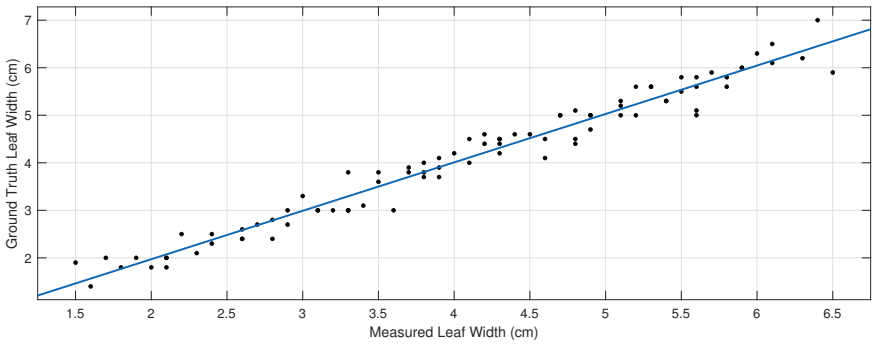

FIGURE B.11: Correlation between ground truth and measured leaf width for Tomato plant

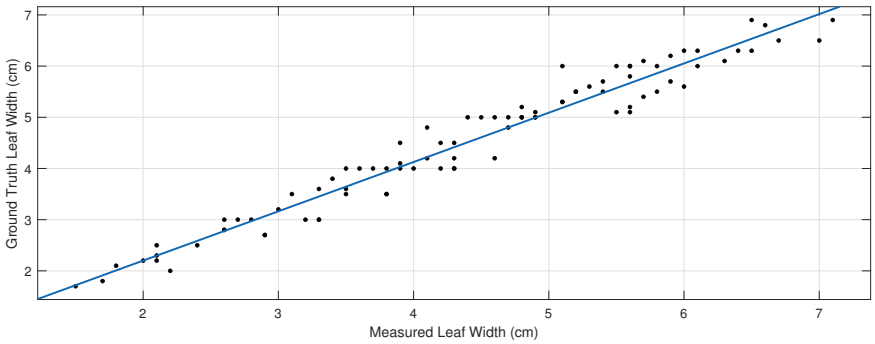

FIGURE B.12: Correlation between ground truth and measured leaf width for Lettuce plant

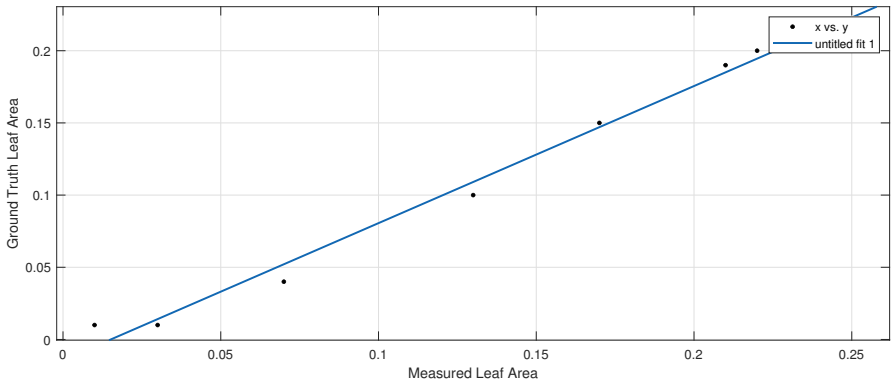

FIGURE B.13: Correlation between ground truth and measured values for leaf area (cm^2) for Cauliflower plant

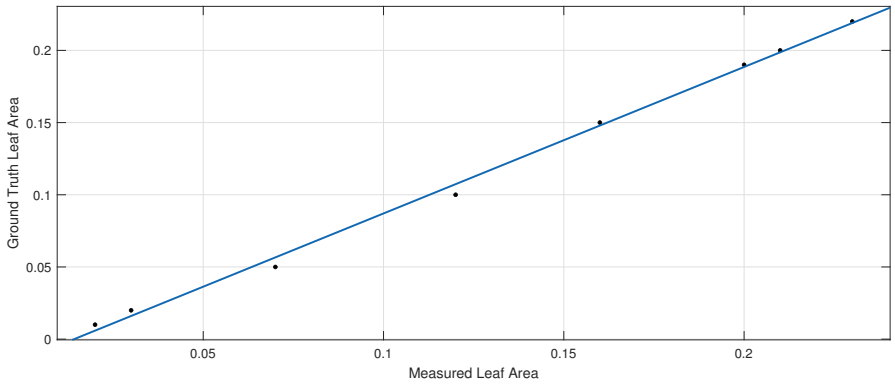

FIGURE B.14: Correlation between ground truth and measured values for leaf area (cm^2) for Tomato plant

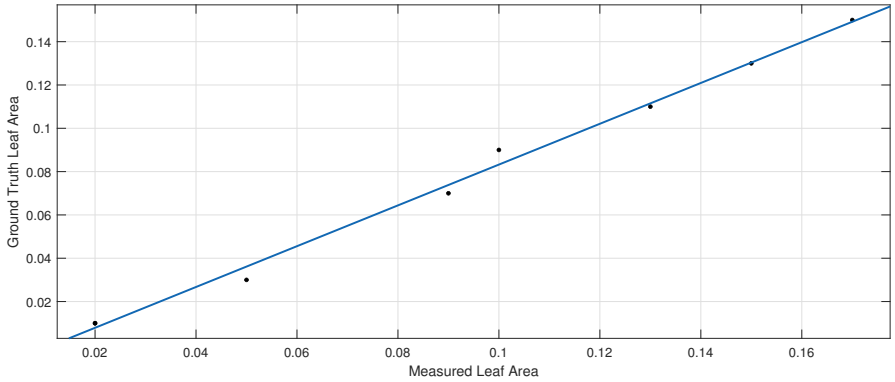

FIGURE B.15: Correlation between ground truth and measured values for leaf area (cm^2) for Maize plant

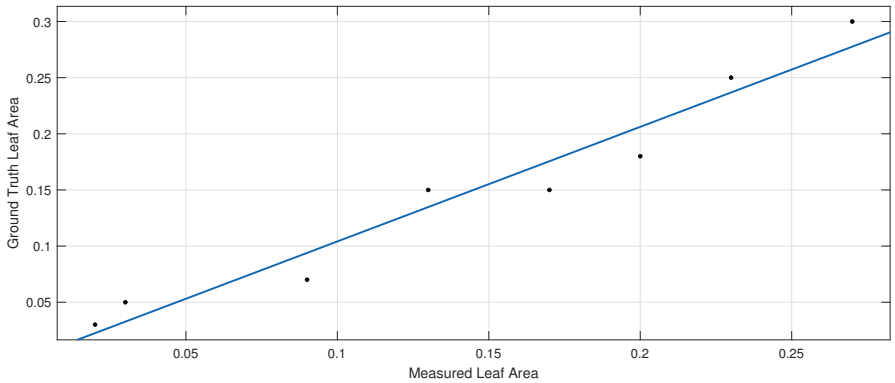

FIGURE B.16: Correlation between ground truth and measured values for leaf area (cm^2) for Lettuce plant

References

[1] URL: https://www.hortnz.co.nz/about-us/.

[2] Caroline A. Schneider, Wayne S. Rasband, and Kevin Eliceiri. "NIH Image to ImageJ: 25 years of image analysis". In: *Nature Methods* 9 (July 2012).

[3] Marco Attene, Bianca Falcidieno, and Michela Spagnuolo. "Hierarchical mesh segmentation based on fitting primitives". In: *The Visual Computer* 22.3 (Mar. 2006), pp. 181–193.

[4] Tavor Baharav, Mohini Bariya, and Avideh Zakhor. "In situ height and width estimation of sorghum plants from 2.5D infrared images". In: *Electronic Imaging* (2017).

[5] Jenny Balfer, F. Schöler, and V. Steinhage. "Semantic skeletonization for structural plant analysis". In: *FSPM2013 - 7th International Conference on Functional-Structural Plant Models*. 2013.

[6] Bruce G. Baumgart. "Geometric modeling for computer vision." In: *Computer Science*. 1974.

[7] Joshua R. Ben-Arie et al. "Development of a pit filling algorithm for LiDAR canopy height models". In: *Computers & Geosciences* 35.9 (2009), pp. 1940–1949.

[8] Yizhak Ben-Shabat, Michael Lindenbaum, and Anath Fischer. "3D Point cloud classification and segmentation using 3D modified fisher vector representation for convolutional neural networks". In: *CoRR* (2017).

[9] Sergej Bergsträsser et al. "HyperART: Non-invasive quantification of leaf traits using hyperspectral absorption-reflectance-transmittance imaging". In: *Plant Methods* 11 (Jan. 2015).

[10] Paul J. Besl and Neil D. McKay. "Method for registration of 3D shapes". In: *Sensor fusion IV: control paradigms and data structures*. Ed. by Paul S. Schenker. Vol. 1611. SPIE, 1992, pp. 586–606.

[11] Bernhard Biskup, Hanno Scharr, and Uli Schurr. "A stereo imaging system for measuring structural parameters of plant canopies". In: *Plant, Cell & Environment* 30 (Nov. 2007), pp. 1299–308.

[12] Bernhard Biskup et al. "A stereo imaging system for measuring structural parameters of plant canopies". In: *Plant, Cell & Environment* 30.10 (2007), pp. 1299–1308.

[13] Dobrina Boltcheva et al. "A spectral clustering approach of vegetation components for describing plant topology and geometry from terrestrial waveform LiDAR data". In: *FSPM2013 - 7th International Conference on Functional-Structural Plant Models*. May 2013.

[14] Alexandre Boulch et al. "SnapNet: 3D point cloud semantic labeling with 2D deep segmentation networks". In: *Computers & Graphics* 71 (2018), pp. 189–198.

[15] Alexander Bucksch and Stefan Fleck. "Automated detection of branch dimensions in woody skeletons of fruit tree canopies". In: *SilviLaser 2009 proceedings, 14.-16. October 2009 Austin,Texas* 77 (Jan. 2009).

[16] Alexander Bucksch and Roderik Lindenbergh. "CAMPINO: A skeletonization method for point cloud processing". In: *ISPRS Journal of Photogrammetry and Remote Sensing* 63.1 (2008), pp. 115–127.

[17] Alexander Bucksch, Roderik Lindenbergh, and Massimo Menenti. "SkelTre - fast skeletonisation for imperfect point cloud data of botanic trees." In: *Eurographics Workshop on 3D Object Retrieval, EG 3DOR*. Jan. 2009, pp. 13–20.

[18] Llorenç Cabrera-Bosquet et al. "High-throughput estimation of incident light, light interception and radiation-use efficiency of thousands of plants in a phenotyping platform". In: *New Phytologist* 212.1 (2016), pp. 269–281.

[19] Jonathan L. Carrivick, Mark W. Smith, and Duncan J. Quincey. "Structure from motion in the geosciences". In: *Wiley Publishing* (2016).

[20] Supawadee Chaivivatrakul et al. "Automatic morphological trait characterization for corn plants via 3D holographic reconstruction". In: *Computers and Electronics in Agriculture* 109 (2014), pp. 109–123.

[21] Ayan Chaudhury. "Computer vision problems in 3D plant phenotyping". PhD thesis. University of Western Ontario, Canada, 2017.

[22] Ayan Chaudhury et al. "Machine vision system for 3D plant phenotyping". In: *IEEE/ACM Transactions on Computational Biology and Bioinformatics* 16.6 (2019), pp. 2009–2022.

[23] Yann Chéné et al. "On the use of depth camera for 3D phenotyping of entire plants". In: *Computers and Electronics in Agriculture* 82 (2012), pp. 122–127.

[24] Paolo Cignoni et al. "MeshLab: an open-source mesh processing tool". In: *Eurographics Italian Chapter Conference*. Ed. by Vittorio Scarano, Rosario De Chiara, and Ugo Erra. The Eurographics Association, 2008.

[25] Randy T. Clark et al. "Three-dimensional root phenotyping with a novel imaging and software platform". In: *Plant Physiology* 156.2 (2011), pp. 455–465.

[26] Robert L. Cook. "Stochastic sampling in computer graphics". In: *ACM Trans. Graph.* 5.1 (Jan. 1986), pp. 51–72.

[27] Andrea Corti et al. "A metrological characterization of the Kinect V2 time-of-flight camera". In: *Robotics and Autonomous Systems* 75 (Oct. 2015).

[28] Corrado Costa et al. "Plant phenotyping research trends, a science mapping approach". In: *Frontiers in Plant Science* 9 (2019).

[29] Jean-François Côté et al. "The structural and radiative consistency of three-dimensional tree reconstructions from terrestrial lidar". In: *Remote Sensing of Environment* 113.5 (2009), pp. 1067–1081.

[30] Jeffrey A. Cruz et al. "Multi-modality imagery database for plant phenotyping". In: *Machine Vision and Applications* 27.5 (July 2016), pp. 735–749.

[31] W. Bruce Culbertson, Thomas Malzbender, and Greg Slabaugh. "Generalized voxel coloring". In: *Vision Algorithms: Theory and Practice*. Ed. by Bill Triggs, Andrew Zisserman, and Richard Szeliski. Berlin, Heidelberg: Springer Berlin Heidelberg, 2000, pp. 100–115.

[32] Sylvain Delagrange, Christian Jauvin, and Pascal Rochon. "PypeTree: a tool for reconstructing tree perennial tissues from point clouds". In: *Sensors (Basel, Switzerland)* 14 (Mar. 2014), pp. 4271–89.

[33] D. Dey, L. Mummert, and R. Sukthankar. "Classification of plant structures from uncalibrated image sequences". In: *2012 IEEE Workshop on the Applications of Computer Vision (WACV)*. Jan. 2012, pp. 329–336.

[34] E. W. Dijkstra. "A note on two problems in connexion with graphs". In: *Numerische Mathematik* 1.1 (Dec. 1959), pp. 269–271. ISSN: 0945-3245.

[35] Tino Dornbusch et al. "Measuring the diurnal pattern of leaf hyponasty and growth in Arabidopsis - a novel phenotyping approach using laser scanning". In: *Functional Plant Biol.* 39.11 (2012), pp. 860–869.

[36] T. Duan et al. "Dynamic quantification of canopy structure to characterize early plant vigour in wheat genotypes". In: *Journal of Experimental Botany* 67.15 (June 2016), pp. 4523–4534.

[37] Jan Dupuis et al. "A multi-resolution approach for an automated fusion of different low-cost 3D sensors". In: *Sensors* 14 (Apr. 2014), pp. 7563–79.

[38] Jan Dupuis et al. "The impact of different leaf surface tissues on active 3D laser triangulation measurements". In: *Photogrammetrie - Fernerkundung - Geoinformation* 2015 (Dec. 2015), pp. 437–447.

[39] Charles Dyer. *Volumetric scene reconstruction from multiple views*. Vol. 628. Mar. 2001, pp. 469–489.

[40] Herbert Edelsbrunner and Ernst P. Mücke. "Three-dimensional alpha shapes". In: *ACM Trans. Graph.* 13.1 (Jan. 1994), pp. 43–72.

[41] Liviu Ene, Erik Næsset, and Terje Gobakken. "Single tree detection in heterogeneous boreal forests using airborne laser scanning and area-based stem number estimates". In: *International Journal of Remote Sensing* 33.16 (2012), pp. 5171–5193.

[42] J. Estornell et al. "Tree extraction and estimation of walnut structure parameters using airborne LiDAR data". In: *International Journal of Applied Earth Observation and Geoinformation* 96 (2021), p. 102273.

[43] Pedro F. Felzenszwalb and Daniel P. Huttenlocher. "Efficient graph-based image segmentation". In: *International Journal of Computer Vision* 59.2 (Sept. 2004), pp. 167–181.

[44] Martin A. Fischler and Robert C. Bolles. "Random sample consensus: a paradigm for model fitting with applications to image analysis and automated cartography". In: *Readings in Computer Vision*. Ed. by Martin A. Fischler and Oscar Firschein. San Francisco (CA): Morgan Kaufmann, 1987, pp. 726–740.

[45] Richard J. Flavel et al. "An image processing and analysis tool for identifying and analysing complex plant root systems in 3D soil using non-destructive analysis: Root1". In: *PLOS ONE* 12.5 (May 2017), pp. 1–18.

[46] Michael Friedli et al. "Terrestrial 3D laser scanning to track the increase in canopy height of both monocot and dicot crop species under field conditions". In: *Plant Methods* 12 (Jan. 2016).

[47] Robert T. Furbank and Mark Tester. "Phenomics : technologies to relieve the phenotyping bottleneck". In: *Trends in Plant Science* 16.12 (2011), pp. 635–644. ISSN: 1360-1385.

[48] William Gelard et al. “3D plant phenotyping in sunflower using architecture-based organ segmentation from 3D point clouds”. In: *5th International Workshop on Image Analysis Methods for the Plant Sciences*. 2016.

[49] William Gelard. et al. “Model-based segmentation of 3D point clouds for phenotyping sunflower plants”. In: *Proceedings of the 12th International Joint Conference on Computer Vision, Imaging and Computer Graphics Theory and Applications - Volume 4: VISAPP, (VISIGRAPP 2017)*. SciTePress, 2017, pp. 459–467.

[50] Jason Geng. “Structured-light 3D surface imaging: A tutorial”. In: *Advances in Optics and Photonics* 3 (June 2011), pp. 128–160.

[51] Christophe Godin. “Representing and encoding plant architecture: A review”. In: *Annals of Forest Science* 57 (June 2000).

[52] Franck Golbach et al. “Validation of plant part measurements using a 3D reconstruction method suitable for high-throughput seedling phenotyping”. In: *Machine Vision and Applications* 27.5 (July 2016), pp. 663–680.

[53] Mahmood Reza Golzarian et al. “Accurate inference of shoot biomass from high-throughput images of cereal plants”. In: *Plant Methods*. 2010.

[54] T. Grift et al. “A review of automation and robotics for the bio-industry”. In: *Journal of Biomechatronics Engineering*. 2008.

[55] Paul Guerrero et al. “PCPNET: learning local shape properties from raw point clouds”. In: *CoRR* (2017).

[56] Qinghua Guo et al. “Crop 3D—a LiDAR based platform for 3D high-throughput crop phenotyping”. In: *Science China Life Sciences* 61.3 (Mar. 2018), pp. 328–339.

[57] Tai Guo et al. “Detection of wheat height using optimized multi-scan mode of LiDAR during the entire growth stages”. In: *Computers and Electronics in Agriculture* 165 (2019), p. 104959. ISSN: 0168-1699.

[58] Sandeep Gupta, Holger Weinacker, and Barbara Koch. “Comparative analysis of clustering-based approaches for 3-D single tree detection using airborne fullwave lidar data”. In: *Remote Sensing* 2.4 (2010), pp. 968–989.

[59] Liang Han et al. “Clustering field-based maize phenotyping of plant-height growth and canopy spectral dynamics using a UAV remote-sensing approach”. In: *Frontiers in Plant Science* 9 (2018), p. 1638.

[60] Richard Hartley and Andrew Zisserman. *Multiple view geometry in computer vision*. 2nd ed. Cambridge University Press, 2004.

[61] Anja Hartmann et al. “HTPheno: An image analysis pipeline for high-throughput plant phenotyping”. In: *BMC Bioinformatics*. 2010.

[62] Kaiming He et al. “Mask R-CNN”. In: *CoRR* abs/1703.06870 (2017).

[63] Gerie van der Heijden et al. “SPICY: towards automated phenotyping of large pepper plants in the greenhouse”. In: *Functional Plant Biology - FUNCT PLANT BIOL* 39 (Jan. 2012).

[64] Franck Hétroy-Wheeler, Eric Casella, and Dobrina Boltcheva. “Segmentation of tree seedling point clouds into elementary units”. In: *International Journal of Remote Sensing* 37.13 (2016), pp. 2881–2907.

[65] Bernhard Höfle and M. Hollaus. "Urban vegetation detection using high density full-waveform airborne LIDAR data - Combination of object-based image and point cloud analysis". In: *International Archives of the Photogrammetry, Remote Sensing and Spatial Information Sciences - ISPRS Archives* 38 (Jan. 2010).

[66] Johan Holmgren et al. "Prediction of stem attributes by combining airborne laser scanning and measurements from harvesters". In: *Silva Fennica* 46 (Jan. 2012).

[67] Fumiki Hosoi, Kazushige Nakabayashi, and Kenji Omasa. "3-D modeling of tomato canopies using a high-resolution portable scanning Lidar for extracting structural information". In: *Sensors (Basel, Switzerland)* 11 (2011), pp. 2166–2174.

[68] Fumiki Hosoi and Kenji Omasa. "Estimation of vertical plant area density profiles in a rice canopy at different growth stages by high-resolution portable scanning lidar with a lightweight mirror". In: *ISPRS Journal of Photogrammetry and Remote Sensing* 74 (2012), pp. 11–19. ISSN: 0924-2716.

[69] Fengjun Hu et al. "Discrete point cloud filtering and searching based on VGSO algorithm". In: *Proceedings - 27th European Conference on Modelling and Simulation, ECMS 2013*. May 2013, pp. 850–856.

[70] Yang Hu et al. "Automatic non-destructive growth measurement of leafy vegetables based on Kinect". In: *Sensors* 18 (Mar. 2018), p. 806.

[71] Kenta Itakura, Itchoku Kamakura, and Fumiki Hosoi. "Three-dimensional monitoring of plant structural parameters and chlorophyll distribution". In: *Sensors* 19 (Jan. 2019), p. 413.

[72] N. Ivanov et al. "Computer stereo plotting for 3D reconstruction of a maize canopy". In: *Agricultural and Forest Meteorology* 75.1 (1995), pp. 85–102.

[73] Miguel Izard et al. "3D maize plant reconstruction based on georeferenced overlapping LiDAR point clouds". In: *Remote Sensing* 7 (Dec. 2015), pp. 17077–17096.

[74] A. K. Jain, M. N. Murty, and P. J. Flynn. "Data clustering: a review". In: *ACM Computing Surveys* 31.3 (1999).

[75] Sylvain Jay et al. "In-field crop row phenotyping from 3D modeling performed using Structure from Motion". In: *Computers and Electronics in Agriculture* 110 (2015), pp. 70–77.

[76] Jianbo Shi and J. Malik. "Normalized cuts and image segmentation". In: *IEEE Transactions on Pattern Analysis and Machine Intelligence* 22.8 (Aug. 2000), pp. 888–905.

[77] Harri Kaartinen et al. "An international comparison of individual tree detection and extraction using airborne laser scanning". In: *Remote Sensing* 4.4 (2012), pp. 950–974.

[78] Yinghai Ke and Lindi J. Quackenbush. "A review of methods for automatic individual tree-crown detection and delineation from passive remote sensing". In: *International Journal of Remote Sensing* 32.17 (2011), pp. 4725–4747.

[79] Maria Klodt and Daniel Cremers. "High-resolution plant shape measurements from multi-view stereo reconstruction". In: *Computer Vision - ECCV 2014 Workshops*. Ed. by Lourdes Agapito, Michael M. Bronstein, and Carsten Rother. Cham: Springer International Publishing, 2015, pp. 174–184.

[80] Barbara Koch, Ursula Heyder, and Holger Weinacker. "Detection of individual tree crowns in airborne Lidar data". In: *Photogrammetric Engineering & Remote Sensing* 72.4 (2006), pp. 357–363.

[81] Barbara Koch et al. "Airborne laser data for stand delineation and information extraction". In: *International Journal of Remote Sensing* 30 (Feb. 2009), pp. 935–963.

[82] Jack Koci et al. "Assessment of UAV and ground-based structure from motion with multi-view stereo photogrammetry in a Gullied Savanna Catchment". In: *ISPRS International Journal of Geo-Information* 6.11 (2017).

[83] Philipp Krähenbühl and Vladlen Koltun. "Efficient inference in fully connected CRFs with Gaussian edge potentials". In: *CoRR* (2012).

[84] P. Kumar, J. Connor, and S. Mikiavcic. "High-throughput 3D reconstruction of plant shoots for phenotyping". In: *2014 13th International Conference on Control Automation Robotics Vision (ICARCV)*. Dec. 2014.

[85] Kiriakos N. Kutulakos and Steven M. Seitz. "A theory of shape by space carving". In: *International Journal of Computer Vision* 38.3 (July 2000), pp. 199–218.

[86] Timo Lahivaara et al. "Bayesian approach to tree detection based on airborne laser scanning data". In: *IEEE Transactions on Geoscience and Remote Sensing* 52.5 (2014), pp. 2690–2699.

[87] P. Lancaster and K. Salkauskas. "Surfaces generated by moving least squares methods". In: *Mathematics of Computation*. Vol. 137. 1981, pp. 141–158.

[88] Morten Larsen et al. "Comparison of six individual tree crown detection algorithms evaluated under varying forest conditions". In: *International Journal of Remote Sensing* 32.20 (2011), pp. 5827–5852.

[89] Franz Leberl et al. "Point clouds: Lidar versus 3D vision". In: *Photogrammetric Engineering and Remote Sensing* 76 (2010), pp. 1123–1134.

[90] Michael A. Lefsky et al. "Lidar remote sensing for ecosystem studies". In: *BioScience* 52.1 (Jan. 2002), pp. 19–30.

[91] L. Li et al. "A reverse engineering system for rapid manufacturing of complex objects". In: *Robotics and Computer-Integrated Manufacturing* 18.1 (2002), pp. 53–67.

[92] Lei Li, Qin Zhang, and Danfeng Huang. "A review of imaging techniques for plant phenotyping". In: *Sensors* 14.11 (2014), pp. 20078–20111.

[93] Penglei Li et al. "Estimating aboveground and organ biomass of plant canopies across the entire season of rice growth with terrestrial laser scanning". In: *International Journal of Applied Earth Observation and Geoinformation* 91 (2020), p. 102132.

[94] Yangyan Li et al. "Analyzing growing plants from 4D point cloud data". In: *ACM Trans. Graph.* 32.6 (Nov. 2013).

[95] S-X Liu et al. "On the relationship between multi-view data capturing and quality of rendered virtual view". In: *The Imaging Science Journal* 57.5 (2009), pp. 250–259.

[96] Suxing Liu et al. "Novel low cost 3D surface model reconstruction system for plant phenotyping". In: *Journal of Imaging* 3.3 (2017).

[97] Yotam Livny et al. "Automatic reconstruction of tree skeletal structures from point clouds". In: *ACM SIGGRAPH Asia 2010 Papers* 29.6 (2010).

[98] J. Long, E. Shelhamer, and T. Darrell. "Fully convolutional networks for semantic segmentation". In: *2015 IEEE Conference on Computer Vision and Pattern Recognition (CVPR)*. 2015, pp. 3431–3440.

[99] William E. Lorensen and Harvey E. Cline. "Marching cubes: a high resolution 3D surface construction algorithm". In: *SIGGRAPH Comput. Graph.* 21.4 (Aug. 1987), pp. 163–169.

[100] Lu Lou et al. "A cost-effective automatic 3D reconstruction pipeline for plants using multi-view images". In: *Advances in Autonomous Robotics Systems*. Cham: Springer International Publishing, 2014.

[101] David G. Lowe. "Distinctive image features from scale-invariant keypoints". In: *International Journal of Computer Vision* 60 (Nov. 2004), pp. 91–110.

[102] Shezhou Luo et al. "Maize and soybean heights estimation from unmanned aerial vehicle (UAV) LiDAR data". In: *Computers and Electronics in Agriculture* 182 (2021), p. 106005.

[103] Ulrike von Luxburg. "A tutorial on spectral clustering". In: *Statistics and Computing* 17.4 (Dec. 2007), pp. 395–416.

[104] Stefan Mairhofer et al. "RooTrak: automated recovery of three-dimensional plant root architecture in soil from X-Ray microcomputed tomography images using visual tracking". In: *Plant Physiology* 158.2 (2012), pp. 561–569.

[105] Matti Maltamo, Erik Næsset, and Jari Vauhkonen. *Forestry applications of airborne laser scanning: concepts and case studies*. Springer, Jan. 2014. ISBN: 978-94-017-8662-1.

[106] Jianchang Mao and A.K. Jain. "A self-organizing network for hyperellipsoidal clustering (HEC)". In: *Proceedings of 1994 IEEE International Conference on Neural Networks (ICNN'94)*. Vol. 5. 1994, 2967–2972 vol.5.

[107] Adam J. Mathews and Jennifer L. R. Jensen. "Visualizing and quantifying vineyard canopy LAI using an unmanned aerial vehicle (UAV) collected high density structure from motion point cloud". In: *Remote Sensing* 5 (2013), pp. 2164–2183.

[108] C. L. McCarthy, N. H. Hancock, and S. R. Raine. "Applied machine vision of plants: a review with implications for field deployment in automated farming operations". In: *Intelligent Service Robotics* 3.4 (Oct. 2010), pp. 209–217.

[109] Ryan F. McCormick, Sandra K. Truong, and John E. Mullet. "3D Sorghum reconstructions from depth images identify QTL regulating shoot architecture". In: *Plant Physiology* 172.2 (2016), pp. 823–834.

[110] Donald Meagher. "Octree encoding: a new technique for the representation, manipulation and display of arbitrary 3D objects by computer". In: *Computer Graphics and Image Processing* (Oct. 1980).

[111] Jie Mei et al. "3D tree modeling from incomplete point clouds via optimization and L1-MST". In: *International Journal of Geographical Information Science* 31.5 (2017), pp. 999–1021.

[112] Ralf Metzner et al. "Direct comparison of MRI and X-ray CT technologies for 3D imaging of root systems in soil: potential and challenges for root trait quantification". In: *Plant Methods* 11.1 (Mar. 2015), p. 17.

[113] Massimo Minervini et al. "Finely-grained annotated datasets for image-based plant phenotyping". In: *Pattern Recognition Letters* 81 (2016), pp. 80–89.

[114] Kumud B. Mishra et al. “Plant phenotyping: a perspective”. In: *Indian Journal of Plant Physiology* 21.4 (Dec. 2016), pp. 514–527.

[115] M. Moriondo et al. “Use of digital images to disclose canopy architecture in olive tree”. In: *Scientia Horticulturae* 209 (2016), pp. 1–13.

[116] Felix Morsdorf et al. “LIDAR-based geometric reconstruction of boreal type forest stands at single tree level for forest and wildland fire management”. In: *Remote Sensing of Environment* 92.3 (2004), pp. 353–362.

[117] Mark Müller-Linow et al. “The leaf angle distribution of natural plant populations: assessing the canopy with a novel software tool”. In: *Plant Methods* 11.1 (Feb. 2015), p. 11.

[118] C. V. Nguyen et al. “3D Scanning system for automatic high-resolution plant phenotyping”. In: *2016 International Conference on Digital Image Computing: Techniques and Applications (DICTA)*. Nov. 2016, pp. 1–8.

[119] Thuy Nguyen et al. “Comparison of structure-from-motion and stereo vision techniques for full in-field 3D reconstruction and phenotyping of plants: an investigation in sunflower”. In: *ASABE*. 2016.

[120] Thuy Nguyen et al. “Structured light-based 3D reconstruction system for plants”. In: *Sensors* 15 (Aug. 2015), pp. 18587–612.

[121] Ivan Nikolov. and Claus Madsen. “Interactive environment for testing sfm image capture configurations”. In: *Proceedings of the 14th International Joint Conference on Computer Vision, Imaging and Computer Graphics Theory and Applications - GRAPP,* INSTICC. SciTePress, 2019, pp. 317–322.

[122] John Oliensis. “A critique of structure-from-motion algorithms”. In: *Computer Vision and Image Understanding* 80 (2000), pp. 172–214.

[123] Kenji Omasa, Fumiki Hosoi, and Atsumi Konishi. “3D LIDAR imaging for detecting and understanding plant responses and canopy structure”. In: *Journal of Experimental Botany* 58 (Feb. 2007), pp. 881–98.

[124] Kenji Omasa and Masaki Kouda. “3D Color video microscopy of intact plants: a new method for measuring shape and growth.” In: *Environment Control in Biology* 36 (1998), pp. 217–226.

[125] Kenji Omasa et al. “Accurate estimation of forest carbon stocks by 3-D remote sensing of individual trees”. In: *Environmental Science & Technology* 37.6 (2003), pp. 1198–1201.

[126] Anthony Paproki et al. “A novel mesh processing based technique for 3D plant analysis”. In: *BMC Plant Biology* 12.1 (May 2012), p. 63.

[127] Abhipray Paturkar, Gaurab Sen Gupta, and Donald Bailey. “3D reconstruction of plants under outdoor conditions using image-based computer vision”. In: *International Conference on Recent Trends in Image Processing & Pattern Recognition*. 2018.

[128] Abhipray Paturkar, Gaurab Sen Gupta, and Donald Bailey. “Effect on quality of 3D model of plant with change in number and resolution of images used : an investigation”. In: *International Conference on Signal and Data Processing*. 2019.

[129] Abhipray Paturkar, Gaurab Sen Gupta, and Donald Bailey. “Non-destructive and cost-effective 3D plant growth monitoring system in outdoor conditions”. In: *Multimedia Tools and Applications* (Apr. 2020).

[130] Abhipray Paturkar, Gaurab Sen Gupta, and Donald Bailey. "Overview of image-based 3D vision systems for agricultural applications". In: *International Conference on Image and Vision Computing New Zealand (IVCNZ)*. Dec. 2017, pp. 1–6.

[131] Abhipray Paturkar, Gourab Sen Gupta, and Donald Bailey. "Plant trait segmentation for plant growth monitoring". In: *2020 35th International Conference on Image and Vision Computing New Zealand (IVCNZ)*. 2020, pp. 1–6.

[132] Abhipray Paturkar, Gourab Sen Gupta, and Donald Bailey. "Making use of 3D models for plant physiognomic analysis: a review". In: *Remote Sensing* 13.11 (2021).

[133] Stefan Paulus. "Measuring crops in 3D: using geometry for plant phenotyping". In: *Plant Methods* 15 (Dec. 2019).

[134] Stefan Paulus et al. "Automated analysis of barley organs using 3D laser scanning: an approach for high throughput phenotyping". In: *Sensors* 14 (July 2014), pp. 12670–12686.

[135] Stefan Paulus et al. "High-precision laser scanning system for capturing 3D plant architecture and analysing growth of cereal plants". In: *Biosystems Engineering* 121 (2014), pp. 1–11.

[136] Stefan Paulus et al. "Limits of active laser triangulation as an instrument for high precision plant imaging". In: *Sensors* 14 (Feb. 2014), pp. 2489–509.

[137] Stefan Paulus et al. "Low-cost 3D systems: suitable tools for plant phenotyping." In: *Sensors (Basel, Switzerland)* 14 (Feb. 2014), pp. 3001–18.

[138] Stefan Paulus et al. "Surface feature based classification of plant organs from 3D laserscanned point clouds for plant phenotyping". In: *BMC Bioinformatics* 14.1 (July 2013), p. 238.

[139] Nick Pears, Yonghuai Liu, and Pete Bunting. *3D Imaging, analysis and applications*. Springer London : Imprint: Springer, 2012.

[140] Gustavo Pereyra Irujo et al. "GlyPh: A low-cost platform for phenotyping plant growth and water use". In: *Functional Plant Biology* 39 (Jan. 2012), p. 905.

[141] Norbert Pfeifer, Ben Gorte, and Daniel Winterhalder. "Automatic reconstruction of single trees from terrestrial laser scanner data". In: *International Archives of Photogrammetry. Remote Sensing and Spatial Information Sciences* 35 (Jan. 2004).

[142] J. Phattaralerphong and H. Sinoquet. "A method for 3D reconstruction of tree crown volume from photographs: assessment with 3D-digitized plants". In: *Tree Physiology* 25.10 (Oct. 2005), pp. 1229–1242.

[143] Gerrit Polder and J.W. Hofstee. "Phenotyping large tomato plants in the greenhouse usig a 3D light-field camera". In: *American Society of Agricultural and Biological Engineers Annual International Meeting 2014, ASABE 2014* 1 (Jan. 2014), pp. 153–159.

[144] Richard James Pollock. "The automatic recognition of individual trees in aerial images of forests based on a synthetic tree crown image model". PhD thesis. The University of British Columbia (Canada), 1996.

[145] Sorin C Popescu, Randolph H Wynne, and Ross F Nelson. "Measuring individual tree crown diameter with lidar and assessing its influence on estimating forest volume and biomass". In: *Canadian Journal of Remote Sensing* 29.5 (2003), pp. 564–577.

[146] R. C. Prim. "Shortest connection networks and some generalizations". In: *The Bell System Technical Journal* 36.6 (Nov. 1957), pp. 1389–1401.

[147] Charles R. Qi et al. "PointNet: deep learning on point sets for 3D classification and segmentation". In: *Proceedings of the IEEE Conference on Computer Vision and Pattern Recognition (CVPR)*. July 2017.

[148] Charles Ruizhongtai Qi et al. "Frustum pointNets for 3D object detection from RGB-D data". In: *CoRR* (2017).

[149] Charles Ruizhongtai Qi et al. "PointNet++: deep hierarchical feature learning on point sets in a metric space". In: *Advances in Neural Information Processing Systems 30*. Ed. by I. Guyon et al. Curran Associates, Inc., 2017, pp. 5099–5108.

[150] Long Quan et al. "Image-based plant modeling". In: *ACM Transactions on Graphics*. Vol. 25. 3. 2006, pp. 599–604.

[151] J. Reitberger et al. "3D segmentation of single trees exploiting full waveform LIDAR data". In: *ISPRS Journal of Photogrammetry and Remote Sensing* 64.6 (2009), pp. 561–574.

[152] Jayakumari Reji et al. "Multi-temporal estimation of vegetable crop biophysical parameters with varied nitrogen fertilization using terrestrial laser scanning". In: *Computers and Electronics in Agriculture* 184 (2021), p. 106051.

[153] Fabio Remondino and D. Stoppa. *TOF range-imaging cameras*. Springer, July 2013, pp. 1–240.

[154] Vezočnik Rok et al. "Use of terrestrial laser scanning technology for long term high precision deformation monitoring". In: *Sensors* 9 (Dec. 2009).

[155] Johann Christian Rose, Stefan Paulus, and Heiner Kuhlmann. "Accuracy analysis of a multi-view stereo approach for phenotyping of tomato plants at the organ level". In: *Sensors* 15 (2015), pp. 9651–9665.

[156] Riccardo Rossi et al. "Performances Evaluation of a Low-Cost Platform for High-Resolution Plant Phenotyping". In: *Sensors* 20.11 (2020).

[157] David Rousseau et al. "Multiscale imaging of plants: Current approaches and challenges". In: *Plant Methods* 11 (Dec. 2015).

[158] Francisco Rovira-Más, Quanyi Zhang, and John Reid. "Creation of three-dimensional crop maps based on aerial stereoimages". In: *Biosystems Engineering* 90 (2005), pp. 251–259.

[159] R. B. Rusu, N. Blodow, and M. Beetz. "Fast point feature histograms FPFH for 3D registration". In: *2009 IEEE International Conference on Robotics and Automation*. May 2009, pp. 3212–3217.

[160] R. B. Rusu et al. "Aligning point cloud views using persistent feature histograms". In: *2008 IEEE/RSJ International Conference on Intelligent Robots and Systems*. Sept. 2008, pp. 3384–3391.

[161] Jianbo S. and J. Malik. "Normalized cuts and image segmentation". In: *IEEE Transactions on Pattern Analysis and Machine Intelligence* 22.8 (2000), pp. 888–905.

[162] Thiago Santos and Julio Ueda. "Automatic 3D plant reconstruction from photographies, segmentation and classification of leaves and internodes using clustering". In: *FSPM2013 - 7th International Conference on Functional-Structural Plant Models*. June 2013.

[163] Thiago Teixeira Santos et al. "3D Plant modeling: localization, mapping and segmentation for plant phenotyping using a single hand-held camera". In: *Computer Vision - ECCV 2014 Workshops*. Ed. by Lourdes Agapito, Michael M. Bronstein, and Carsten Rother. Cham: Springer International Publishing, 2015, pp. 247–263.

[164] Hanno Scharr et al. "Fast high resolution volume carving for 3D plant shoot reconstruction". In: *Frontiers in Plant Science* 8 (2017), p. 1680.

[165] Daniel Scharstein and Richard Szeliski. "A taxonomy and evaluation of dense two-frame stereo correspondence algorithms". In: *Int. J. Comput. Vision* 47.1-3 (Apr. 2002), pp. 7–42.

[166] Julius Schöning and Gunther Heidemann. "Evaluation of multi-view 3D reconstruction software". In: *Computer Analysis of Images and Patterns*. Ed. by George Azzopardi and Nicolai Petkov. Cham: Springer International Publishing, 2015, pp. 450–461.

[167] Hannes Schulz et al. "Plant root system analysis from MRI images". In: *Computer Vision, Imaging and Computer Graphics Theory and Application*. Vol. 359. Jan. 2013, pp. 411–425.

[168] Steven M. Seitz and Charles R. Dyer. "Photorealistic scene reconstruction by voxel coloring". In: *International Journal of Computer Vision* 35.2 (Nov. 1999), pp. 151–173.

[169] Ariel Shamir. "A survey on mesh segmentation techniques". In: *Computer Graphics Forum* 27.6 (2008), pp. 1539–1556.

[170] Weinan Shi et al. "Plant-part segmentation using deep learning and multi-view vision". In: *Biosystems Engineering* 187 (2019), pp. 81–95.

[171] Noah Snavely, Steven Seitz, and Richard Szeliski. "Photo tourism: exploring photo collections in 3D". In: *ACM Trans. Graph.* 25 (July 2006), pp. 835–846.

[172] P. Sodhi, S. Vijayarangan, and D. Wettergreen. "In-field segmentation and identification of plant structures using 3D imaging". In: *2017 IEEE/RSJ International Conference on Intelligent Robots and Systems (IROS)*. Sept. 2017, pp. 5180–5187.

[173] Paloma Sodhi. "In-field plant phenotyping using model-free and model-based methods". In: *IEEE/RSJ International Conference on Intelligent Robots and Systems IROS*. 2017.

[174] Svein Solberg, Erik Næsset, and Ole Bollandsås. "Single tree segmentation using airborne laser scanner data in a structurally heterogeneous spruce forest". In: *Photogrammetric Engineering & Remote Sensing* 72.12 (2006), pp. 1369–1378.

[175] Yu Song. "Modelling and analysis of plant image data for crop growth monitoring in horticulture". PhD thesis. University of Warwick, Coventry, UK, 2008.

[176] David R. Streutker and Nancy F. Glenn. "LiDAR measurement of sagebrush steppe vegetation heights". In: *Remote Sensing of Environment* 102.1 (2006), pp. 135–145.

[177] Ram Subramanian, Edgar P. Spalding, and Nicola J. Ferrier. "A high throughput robot system for machine vision based plant phenotype studies". In: *Machine Vision and Applications* 24.3 (Apr. 2013), pp. 619–636.

[178] Ping Tan et al. “Image-based tree modeling”. In: *ACM Transactions on Graphics*. Vol. 26. 3. 2007, p. 87.

[179] Shijun Tang, Pinliang Dong, and Bill P. Buckles. “Three-dimensional surface reconstruction of tree canopy from lidar point clouds using a region-based level set method”. In: *International Journal of Remote Sensing* 34.4 (2013), pp. 1373–1385.

[180] Poching Teng et al. “Accuracy assessment in 3D remote sensing of rice plants in paddy field using a small UAV”. In: *Eco-Engineering* 28 (2016), pp. 107–112.

[181] Suresh Thapa et al. “A novel liDAR-based instrument for high-throughput, 3D measurement of morphological traits in maize and sorghum.” In: *Sensors* 18 (4 Apr. 2018).

[182] W. Tiller. “Rational B-splines for curve and surface Representation”. In: *IEEE Computer Graphics and Applications* 3.6 (1983), pp. 61–69.

[183] Beau Tippetts et al. “Review of stereo vision algorithms and their suitability for resource-limited systems”. In: *Journal of Real-Time Image Processing* 11.1 (2016), pp. 5–25.

[184] Sébastien Tisné et al. “Phenoscope: an automated large-scale phenotyping platform offering high spatial homogeneity”. In: *The Plant Journal* 74.3 (2013), pp. 534–544.

[185] Christopher N. Topp et al. “3D phenotyping and quantitative trait locus mapping identify core regions of the rice genome controlling root architecture”. In: *Proceedings of the National Academy of Sciences* 110.18 (2013), E1695–E1704.

[186] R. Y. Tsai and R. K. Lenz. “Real time versatile robotics hand/eye calibration using 3D machine vision”. In: *IEEE International Conference on Robotics and Automation*. Apr. 1988, 554–561 vol.1.

[187] Darren Turner, Arko Lucieer, and Christopher Watson. “An automated technique for generating georectified mosaics from ultra-high resolution unmanned aerial vehicle (UAV) imagery, based on structure from motion (SfM) point clouds”. In: *Remote Sensing* 4 (2012), pp. 1392–1410.

[188] H. Uchiyama et al. “An easy-to-setup 3D phenotyping platform for KOMATSUNA dataset”. In: *2017 IEEE International Conference on Computer Vision Workshops (ICCVW)*. 2017, pp. 2038–2045.

[189] *United Nations Sustainable Development Goals*. https://sustainabledevelopment.un.org/sdgs.

[190] Breght Vandenberghe, Stephen Depuydt, and Arnout Van Messem. “How to make sense of 3D representations for plant phenotyping: a compendium of processing and analysis techniques”. In: *OSI Preprints* (Nov. 2018).

[191] Jari Vauhkonen. “Estimating crown base height for Scots pine by means of the 3D geometry of airborne laser scanning data”. In: *International Journal of Remote Sensing* 31.5 (2010), pp. 1213–1226.

[192] Jari Vauhkonen et al. “Comparative testing of single-tree detection algorithms under different types of forest”. In: *Forestry: An International Journal of Forest Research* 85.1 (Oct. 2011), pp. 27–40.

[193] Manuel Vázquez-Arellano et al. “3D Imaging systems for agricultural applications a review”. In: *Sensors* 16 (July 2016), p. 1039.

[194] A. Verroust and F. Lazarus. "Extracting skeletal curves from 3D scattered data". In: *Proceedings Shape Modeling International '99. International Conference on Shape Modeling and Applications*. 1999, pp. 194–201.

[195] Miguel Vieira and Kenji Shimada. "Surface mesh segmentation and smooth surface extraction through region growing". In: *Computer Aided Geometric Design* 22.8 (2005), pp. 771–792.

[196] *VisualSFM*. http://ccwu.me/vsfm/.

[197] Mirwaes Wahabzada et al. "Automated interpretation of 3D laserscanned point clouds for plant organ segmentation". In: *BMC Bioinformatics* 16.1 (Aug. 2015), p. 248.

[198] P.J. Walklate. "A laser scanning instrument for measuring crop geometry". In: *Agricultural and Forest Meteorology* 46.4 (1989), pp. 275–284.

[199] Achim Walter et al. "Dynamics of seedling growth acclimation towards altered light conditions can be quantified via GROWSCREEN: A setup and procedure designed for rapid optical phenotyping of different plant species". In: *The New phytologist* 174 (Feb. 2007), pp. 447–55.

[200] Weiyue Wang et al. "SGPN: Similarity group proposal network for 3D point cloud instance segmentation". In: *Proceedings of the IEEE Conference on Computer Vision and Pattern Recognition (CVPR)*. June 2018.

[201] Wenping Wang, Helmut Pottmann, and Yang Liu. "Fitting B-spline curves to point clouds by curvature-based squared distance minimization". In: *ACM Transactions on Graphics* 25.2 (2006).

[202] Yunsheng Wang, Holger Weinacker, and Barbara Koch. "A Lidar point cloud based procedure for vertical canopy structure analysis and 3D single tree modelling in forest". In: *Sensors* 8.6 (2008), pp. 3938–3951.

[203] Chunlei Xia et al. "In situ 3D segmentation of individual plant leaves using a RGB-D camera for agricultural automation". In: *Sensors* 15 (Aug. 2015), pp. 20463–79.

[204] Shunfu Xiao et al. "A fast and accurate approach to the extraction of leaf midribs from point clouds". In: *Remote Sensing Letters* 11.3 (2020), pp. 255–264.

[205] Xiaowei Yu et al. "Automatic detection of harvested trees and determination of forest growth using airborne laser scanning". In: *Remote Sensing of Environment* 90.4 (2004), pp. 451–462.

[206] Cha Zhang and Tsuhan Chen. "Efficient feature extraction for 2D/3D objects in mesh representation". In: *Proceedings 2001 International Conference on Image Processing*. Vol. 3. 2001, pp. 935–938.

[207] Song Zhang. "High-speed 3D shape measurement with structured light methods: A review". In: *Optics and Lasers in Engineering* 106 (2018), pp. 119–131.

[208] Yu Zhang et al. "3D monitoring for plant growth parameters in field with a single camera by multi-view approach". In: *Journal of Agricultural Meteorology* 74 (2018), pp. 129–139.

[209] Yu Zhang et al. "Estimating 3D leaf and stem shape of nursery paprika plants by a novel multi-camera photography system". In: *Sensors* 16.6 (2016).

[210] Z. Zhang. "Microsoft Kinect sensor and its effect". In: *IEEE MultiMedia* 19.2 (Feb. 2012), pp. 4–10.

[211] Zhen Zhen et al. "Agent-based region growing for individual tree crown delineation from airborne laser scanning (ALS) data". In: *International Journal of Remote Sensing* 36.7 (2015), pp. 1965–1993.

[212] Jing Zhou et al. "Evaluating Geometric Measurement Accuracy Based on 3D Reconstruction of Automated Imagery in a Greenhouse". In: *Sensors* 18.7 (2018).

[213] Yin Zhou and Oncel Tuzel. "VoxelNet: end-to-end learning for point cloud based 3D object detection". In: *CoRR* (2017).